UNIVERSITÀ DEGLI STUDI DI PADOVA

DIPARTIMENTO DI SCIENZE CHIRURGICHE ONCOLOGICHE E GASTROENTEROLOGICHE

---

Scuola di Dottorato di Ricerca in
**Oncologia e Oncologia Chirurgica**
**CICLO XXVII**

# Targeting immunosuppressive myeloid cells using nanocarriers to improve cancer immunotherapy

**Direttore della Scuola**: Ch.ma Prof.ssa Paola Zanovello

**Supervisore**: Ch.mo Prof. Vincenzo Bronte

Ch.ma Dr.ssa Susanna Mandruzzato

**Dottoranda**: Maria Stella Sasso

# Table of Contents

# Summary

In the last decade, different cancer immunotherapy approaches have been proved to produce objective clinical responses and survival benefits in cancer patients who failed conventional treatment options. However, the efficacy of cancer immunotherapy is known to be limited by tumor-induced expansion of immunosuppressive and tumor-promoting immune populations, including cells of myeloid origin (such as tumor associated macrophages –TAMs-, and myeloid-derived suppressor cells –MDSCs-). The development of increasingly powerful and widely applicable immunotherapies is therefore dependent on the availability of supporting treatments able to reduce tumor-associated immunosuppression, with good efficacy and low toxicity. Drug delivery nanosystems have been shown to improve pharmacological proprieties of anti-cancer drugs by increasing drug half-life, enhancing accumulation into tumor tissues and reducing off-target toxicity. In addition, the use of RNA delivery nanosystems is currently being explored for the development of RNA intereference (RNAi)-based anti-cancer therapeutics. The use of drug and RNA delivery nanosystems to target tumor-associated immune cells, besides tumor cells, is a far less explored approach, which is currently showing promise as tool to improve cancer immunotherapy.

In the present work we investigated two different nanotechnology-based tools to modulate the presence and function of tumor-associated myeloid cells: a modified form of gemcitabine encapsulated into lipid nanocapsules (LNC-GemC12), and ployarginine-coated nanocapsules (PolyArg NCs) loaded with short hairpin (sh) RNAs, for *in vivo* RNAi-based gene silencing.

LNC-GemC12 and free gemcitabine hydrochloride (GemHCl, the current standard gemcitabine formulation) were found to selectively deplete both splenic and tumor-infiltrating monocytic (M-) MDSCs, following administration at a very low drug dose to EG7-OVA tumor bearing mice. Remarkably, LNC-GemC12 administration was associated with a stronger and more durable reduction of tumor-infiltrating M-MDSCs as compared with GemHCl, which resulted in the attenuation of MDSC suppressive activity towards T cells. More importantly, treatment of EG7-OVA tumor bearing mice with LNC-GemC12, prior to adoptive cell transfer therapy (ACT) with OVA-specific T lymphocytes, significantly extended mouse survival as compared to mice receiving ACT alone. Conversely, preconditioning with GemHCl at the same dose did not result in a similar survival benefit.

PolyArg NCs were loaded with a fluorinated shRNA specific for mouse C/EBPβ transcription factor, which is known to be required for tumor-induced MDSC expansion and acquisition of immunosuppressive functions. PolyArg NCs loaded with the C/EBPβ-specific shRNA (NC-

shC/EBPβ) efficiently down-regulated target gene expression in an immortalized MDSC cell line. *In vivo*, we reported a significant reduction of C/EBPβ mRNA levels in splenic and tumor-infiltrating myeloid cells, following repeated administration of NC-shC/EBPβ to mice bearing MCA203 subcutaneous sarcomas.

The present data support the use of LNC-GemC12 as MDSC-targeted agent in cancer immunotherapy, notably in combination with ACT. As compared with standard MDSC-depleting chemotherapeutic drug formulations, LNC-GemC12 bears the potential of achieving significant effects at very low, likely not toxic, drug doses. Moreover, the use of a drug already employed in clinical oncology, combined with a biocompatible delivery nanosystem, might facilitate clinical translation. We also provided an initial evidence that shRNA-loaded PolyArg NCs allow to downregulate target gene expression in myeloid cells *in vivo*, and could be exploited to therapeutically modulate tumor-associated myeloid cells.

# Riassunto

Nell'ultimo decennio l'impiego di diversi tipi di immunoterapia dei tumori ha consentito di ottenere risposte cliniche e un miglioramento della sopravvivenza in pazienti non rispondenti alle terapie convenzionali. Tuttavia, l'efficacia dell'immunoterapia del cancro è limitata dalla presenza di popolazioni di cellule immunitarie con proprietà immunosoppressive e pro-tumorali che si espandono durante la patogenesi della malattia. Tali cellule comprendono popolazioni di origine mieloide, quali i macrofagi associati al tumore (*tumor associated macrophages, TAMs*), e cellule soppressive di derivazione mieloide (*myeloid derived suppressor cells, MDSCs*). Pertanto, per lo sviluppo di protocolli d'immunoterapia ottimali sono necessari trattamenti di supporto, con buona efficacia e bassa tossicità, in grado di contrastare l'immunosoppressione indotta dal tumore. Diversi studi preclinici e clinici hanno dimostrato che i nanosistemi per il trasporto di farmaci antitumorali sono in grado di migliorarne le proprietà farmacologiche aumentandone l'emivita, favorendone l'accumulo nel sito tumorale e limitando la tossicità a carico di tessuti sani. Inoltre, i nanosistemi per il trasporto di RNA sono attualmente impiegati nello sviluppo di terapie antineoplastiche che utilizzano approcci di silenziamento genico *in vivo* basati sul meccanismo dell'Interferenza a RNA (RNAi). L'uso di nanosistemi per il trasporto di farmaci ed RNA che hanno come target le cellule sistema immunitario, oltre alle cellule tumorali, sembra essere un nuovo e promettente approccio per potenziare l'efficienza dell'immunoterapia dei tumori.

In questo lavoro abbiamo valutato l'efficacia di due diverse formulazioni di nanotrasportatori, caricati con farmaci o RNA, come agenti immunomodulanti per alterare la presenza e/o funzione delle cellule mieloidi associate al tumore. La prima formulazione consiste in una forma modificata di gemcitabina incapsulata in nanocapsule lipidiche (LNC-GemC12); la seconda è costituita da nanocapsule rivestite di poliarginina (PolyArg NCs) caricate con *short hairpin* (sh) RNA, per il silenziamento genico *in vivo* mediante RNAi.

Nel modello tumorale murino EG7-OVA, la somministrazione di LNC-GemC12 e di gemcitabina idrocloruro (GemHCl, l'attuale formulazione standard per la gemcitabina), ad un dosaggio molto basso, causa una deplezione selettiva delle MDSC monocitarie (M-MDSCs) nella milza e nel sito tumorale. In particolare, alla somministrazione di LNC-GemC12, rispetto alla GemHCl, si associa una riduzione più intensa e prolungata delle M-MDSCs tumorali ed una conseguente attenuazione dell'attività soppressiva delle MDSC infiltranti il tumore nei confronti dei linfociti T. Inoltre, nello stesso modello, il trattamento con LNC-GemC12 prima della somministrazione di una terapia di trasferimento cellulare adottivo (ACT) con linfociti T OVA-specifici, risulta in un

miglioramento della sopravvivenza rispetto al solo trattamento mediante ACT. In confronto, il pre-trattamento con GemHCl alla stessa dose non si associa ad un'estensione della sopravvivenza dopo ACT.

Nella seconda parte di questo lavoro, le PolyArg NC sono state caricate con un shRNA fluorinato specifico per il fattore di trascrizione murino C/EBPβ, la cui espressione è necessaria per l'espansione e l'induzione di funzioni immunosoppressive nelle MDSC. Le PolyArg NC caricate con l'shRNA C/EBPβ-specifico (NC-shC/EBPβ) sono state impiegate con successo per ridurre l'espressione del gene bersaglio in una linea cellulare di MDSC immortalizzate. Successivamente, abbiamo valutato il funzionamento di questo sistema *in vivo* in un modello murino di sarcoma sottocutaneo. In questo modello abbiamo riportato una riduzione significativa nei livelli di mRNA di C/EBPβ nelle cellule mieloidi spleniche e intratumorali a seguito della somministrazione ripetuta di NC-shC/EBPβ.

I dati ottenuti in questo lavoro supportano la validità dell'uso delle LNC-GemC12 come agente per la modulazione delle MDSC nell'immunoterapia del cancro, in particolare in combinazione con l'ACT. Rispetto alle formulazioni standard di agenti chemioterapici in grado di ridurre la frequenza delle MDSC, le LNC-GemC12 hanno il potenziale di fornire un'efficacia terapeutica a dosaggi di farmaco molto bassi e verosimilmente non tossici. In aggiunta, l'utilizzo di un farmaco già in uso nella pratica clinica, combinato con una formulazione di nano capsule lipidiche biocompatibili, potrebbe facilitare la traslazione in ambito clinico di questo approccio. Nel presente studio, abbiamo inoltre fornito una prima validazione dell'efficacia *in vivo* delle PolyArg NC caricate con shRNA come strumento per ridurre l'espressione di geni bersaglio nelle cellule mieloidi associate al tumore, potenzialmente impiegabile come agente immunomodulante nella terapia del cancro.

# Introduction

The interaction between immune cells and tumor cells is currently recognized to play a critical role in cancer pathogenesis[1]. In cancer, the immune system acts like a double-edged sword, since it includes both components able to detect and destroy tumor cells (as cytotoxic T cells and Natural Killer cells) and cells that suppress this anti-tumor response and/or directly support tumor proliferation, invasion and metastasis[2]. With the substantial progresses made in the last 20 years in the field of cancer immunotherapy (i.e. harnessing the immune system to destroy tumors), a growing consideration has been given to the concept that the immunosuppressive cell subsets, which support cancer pathogenesis, are also a major obstacle to the efficacy of immunotherapeutic approaches [3]. Based on this concept, along with the development of increasingly refined and effective strategies to directly potentiate the immune-mediated cytotoxicity (e.g. by the generation of highly potent and versatile engineered T cytotoxic cells[4]) also new approaches to specifically eliminate or modulate tumor-associated immunosuppressive and tumor promoting cells have been investigated. The combination of these complementary strategies is ultimately expected to maximize the efficacy of cancer immunotherapy.

Immune populations known to support cancer progression by different mechanisms include T regulatory cells (Tregs) and cells of myeloid origin, such as tumor associated macrophages (TAMs), myeloid-derived suppressor cells (MDSCs), and dendritic cells (DCs). Tregs are a peculiar population of T lymphocytes endowed with immunosuppressive functions. Tumor-infiltrating Tregs may be either natural occurring T regs, generated during thymic development and recruited in the tumor site by tumor-derived chemokines[5,6] and induced Tregs that differentiate *in situ* from $CD4^+$ T lymphocytes under the influence of microenvironmental stimuli[7]. DCs are strictly required to mount an adaptive immune response against tumor cells, since these cells are highly specialized antigen presenting cells, with the unique ability to activate naïve T lymphocytes[8]. However, in cancer DCs are often prone to bear an immature and dysfunctional state, characterized by low costimulatory molecule expression and poor activating abilities[9]. Moreover these cells may also exert an active immunosuppressive function, mainly relying on the expression of the enzyme indoleamine 2,3-dioxygenase (IDO). IDO expression by DCs results in the microenvironnemental depletion of L-Tryptophan, and in the accumulation of its catabolites, which both inhibit T cell activation and function[10].

Among populations of myeloid origin, MDSCs and TAMs exert the strongest immunosuppressive and tumor-promoting functions. These two populations are extensively described below. The following paragraphs will also provide an overview of cancer immunotherapy approaches, which

have so far achieved the best results in clinical evaluations, and of current successes and challenges in the use of delivery nanosystems in oncology. Last paragraphs will be dedicated to the application of delivery nanosystems in cancer immunotherapy and notably in the modulation of tumor-promoting and immunosuppressive cell populations.

## 1. Myeloid-derived suppressor cells (MDSCs)

Myeloid-derived suppressor cells (MDSCs) are an immune population of myeloid origin characterized by a strong immunosuppressive activity and heterogeneous composition, including monocytic and granulocytic cells, and more immature precursor cells. In mice, MDSCs were originally identified as $CD11b^{+}Gr1^{+}$ cells that expanded during cancer growth, accumulating both within the tumor site and in peripheral lymphoid organs, notably in the spleen[11]. The initial identification and most information on MDSCs derive from studies in tumor models; however, their expansion has been reported also under other pathological conditions, including parasitic infection[12-14] polymicrobial sepsi [15], autoimmunity[16], inflammatory bowel disease[17] and trauma[18]. Currently, the monocytic and granulocytic fraction of mouse MDSCs are commonly distinguished on the basis of the differential expression of Ly6C and Ly6G markers (two protein isoforms recognized by anti-Gr1 antibody): monocitic (M-)MDSCs have a $CD11b^{+}Ly6G^{-}Ly6C^{high}$phenotype, while polymorphonuclear/granulocytic (PMN-)MDSCs are $CD11b^{+}Ly6G^{+}Ly6C^{int/low}$ [19]. Alternatively, M- and PMN-MDSCs have been discriminated based on the intensity of Gr1 marker, since $CD11b^{+}Gr1^{high}$ cells substantially correspond to $Ly6G+Ly6C^{int/low}$ PMN-MDSCs, while the $CD11B^{+}Gr1^{int/low}$ fraction include M-MDSCs[20,21]. M-MDSCs also express common markers of inflammatory monocytes as F4/80, CD115, and CCR2[20-22]. Indeed, M-MDSC phenotypically resemble mouse $Ly6C^{high}$ inflammatory monocytes[10], and are likely to represent, at least in part, a peculiar cancer-induced functional state of monocytes, with the fundamental distinction that inflammatory monocytes do not bear immunosuppressive functions. Similarly, PMN-MDSCs phenotipically resemble normal granulocytes, except for the increased expression of markers that are poorly expressed by granulocytes, such as CD244 and CD115 [23]. For these reasons, the unambiguous definition of the MDSC populations requires assessment of immunosuppressive functions by *ex-vivo* or *in vivo* assays, and other functional evaluations. For instance, mouse PMN-MDSCs have been reported to have lower phagocytic ability, lower Tumor Necrosis Factor (TNF)α expression and higher ARG1 and myeloperoxidase expression and ROS production as compared with neutrophils[23]. Likewise, the expression of proteins related to MDSC suppressive activity, as ARG1 and inducible Nitric Oxide synthase (iNOS, see below), may allow to identify

better M-MDSCs. Of note, MDSCs isolated from the spleen of tumor-bearing mice have been reported to include cells with morphologic, phenotypic and functional features of myeloid precursor cells, which are not found in the spleen of healthy mice[21,24,25]. Indeed, the spleen is a unique site of cancer-associated extramedullary hematopoiesis in mice, and there is evidence that splenic hematopoiesis might occur also in cancer patients[26].

Like mouse MDSCs, human MDSCs comprise monocytic and granulocytic subsets, although for each subset multiple phenotypes have been reported, accounting for the higher heterogeneity and complexity in human MDSC definition as compared to mouse MDSCs[27]. Most commonly reported fenotypes are $CD14^{+}IL4R\alpha^{+}$, $CD14^{+}/HLA\text{-}DR^{low/-}$ and $CD15^{-}/CD14^{+}/CD33^{high}/HLA\text{-}DR^{low/-}$ for human M-MDSCs; $CD15^{+}IL4R\alpha^{+}$, $CD14^{-}/CD15^{+}/CD11b^{+}$ and $CD15^{high}/FSC^{low}/SSC^{high}$ for PMN-MDSCs[19]. In addition, human MDSCs include a more immature subset, which is not stained by lineage marker cocktails and expresses the common myeloid markers CD33 and CD11b ($Lin^{-}/HLA\text{-}DR^{-}/CD33^{+}/CD11b^{+}$ phenotype)[19].

MDSC expansion in peripheral blood of cancer patients or, less often, in tumor clinical specimens, has been described in multiple cancer types[27]. Remarkably, various studies on different human solid tumors reported the existence of a positive correlation between higher circulating MDSC frequency or absolute numbers and clinical parameters as increasingly advanced cancer stages, greater metastatic burden, and worse patient prognosis[28-31]. In the same studies, MDSC ability to suppress T cell proliferation and IFNγ secretion was assessed by *ex vivo* assays, thus confirming the immunosuppressive nature of these cells.

Different tumor-derived factors, including prostaglandins, granulocyte-macrophage colony stimulating factor (GM-CSF), granulocyte colony stimulating factor (G-CSF), macrophage colony stimulating factor (M-CSF), stem cell factor (SCF), and vascular endothelial growth factor (VEGF) have been shown to promote MDSC expansion, mostly identified in mouse tumor models[11]. Pro-inflammatory mediators released by both tumor cells and tumor-activated infiltrating immune cells, as interleukin-1β (IL-1β), IL-6, IL-4, IL-10, IL-13, S100 calcium binding protein A8 and A9 (S100A8 and S100A9), interferon gamma (IFN-γ), induce the activation of immunosuppressive and tumor-promoting functions in myeloid cells[11].

The above reported signals are known to activate different transcription factors, which regulate MDSC expansion, survival and suppressive programs. Among these factors a major role is played by proteins of the signal transducer and activator of transcription family (STAT), notably STAT3, STAT1 and STAT6, and by nuclear factor κB (NF-κB) and CCAAT/enhancer-binding protein-β (C/EBPβ)[10].

MDSCs exploit different mechanisms to inhibit T cell recruitment, activation and proliferation, which have been extensively investigated in mouse tumor models. One of the first described mechanisms is the upregulation of the L-arginine metabolizing enzyme ARG1. T cell proliferation is possibly inhibited by the activation of intracellular regulatory pathways, which sense amino acid starvation and accumulation of catabolytes and repress protein synthesis[32]. Notably, L-arginine depletion from the tumor microenvironment impairs T cell activation by blocking the re-expression of the CD3 ζ chain of the TCR complex after antigen stimulation[33]. In addition, MDSC cell metabolism results in the local depletion of extracellular cysteine, which is also required for T cell activation and function[34].

Another known mechanism of MDSC-mediated immune suppression is the release of reactive oxygen and nitrogen species (ROS/RNS). Nitric oxide (NO) production by iNOS, upregulated in MDSCs, results in the block of signaling pathways downstream of the IL-2 receptor, thus impairing T cell activation and proliferation[35]. Human peripheral blood mononuclear cells (PBMCs) exposure to NO reduces IL-2 expression and release, thus impairing T cell proliferation[36].

The simultaneous activity of ARG1 and iNOS has been shown to exert a synergistic immunosuppressive function, by resulting in an enhanced production of superoxide anion $0_2^-$ by the iNOS reductase domain[37]. L-arginine substrate consumption by ARG1 is thought to shift iNOS enzymatic activity from NO production to superoxide anion ($O_2^-$) production, due to the reduced concentration of the amino acid substrate; the superoxide anion in turn reacts with NO to produce peroxinitrite (ONOO–), a potent nitrating agent[32,38]. MDSC-derived peroxinitrite was shown to impair antigen recognition of $CD8^+$ T cells by nitrating T cell receptor (TCR) and CD8 molecules on their surface, and in this way preventing the proper binding to major histocompatibility complexes (MHC) loaded with antigenic peptides[39]. Moreover, peroxinitrite nitrates the CC-chemokine ligand 2 (CCL2) released within the tumor microenvironment, thus inhibiting T cell recruitment mediated by this chemokine[40].

In addition, in mouse tumor models MDSC-mediated immune suppression was shown to depend on the production of reactive oxygen species (ROS), mainly including $H_2O2$[41]. Consistently, the presence of circulating, activated granulocytes in cancer patients was found to correlate with reduced T-cell receptor ζ chain expression and decreased cytokine production by T cells, and granulocyte-mediated immunosuppression appeared to be mainly due to $H_2O_2$ production[42].

In works considering separately M-MDSC and PMN-MDSC immunosuppressive activity, M-MDSC-mediated suppression was found to be more dependent on NO release, while PMN-MDSCs produced greater amounts of ROS and lower amount of NO as compared with M-

MDSC[20,43]. In addition, although PMN-MDSCs generally represent a more abundant population in spleens of tumor bearing mice, M-MDSCs exerted a stronger immune suppressive activity on a per-cell basis[20,22,25,44].

Besides restraining cell function, MDSCs have also reported to inhibit Natural killer (NK) cells[45-47] and to promote the differentiation and expansion of Tregs. Notably, $Gr1^+CD115^+$MDSCs, likely corresponding to the monocytic subset, were found to induce the *in vivo* expansion of Tregs by mechanisms involving both soluble factors (IFNγ, IL-10) and expression of the CD40 receptor [48,49]. In addition, M-MDSCs were reported to recruit Tregs in tumors by secreting CCR5-binding chemokines[50].

Recently, a new potential mechanism of tumor promotion by MDSCs has been discovered, since $CD11b^+Gr1^+$cells (possibly corresponding to MDSCs) were found to strongly infiltrate benign prostate tumors and favor the evasion of tumor cell senescence, thus promoting the progression to malignancy[51].

In addition to direct immunosuppressive and pro-tumor functions, MDSCs also contribute to replenish the tumor-associated macrophage (TAM) pool. MDSC recruited into the tumor site have the ability to differentiate in pro-tumoral TAMs under microenvironment stimuli as hypoxia, a property that is likely due to the M-MDSC component, since monocytes are natural macrophage precursors[52]. Consistently, selective depletion of monocytes in blood and lymphoid organs, including splenic immunosuppressive M-MDSCs, by the chemotherapeutic drug trabectedin resulted in TAM reduction in multiple mouse cancer models[53]. Other studies demonstrating TAM differentiation from $Ly6C^+$ monocytes[54,55] further support M-MDSC contribution to the generation of TAMs, since the monocytic phenotype may indeed identify immunosuppressive M-MDSCs in cancer model, as discussed above.

## 2. Tumor associated macrophages (TAMs)

In mice, TAMs primarily descend from circulating inflammatory monocytes and M-MDSCs and are maintained by both monocyte recruitment and differentiation, and *in situ* TAM proliferation [54,55]. However, it is worth to note that macrophage populations found in peripheral tissues, in healthy and disease, are extremely heterogeneous. Moreover, tissue-resident macrophage populations descending from primitive yolk-sack-derived macrophages or from fetal liver monocytes, rather than from blood monocytes, have recently been identified[56-58]. These resident macrophages are maintained by self-renewing during the adult life, without being replenished by the circulating monocyte pool.

Mouse macrophages are phenotypically identified based on the expression of CD11b, F4/80 and CD115 (colony stimulating factor 1 receptor, CSF-1R) markers and absence of expression of Ly6G marker, while in humans macrophages express CD68, CD163, CD16, CD312 and CD115 antigens[59]. However, in mice TAMs may also express classical DC markers such as MHCII and CD11c[54], thus rendering difficult the unambiguous definition of this population only based on their phenotypic characterization. Functional assays and gene expression profiling can provide additional tools to better define TAM populations[54].

TAMs have been reported to bear an alternative functional polarization, termed "M2", in opposition to the classical pro-inflammatory activation status, or "M1". The M1 and M2 states are induced by different environmental factors, including cytokines and toll-like receptor ligands, and are characterized by specific functional properties. M1 macrophages are efficient antigen-presenting cells, have an high production of reactive oxygen and nitrogen species, exert a strong cytotoxic activity against pathogens and tumor cells, express high levels of pro-inflammatory cytokines, and promote a "Th1-oriented" T cell response. Conversely, M2 macrophages have poor antigen presenting abilities, express high level of mannose, scavenger and galactose-type receptors, produce low amounts of pro-inflammatory cytokines and high levels of the anti-inflammatory cytokine IL-10, and are typically involved in the resolution of inflammation and tissue remodeling[60]. However, the dichotomic M1/M2 distinction is oversimplified, since cells may bear intermediate phenotypes and functions [61]. In addition, although TAMs are generally thought to bear an M2-like phenotype, at least in advanced tumors, the M2 phenotypic signature does not always characterize TAMs in experimental cancer models[54].

Beyond the M1-M2 phenotypic distinction, which is not always straightforward, TAMs have been generally reported to play a strong pro-tumor role. Different pro-tumor functions have been described for TAMs, including suppression of anti-tumor immunity, promotion of cancer cell growth, angiogenesis and metastasis (Fig. 1). Consistently, TAMs are an independent negative prognostic factor in human cancers[62,63].

Tumor-associated monocytes/macrophages upregulate the membrane molecule programmed death ligand 1 (PD-L1), which binds to the inhibitory receptor PD1 on T cell membrane, thus restraining T cell proliferation and function[64,65]. In a recent work, PD-L1 was reported to be upregulated in tumor-infiltrating MDSCs and macrophages upon exposure to hypoxia, via hypoxia inducible factor-1α (HIF-1α) activation[66]. In addition, TAMs may express the non-classical HLA molecules HLA-G and HLA-E, in membrane-bound or soluble form, which binds inhibitory receptors on NK cells[67].

TAMs have been reported to secrete Treg-attracting chemokines, including CCL22[5], CCL20[6] and CCL5[68,69]. TGF-β and IL-10 released by TAMs may contribute to the local induction of Tregs differentiation from $CD4^+$ T cells and also exert an inhibitory activity on T cytotoxic and helper cells[70]. Mouse TAMs, as MDSCs, express the enzyme ARG1[33,71], which locally depletes L-arginine, thus impairing T cell activation and proliferation, as discussed above.

Besides contributing to tumor-associated immunosuppression, TAMs are known to directly support critical steps of cancer pathogenesis. First, TAMs participate in tumor-induced neo-angiogenesis, which is required for continuous tumor growth and progression to malignancy[1]. One of the main mechanisms of angiogenesis promotion is macrophage-dependent VEGF release [72,73]. Notably, TAMs have been recently reported to induce VEGF secretion by endothelial cells through the release of the WNT family ligand WNT7B[74]. Pro-angiogenic myeloid cells are characterized by the expression of the Angiopoietin2 (ANG2) receptor TIE2 [75]. $Tie2^+$ macrophages interact with ANG2 expressing endothelial cells and this signalling pathway results in macrophage association with blood vessels and pro-angiogenic function[76].

TAMs express high level of different proteases, which support tumor cell mobility and invasion through the degradation and remodeling of the extracellular matrix[77]. In addition, macrophages directly stimulate tumor cell migration through the secretion of paracrine factors. In the PyMT breast cancer model, Wyckoff et coworkers described a paracrine signalling loop consisting in the stimulation of tumor cell motility by TAM-derived EGF and induction of TAM migration by tumor-derived CSF-1, resulting in the coordinated migration of both cell types[78]. A different TAM-derived molecule, protein acidic and rich in cysteine (SPARC), also known as osteonectin, was reported to favor cancer cell migration by promoting the interaction between cancer cells and the extracellular matrix[79]. In addition perivascular TAMs were shown to directly interact with cancer cells and favor their ingress into blood vessels[80].

The combination of pro-angiogenic functions and promotion of cancer cell motility and ingress into blood vessels collectively results in a strong promotion of tumor spread by TAMs. However, the mechanisms underlining the process of distant metastasis formation by circulating tumor cells are still incompletely understood. Myeloid cells are known to play a critical role in this process. Tumor-derived soluble factors, released systemically, can induce the accumulation of myeloid cells at distant sites, thus increasing the efficiency of metastatic cell seeding at those sites, defined pre-metastatic niches. In metastatic lung cancer and melanoma mouse models, the secretion of S100A8 and S100A9 inflammatory mediators in lungs, released in response to soluble factors produced by the primary tumor, was found to mediate myeloid cell recruitment into pre-metastatic sites[81]. In the same models, tumor-induced upregulation of fibronectin in

pre-metastatic lungs was reported to mediate the adhesion of circulating VEGFR1$^{+}$ hematopoietic progenitors expressing the VLA-4 integrin, which were in turn required to support tumor cell seeding[82]. Studies on lung metastasis formation have shown that cancer cells can express pro-coagulant molecules, as the tissue factor, which promote the formation of clots containing platelets and tumor cells in lung vessels [83]. Clotting, in turn, favors the recruitment of myeloid cells at the pre-metastatic site [83,84] by a mechanism involving endothelium activation and expression of the adhesion molecules vascular cell adhesion molecule-1 (VCAM-1) and vascular adhesion protein-1 (VAP-1) [84]. Circulating myeloid cells recruited at pre-metastatic sites may then differentiate into metastasis-associated macrophages, which increase the efficiency of circulating tumor cell extravasation and promote the subsequent growth of metastatic lesions[70,85].

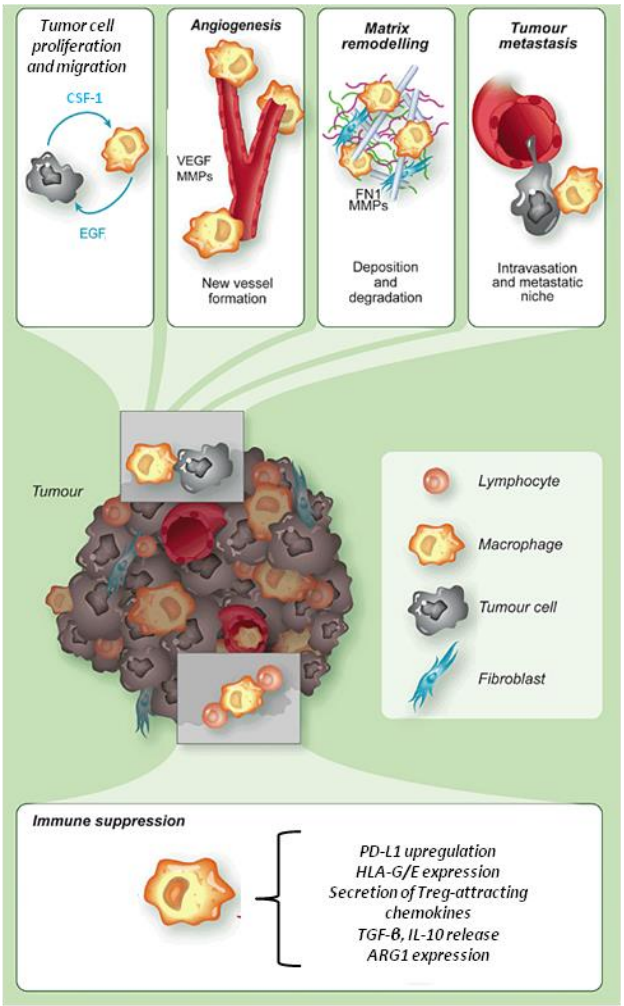


**Figure 1. Tumor-promoting functions of TAMs.** TAMs sustain tumor cell growth, and promote tumor spread by mediating matrix remodeling and supporting tumor cell motility and ingress into blood vessels. TAMs also promote angiogenesis, which is required for continuous growth of the

primary tumor ad favor tumor cell ingress into blood circulation. In addition, TAMs support tumor cell seeding and proliferation at the pre-metastatic niche and mediate tumor-induced immunosuppression by multiple mechanisms.
Adapted from: *P.Allavena and A.Mantovani. Clinical and Experimental immunology 2012.*

## 3. Current approaches for cancer immunotherapy

Cancer immunotherapy exploits immune-mediated cytotoxicity (primarily dependent on $CD8^+$ T cells) to fight tumors. To date, different approaches have been developed to potentiate the immune response against tumor cells, evaluated at clinical and preclinical levels. Approaches that have been studied in clinical trials, and that in some cases leaded to FDA drug approval, include inhibitors of immune checkpoints, cancer vaccines and the adoptive transfer of tumor-specific T cells.

### *3.1. Immune check point inhibitors and cancer vaccines*

Among immune checkpoint inhibitors, ipilimumab, a blocking antibody targeting the inhibitory molecule Cytotoxic T-lymphocyte–associated antigen 4 (CTLA-4), was positively evaluated in a series of clinical trials and in 2011 the drug was finally approved by the FDA for the treatment of unresectable or metastatic melanoma[86]. Notably, in a paper dated 2010, ipilimumab was reported to improve the overall survival of patients with late-stage, metastatic melanoma that failed previous therapies, as compared with patients receiving a gp100 vaccine[87]. Ipilimumab therapeutic effect relies on the block of the immune checkpoint mediated by the CTLA-4 molecules. CTLA-4 competes with the activating receptor CD28 for the binding to B7.1/B7.2 costimulatory molecules on the surface of antigen presenting cells, thus preventing a proper T cell activation upon antigen recognition[86]. Blocking this checkpoint promotes a stronger and sustained T cell activation. In addition, the efficacy of anti-CTLA-4 antibodies may be in part also due to interference with Treg-mediated immunosuppression[88].
Currently, antibodies targeting programmed death-1 (PD-1) receptor, a different T cell and B cell negative regulator, or its ligand PD-L1, are in phase of clinical evaluation. A phase 1 clinical trial evaluating the antitumor activity and safety of a PD-1 blocking antibody (nivolumab) reported durable objective clinical responses in patients with non-small-cell lung cancer, melanoma, or renal–cell cancer[89]. Recently, the overall survival outcomes for advanced melanoma patients

treated with nivolumab were reported and considered positively as compared with previous clinical studies evaluating other treatments in the same population[90]. In addition, treatment of patients with advanced cancers with an antibody targeting PD-L1 was proven to induce durable tumor regression with an objective response rate of 6 to 17%, or prolonged stabilization of disease (12-41% of patients)[91].

Therapeutic cancer vaccines are designed to immunize patients against tumor-associated antigens in order to boost the endogenous immune response. Effective vaccination requires exposition of the immune system to a cancer antigen, which can be the product of a mutated cancer gene, the product of a non-mutated gene overexpressed by cancer cells, or a differentiation antigen associated with the histological cancer type. Antigens have to be associated with immunological adjuvants in order to induce DC maturation and proficient antigen presentation to lymphocytes, ultimately resulting in the induction of an antigen-specific immune response[92]. Various approaches for therapeutic cancer vaccination have been developed, including administration of antigenic peptides or full-length proteins together with adjuvant moieties, viral vectors encoding tumour antigens, vaccine based on full tumor cells and DC-based vaccines[92]. In this latter approach, DCs are isolated from a cancer patient, loaded with antigens *ex vivo*, activated and then re-infused back into the patient. However, most of these approaches showed modest or not significant benefits in clinical trials[92]. A single therapeutic cancer vaccine received FDA approval in 2010 for the treatment of advanced prostate cancer, marketed with the name of Provenge (sipuleucel-T). Sipuleucel-T was prepared by stimulation of isolated peripheral blood mononuclear cells with a fusion protein composed of prostatic acid phosphatase (a tumor-associated differentiation antigen) and GM-CSF, followed by the reinfusion of activated mononuclear cells into the patients. Such vaccination approach resulted in a 4.1 median survival improvement in prostate patients, considered meaningful due to the peculiarity of treated population, which has advanced disease with poor treatment options[93]. Another example of successful cancer vaccine is a peptide vaccine for melanoma, consisting in gp100 peptide administer together with incomplete Freund's adjuvant and IL-2 infusion, which resulted in an higher response rate and longer progression-free survival (2.2 months) in patients with advanced melanoma as compared with patients treated with IL-2 alone[94].

## *3.2. Adoptive T cell therapy (ACT)*

Adoptive T cell therapy (ACT) consists in the infusion of *in vitro* generated cytotoxic lymphocytes (CTLs) with tumor antigen specificity. In first pivotal works on melanoma, CTLs were obtained by

*ex-vivo* selection and expansion of tumor-infiltrating lymphocytes isolated from patient tumor specimens. This approach gave considerable results in 3 sequential clinical trials on metastatic melanoma patients who failed previous treatment options. These trials reported objective response rates up to 72% and an overall 22% rate of complete tumor regression, which was in most cases durable beyond 3 years[95]. Of note, the efficacy of CTL transfer in melanoma patients was dependent on therapy combination with IL-2 administration, aimed at stimulating proliferation of transferred T cells, and preconditioning lympho-depleting or lympho-depleting/myelo-ablating regimens. Myelo-ablating total body irradiation was followed by the infusion of autologous cryo-preserved $CD34^+$ hematopoietic stem cells from a G-CSF-mobilized pheresis[95]. Combination of chemotherapy-based lympho-depletion (fludarabine plus cyclophosphamide) with total body irradiation was found to increase patient response to ACT as compared to chemotherapy alone[95]. Remarkably increased irradiation doses were found to correlate with improved immune response to ACT in cancer patients and mouse models[95,96]. Different mechanisms are thought to account for the positive impact of increasingly severe preconditioning regimens on ACT efficacy. First, the increased availability of homeostatic cytokines stimulating transferred T cell proliferation and function after depletion of competing endogenous lymphocytes. Other proposed mechanisms are the induction of tissue damage and consequent inflammation, which results in the maturation of antigen presenting cells (APCs), and the depletion of immunosuppressive cellular elements[3]. Notably, at least part of APC activation may be triggered by translocation of bacterial products into the blood following damage to the gut mucosal barrier[97]. Reduced immunosuppression following lympho/myelo-ablating regimens is currently attributed to the elimination of both Tregs and immunosuppressive cells of myeloid origin[3]. Remarkably, in mouse tumor models ACT efficacy is improved by either targeted MDSC depletion with selected chemotherapeutic drugs, in absence of T lymphocyte frequency reduction [21], or attenuation of MDSC-dependent mechanisms of immunosuppression by pharmacological inhibition of ARG1 and iNOS[40,98]. In addition, in conditional knock-out mice lacking the C/EBPβ transcription factor in the hematopoietic compartment, MDSC are poorly expanded during tumor growth and bear poor immunosuppressive functions[99]. In these mice ACT approaches show dramatically increased potency as compared to wild type mice.

The major drawback of preconditioning treatments based on chemotherapy plus total body irradiation, currently employed in clinical setting, is the potential of severe toxicity that limits therapy extension to highly selected patients with a good performance status and normal organ function[100,101]. The development of more effective and widely applicable immunotherapies,

starting from ACT based approaches, is therefore dependent on the availability of supporting treatments aimed at reducing tumor-associated immunosuppression with good efficacy and low toxicity. The search for highly selective strategies to target and neutralize immunosuppressive cells may provide a great advantage in this respect.

Even though ACT based on TIL isolation, *ex vivo* expansion and reinfusion into patients showed efficacy in different clinical trials on melanoma, translating this approach to other human cancers is challenging. Indeed, functional TILs can rarely be isolated from human tumors other than melanoma[3]. Such peculiarity is thought to arise from the lower mutational state and consequent immunogenicity of most cancer types compared to melanoma. If this is true, ACT approaches using TILs can be tailored only for a few other highly mutated cancers, as smoke-related lung cancer[3]. In order to extend ACT applicability to most human tumors, approaches to generate transgenic cytotoxic T cells have been developed in the last years. Such approaches bypass the need of having a relatively strong, naturally occurring anti-tumor T cell response in each single patient, by providing the patients with artificially designed tumor-specific T cells. A first strategy consists in the generation of T cells expressing chimeric antigen receptors (CARs) in which an antibody single-chain variable fragments is joined with TCR and T-cell costimulatory receptor domains, thus conferring non-MHC-restricted specificity for surface antigens. CARs specific for antigens overexpressed in different cancer types have been evaluated in clinical trials. However, first trials have reported treatment limiting toxicities due to strong cytotoxicity against normal tissues, also expressing the targeted antigens, and multiple cytokine release[102-104]. However, good clinical responses and acceptable toxicities have been reported in a series of clinical studies using CD19-targeting CARs for the treatment of B-cell malignancies in adult and pediatric patients[105-107].

A different possibility is to generate *ex vivo* T cells expressing transgenic TCR, which, differently from CARs, allow targeting also tumor-associated intracellular antigens through MHC-I restricted epitope presentation. Coding sequences for antigen-specific TCR can be either isolated from TILs of highly responsive patients or from T lymphocytes of transgenic mice expressing human HLA-A2, after immunization with the selected human tumor-associated antigen. This second approach offers broader applicability. However, since TCRs are generated in a mouse system, there is no thymic negative selection of TCR reactive towards all human proteins. The absence of central tolerance mechanisms may result in episodes of unintended cross-reactivity of the transgenic TCR against normal human tissue antigens[3]. Positive results using a TCR originated in a transgenic mouse system were obtained in a clinical trial targeting the cancer-testis antigen NY-ESO-1, whose expression is restricted to germ cells and certain cancer types[108]. In this trial

objective clinical response was reported in 5/11 patients with melanoma and 4/6 patients with synovial cell sarcoma, after a single infusion of transgenic T cells, plus IL-2 administration and preconditioning chemotherapy, without the onset of autoimmune toxicity.

Based on clinical studies conducted so far, ACT appears to be one of the most potent immunotherapy approaches, able to cause objective and durable clinical responses in patients refractory to standard therapies. Although most clinical successes using ACT were obtained in the treatment of melanoma, new technical advances in the generation of tumor specific cytotoxic T cells are gradually extending ACT efficacy to other cancer types. Importantly, as previously noticed, the development of effective ACT approaches is also dependent on the introduction of new strategies to modulate the immunosuppressive tumor microenveronnement in order to allow transferred T cells to expand end properly exert their function (fig. 2)

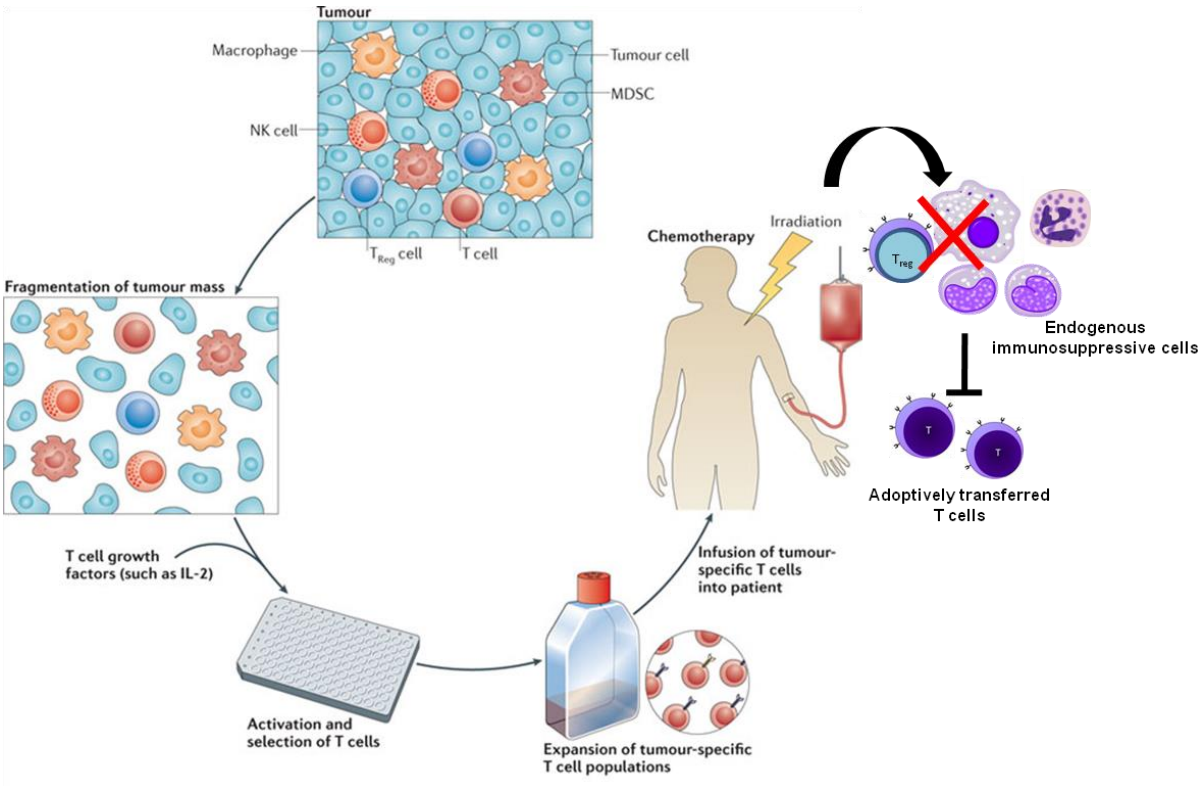


**Figure 2. Depletion of endogenous immunosuppressive cells is required for optimal efficacy of adoptive T cell transfer immunotherapy.**

Classical adoptive T cell therapy (ACT) strategy consists in the isolation of tumor-infiltrating lymphocytes from resected tumor specimens. Tumor-reactive T cells are selected and progressively expanded *in vitro*, and subsequently infused into patients. Prior to T cell infusion, patients undergo a lympho/myeloablating treatment consisting in chemotherapy (fludarabine and cyclophosphamide) plus total body irradiation. Patient preconditioning with chemo/radiotherapy increases ACT efficacy by multiple mechanisms, including depletion of immunosuppressive

cellular elements (Tregs and MDSCs) which would otherwise impair the proliferation and function of transferred T cells.
Adapted from : *Restifo et al .Nat Rev immunol 2012.*

## 4. Use of drug and RNA delivery nanosystems in oncology

The use of nano-sized platforms (nanocarriers) to deliver anticancer drugs has the potential to improve drug therapeutic index by: I) extending drug half-life by offering protection from drug degradation/metabolization and reducing renal excretion; II) increase drug accumulation into the tumor site, while preventing accumulation in most tissue; III) increase selective cell uptake. The *in vivo* behavior of nanocarrier formulations depends on multiple factors, including nanocarrier size, shape, chemical composition, and surface charge. These features influence nanocarrier biodistribution, pharmacokinetic, interaction with the immune system, internalization by target cells, and intracellular fate. Such proprieties cannot be fully predicted based on nanocarrier composition and physico-chemical characteristics, and ultimately have to be determined empirically by experimental evaluation in suitable preclinical models. However, based on all the past research work in the field of cancer nanomedicine, some general rules have been established and are currently accepted as fundamental guidelines for the design of new nanocarriers formulations (fig. 3), which are discussed below.

### *4.1. Passive targeting of the tumor site: the EPR effect*

Nanocarrier size is recognized as one of the most important parameters regulating the *in vivo* fate of delivery systems. A size greater than 2 nm prevents the extravasation of nanoparticulated materials through cell-cell adherent junctions in the endothelial walls, and a size above 8 nm excludes particle from glomerular filtration in the kidney thus reducing clearance rates[109]. Nanocarriers below 200 nm are generally considered to preferentially accumulate within the tumor site, rather than in most peripheral tissues, by the Enhanced Permeability Retention effect (EPR)[109]. The first evidences on the existence of the EPR effect was reported nearly 30 years ago[110] and since then this phenomenon has been largely investigated in mouse tumor models and used as rationale for the passive targeting of the tumor site by nanosystems. The fundamentals of the EPR model rely on the irregular and leaky nature of tumor vasculature. Tumor vessels are formed by neo-angiogenetic processes triggered as soon as the tumor grows and lacks sufficient oxygen and nutrients supply by preexistent blood vessels, which induces cell

hypoxic response, necrosis and inflammation. Hypoxia response and inflammation leads to the release of pro-angiogenic factors (including VEGF, Ang2, and Fibroblast Growth Factor) that stimulate new vessel formations[111]. Due to the unbalanced network of factors orchestrating tumor-driven angiogenesis, tumor vessels are often irregular, discontinuous, with an abnormal or missing basement membrane, and are far more leaky than normal tissue vessels. Tumor vasculature is hence highly permeable and allows the extravasation of macromolecules normally excluded by most peripheral tissues[112] Along with enhanced permeation of tumor vasculature, the EPR model presupposes the existence of an enhanced retention component, which relies on the defective lymphatic drainage of the tumor site. The intratumoral pressure cause the collapse of lymphatic vessels and the consequent absence of an efficient lymphatic drainage, especially in the center of the tumor mass. This results in the retention of essudated fluids into the tumor interstitium, from which they are slowly re-absorbed in the blood[112]. According to the EPR model, nanoparticulated material can more easily extravasate in the tumor site rather than in most normal tissues, and tend to be retained in the tumor stroma, thus favoring uptake by tumor cells rather than by normal cells.

The EPR has been broadly demonstrated in murine subcutaneous and orthotopic tumor models, but evidence of improved accumulation of nano-sized formulations in human cancers is still limited. Such limitation is in part due to the challenge in precisely evaluating biodistribution in humans, as compared to mouse models. A few studies evaluated in tumor biopsies or tumor exudates the concentration of Doxil®, a formulation of doxorubicin encapsulated into 100 nm PEGylated liposomes that has received FDA approval for the treatment of different human cancers[113]. In the first pharmacokinetic and biodistribution study on Doxil® in humans, the drug was quantified in malignant pleural effusions of cancer patients with ovarian, breast and non-small cell lung cancer. Authors reported markedly enhanced drug amounts in tumor essudates following Doxil® administration than after free doxorubicin administration, thus indicating improved delivery to the tumor site[114]. However, in a recent paper reviewing biodistribution studies on doxorubicin liposomal formulations, liposomes were found to have an enhanced accumulation in tumor tissues with respect to plasma or surrounding tissues only in sarcoma patients, while this was not true for other tumor types[115]. In addition, an improved efficacy of PEGylated liposomal doxorubicin over free doxorubicin was reported only for Kaposi's sarcoma and multiple myeloma patients, while the two formulations were equivalent on a more solid tumor as breast cancer[116-118]. Kaposi's Sarcoma and multiple myeloma represents particular cases of poorly compact, highly vascularized and leaky tumors, which are easily accessible to nanoparticulated formulations and to which the EPR effect likely applies[119]. Other human tumors

may be less permeable and highly heterogeneous (including highly and poorly perfused zones), thus limiting the access of nanocarriers to the whole tumor mass. The paucity of evidence of improved efficacy of nanoparticulated formulations over standard anticancer therapy has recently challenged the universal validity of the EPR[119]. However, although most clinical evaluations of cancer nanomedicines did not unveil an improved efficacy over standard therapies, the use of some these formulations solved important toxicological issues and was therefore introduced into the clinical practice. Notably, Doxil® showed significantly reduced cardiotoxicity as compared with free doxorubicin, due to reduced exposure of cardiac tissue to the drug[116,120]. Abraxane® (nanoparticulated albumin-bound paclitaxel) avoided the use of non-ionic solvents (such as polyethylated castor oil) included in standard paclitaxel formulations, which were associated to severe toxicities; in this way Abraxane® formulation allowed to increase maximum tolerated paclitaxel doses and clinical efficacy in metastatic breast cancer[121].

## *4.2. Mechanisms of immune recognition of nanocarriers*

When designing tumor-targeted nanomedicines, a prolonged residence time of nanocarriers in the systemic circulation is generally advantageous, since it favors the accumulation of carrier-cargo complexes in the tumor tissue[109]. Doxil® is the prototype of long-term circulating formulation, with a markedly improved pharmacokinetic profile and a far lower clearance as compared with free doxorubicin[114].

In order to increase vascular residence, the delivery nanosystem needs to be protected from renal filtration, as said above, and from excessive uptake by cells of the immune system. Once in the blood stream, nanocarriers tend to interact with serum proteins *via* various attractive forces, including hydrophobic/hyrdophylic and electrostatic bounds, resulting in the formation of a protein corona covering circulating particles, which includes immunoglobulin and complement fragments[122,123]. Nanocarriers have sizes comparable to human viruses and since they are devoid of complement regulator proteins, which normally protect mammal cells by complement activation, they tend to be recognized as non-self and to activate complement pathways[124]. IgG adsorbed on nanocarrier surface and cleaved complement proteins act as opsonins and promote particle uptake by immune cells expressing FcγR and complement receptors, including tissue macrophages and circulating monocytes and neutrophils[125].

Since first works on nanomedicines, the complement system has been shown to be activated upon interaction with nanocarrier surface through both the classical and alternative pathway[126,127]. In general, the rate of particle opsonization and clearance by the immune system

increases for highly charged particles as compared to neutral ones[128]. Notably, cationic nanocarriers strongly interact with anionic serum proteins, resulting in aggregation phenomena[129].

PEGylation, which consists in the decoration of a particle surface with covalently bound, entrapped, or adsorbed polyethylene glycol (PEG) chains, has been widely used to confer "stealth" proprieties, i.e. to mask nanocarriers from the immune system[130]. PEG is hydrophilic and neutrally charged and reduces both opsonization and non-specific binding to cell membranes by steric hindrance and shielding of charged or hydrophobic components in the formulation[123]. The long-term circulating proprieties of Doxil® are indeed attributed to the presence of PEG chains in the liposome outer layer. PEGylation however does not completely prevent particle recognition by the immune system. Reamarkably, PEGylated formulations, as Doxil®, still bear a residual ability to activate the complement system, and occasionally cause complement-related hypersensitivity reaction in patients[124]. In addition, macrophages have been shown to directly bind nanocarriers (notably liposomes) in an opsonin-independent fashion *via* scavenger receptors, including CD14, CD36 and CD51/61, even in presence of a PEG coating[128]. Jones and coworkers examined the *in vivo* clearance of fluorescently-labeled, 300 nm PEGylated nanoparticles by myeloid cells in mice with different genetic backgrounds, evaluating both the plasmatic exposure and the differential uptake by distinct immune populations[131]. BALB/C mice were found to have a faster clearance of particles from the blood, compared to C57BL/6 mice. In both mouse strains T and B lymphocytes showed a poor nanoparticle uptake, while spleen macrophages had higher levels of particle internalization as compared to most other splenic immune subsets[131]. Remarkably, the degree of particle uptake by monocytes and granulocytes was dramatically different between the two strains, since monocytes showed the strongest particle internalization in the blood of C57BL/6 mice, while granulocytes were the population with the highest particle uptake in both the blood and spleen of BALB/C mice[131]. According to this study, both mononuclear phagocytes and granulocytes are involved in particle clearance, which begins in the blood, before reaching blood filtration sites as the spleen and the liver. Interestingly, the relative importance of each immune population on nanoparticle clearance may be strain-related. These differences were explained based on the alternative bias of specific mouse strains towards a Th1-oriented (C57BL/6) or a Th2-oriented (BALB/C) immune polarization[131]. However, many of the biodistribution studies are performed in healthy mice, while pathological states may influence immune response polarization and might result in a different pattern of nanopaticle uptake by immune populations, which should be then evaluated for each specific disease model.

Features promoting particle recognition by immune cells, which are carefully avoided when designing nanosystems for the delivery of tumor-targeted drugs, becomes instead desirable when the main aim is targeting immune cells. However, in approaches aimed at targeting tumor-infiltrating myeloid cells, the use of stealth, long-circulating delivery nanosystems may also be advantageous since, as discussed so far, it promotes accumulation within the tumor site.

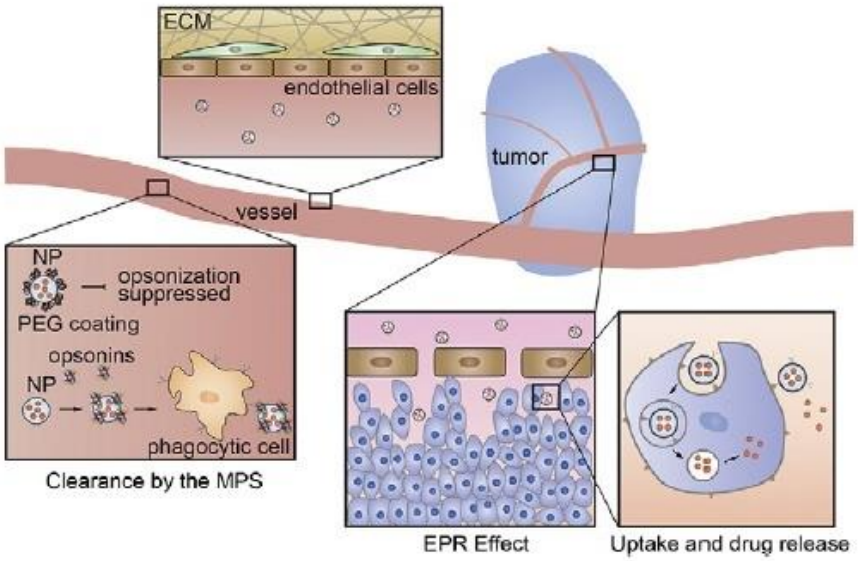


**Figure 3. Main factors affecting drug delivery to tumors by nanosystems.**
Delivery nanosystems must have a size above 8 nm to avoid both extravasation in normal tissues with tight endothelial junctions and glomerular filtration in the kidney. In addition, shielding polymers ad polyethylene glycol (PEG) can be used to minimize nanocarrier opsonization and uptake by immune cells. Reduced nanocarrier clearance by both renal excretion and immune-mediated destruction results in prolonged residence times in blood circulation. In turn, long-circulating nanocarriers accumulate more efficiently in the tumor site by the enhanced permeability and retention Effect (EPR), which relies on the higher permeability of tumors vessels with respect to most peripheral tissues. Once target tissues are reached, the drug payload may be released either in the extracellular space or upon cell uptake and carrier disruption.
From: *Dawidczyk al, . J Control Release 2014.*

## *4.3. Passive versus active tumor targeting*

Along with passive targeting approaches, nanosystems for active tumor cell targeting have been developed. Active targeting relies on the recognition of ligands overexpressed by cancer cells or tumor vessels by cognate molecules decorating nanocarrier surface, including antibodies,

antibody fragments, peptides, nucleic acid ligands and small molecules[115]. The design of actively targeted formulations presents further complexity as compared with systems for passive targeting, since multiple parameters as nanocarrier architecture, ligand conjugation chemistry and the choice of targeted ligands all contribute to determine nanosystem efficacy. This enhanced complexity is also associated to increased costs when the approach is translated from preclinical models to the clinic and ultimately to the pharmaceutical market[132]. Currently there are no FDA-approved targeted nanomedicine formulations, but a few systems are being evaluated in phase I/II clinical trials[115]. In the field of active targeting, targeting ligands expressed by multiple cancer types are generally more appealing, since the broader market potentials of these formulations compensate the costs associated to experimental evaluations. Examples of these ligands are the Transferrine Receptor and the Prostatic Membrane Antigen (PSMA)[115], the latter being expressed on prostate cancer calls and on tumor vessels of most solid tumors, but not in normal endothelium[133]. As an example, Docetaxel-loaded nanoparticles targeting PSMA were found to produce an enhanced drug accumulation into tumor tissues and more potent antitumor efficacy as compared to free docetaxel in mouse tumor models, and had a favorable pharmacokinetic profile in multiple preclinical models[134]. This nanoparticle-based formulation is currently in early phase of clinical evaluation and preliminary data indicate the presence of objective responses to the treatment[134].

Remarkably, targeting tumor cells by recognition of tumor-specific ligands, requires first particle accumulation into target tissue and hence the previously discussed proprieties, such as reduced renal and immune-mediated clearance, extended vascular residence and improved accumulation at the tumor site, are still required for both actively targeted formulations and passive targeting approaches.

Strategies for active targeting of tumor cells will not be extensively described in this context, since the primary focus of the present work will be the targeting of tumor-associated myeloid cells. However, general considerations about the challenges and cost/benefit issues of active targeting approaches presented above also apply to the targeting of myeloid cells, which is discussed in paragraph 5.

## *4.4. Challenges in therapeutic RNA delivery*

Therapeutic silencing of selected genes can be achieved by exploiting RNA interference (RNAi) mechanisms. RNAi cellular machinery operate on both RNA duplexes of exogenous origins and

endogenous RNA molecules, such as microRNAs (miRNAs). miRNAs are transcribed as long stem loop molecules termed pri-miRNAs, and processed into pre-miRNAs through a microprocessor complex involving the endonuclease Drosha. These pre-miRNAs are then exported to the cytoplasm by the exportin-5 transporter, cleaved into small RNA duplexes of approximately 22 nucleotides by the endonuclease Dicer, and ultimately loaded into the RNA-induced silencing complex (RISC). Argonaute 2, a multifunctional protein that is part of the RISC, unwinds the double strand RNA (dsRNA) and one of the strands (guide strand) is selected, while the opposite strand is degraded (passenger strand). The activated RISC complex binds to mRNAs with sequence complementarity to the guide strand resulting in target mRNA silencing by RNA endonucleolytic cleavage, translational repression or destabilization by deadenylation[135,136]. The two latter mechanisms are more common for naturally occurring miRNAs, which usually have partial complementarity to target sequences, while artificial dsRNA of exogenous origins are usually designed to be exactly complementary to target mRNAs and results in their direct cleavage. The dsRNA of exogenous origin can enter the cellular RNAi machinery at different levels: short interfering RNAs (siRNA) are dsRNA oligo of about 22 nt that can be directly loaded onto the RISC. In a similar way, artificial miRNA mimics can be introduced into cell cytoplasm and directly bind to the RISC complex. Short hairpin RNAs (shRNA) can be generated by transcription of transgenes carried by plasmids or lentiviral vectors integrated in the genome and thus undergo an analogous processing pathway to endogenous miRNA precursors. The shRNA molecules can also be chemically synthesized and transfected into cells, where they require to be processed before being loaded on RISC[136].

*In vivo* RNA delivery approaches have to overcome multiple physiological barriers. First, naked RNA tend be rapidly degraded by serum nucleases after introduction in the systemic circulations, so it needs to be protected by nuclease attack by structural modifications and/or encapsulation into delivery systems. Many RNA chemical modification are routinely used to stabilize RNA molecules, including substitution of 2' oxygen with a fluorine atom (fluorination), 2'-O-methylation, locked nucleic acids (LNA), unlockednucleic acids (UNA) and phosphorothioated backbones[137]. Some of these modifications, as 2'-O-methylation and LNA modifications, have also been reported to reduce siRNA immunogenicity *in vivo* by preventing activation of Toll-like receptors (TLR), such as TLR7[138,139]. Chemical modifications may allow facing stability and immunogenicity issues, and may be sufficient to achieve efficient *in vivo* nucleic acid delivery for certain applications. For instance, successful naked LNA delivery to hepatocytes has been shown in non-human primates models[140,141].

However, for other applications the use of RNA delivery systems may be essential to overcome further physiological barriers and achieve meaningful *in vivo* gene silencing. As anticancer drugs, also naked nucleic acids are smaller that the renal filtration limit and are hence rapidly cleared from the blood circulation[142]. Moreover, anticancer RNAi therapeutics, as anticancer drugs, require accumulation into the tumor site by passive or active targeting approaches. To extend blood circulation half-life and consequently accumulation into the tumor site, particle PEGylation is largely exploited for RNA nanocarriers, as for drug delivery systems (see paragraph 4.2 ).

Naked RNA molecules does not readily cross the cell membrane, due to their size and negative charge, and delivery systems can improve cell internalization of RNA molecule. Moreover, since internalization mostly occurs by endocytic mechanisms, delivery vehicles have also to promote RNA escape from the endosomal compartments, in order to avoid its premature degradation[137]. Cationic delivery systems, including cationic lipid nanoparticles and cationic polymers, are particularly suitable to this purpose since they electrostatically interact with the negatively charged cell surface and promote membrane wrapping and cell internalization. Moreover, they have been reported to induce endosomal escape by destabilizing phospholipid layers of the endosomal membranes or by a "proton sponge effect"[123]. This latter effect consists in the buffering the endosomal lumen during endosomal acidification process, which results in an increased ionic concentration, endosome swelling and rupture. In addition, delivery systems may be specifically designed to respond to endosomal acidification by becoming membrane-disruptive, for instance by taking advantage of pH-responsive disruption of PEG shells[143]. However, mechanisms of endosomal escape of delivery nanosystems are still not fully understood, and for many systems the effective RNA release into the cytoplasm remains to be empirically determined.

Several RNAi-based therapeutic have been evaluated in clinical trials for the treatment of various diseases, including cancer[137]. Such therapeutics are based on different delivery vehicles, including cationic polymers (as cyclodextrin and polyethyleneimine-PEI), liposomes and other lipid nanoparticles, and siRNA-polymer conjugates[137,142].

An example of effective RNA delivery systems used in cancer therapy is the ALN–VSP drug, developed at the Alnylam Pharmaceuticals and currently under clinical evaluation. ALN-VSP consists in lipid nanoparticle encapsulating two different siRNA, targeting VEGF and kinesin spindle protein (KSP). ALN-VSP particle contains ionizable lipids, which acquire positive charge at acidic endosomal pH (thus favoring interaction with endosomal membranes and endosomal escape) and also include PEGylated lipids, in order to minimize immune recognition and increase vascular residence[137,144]. siRNAs encapsulated in ALN-VPS include O'2-methylated bases, to

improve nuclease stability and reduce immunogenicity[144]. Moreover, these particles have a size between 80 and 100 nm, which favors accumulation in organs with large endothelial fenestration as spleen and liver, and permeable tumor tissues[144]. ALN-VSP was preclinically evaluated in a mouse liver tumor model, where effective down-regulation of target genes by RNAi mechanism was demonstrated. Moreover pharmacologic effects of VEGF and KSP inhibition was reported, which consisted in a reduced tumor vasculature and block of cell mitosis, respectively, and an overall improvement of mice survival[144]. A clinical evaluation in patients bearing different cancer types with liver involvement, showed antitumor efficacy in both hepatic and extraepatic sites after repeated drug administration, including one complete response. In addition, effective cleavage of target mRNA in tumor biopsies was reported, and drug administration had favorable toxicological profile, thus supporting the further investigation of this drug in clinical setting[144].

Nucleic acid delivery systems specifically aimed at targeting myeloid cell for cancer immunomodulation and immunotherapy will be discussed in the following sections.

## 5. Targeting immunosuppressive and tumor-promoting myeloid cells using nanocarriers

Nanocarriers are known to be easily opsonized and uptaken by myeloid cells in the circulation and in blood filtration organs (spleen and liver) primarily by non-specific binding of circulating IgG and complement activation, as discussed in detail in paragraph 4.2. Thus, myeloid cells can be targeted using delivery nanosystems without the need of functionalization with actively targeting molecules, although this latter approach may increase the degree of uptake by selected cell populations as compared with other cells, as discussed below. Myeloid cell targeting approaches with applications in cancer immunotherapy include DC-targeted vaccines and drug or RNAi-based therapeutics to deplete or functionally modulate immunosuppressive and tumor-promoting cells, as MDSCs ant tumor macrophages.

The use of nanoparticulated vaccines as compared with protein/peptide-based vaccines has the avantage of I) increasing antigen uptake by DCs, by exploiting the size and pathogen-like appearance of nanosystems that favor their internalization by myeloid cells; II) prolong antigen release *in vivo*; III) simultaneously deliver antigens and adjuvant moieties, as TLR ligands[145]. Nanotechnology-based cancer vaccination approaches will not be extensively discussed here, since the development of new cancer vaccines is not among the purposes of this work. Next sections will review a series of studies on either drug or RNA delivery nanosystems aimed at

targeting MDSCs and TAMs, and present some possible future approaches for the development of MDSC- and TAM-targeted nanomedicines. In addition, also nanosystems developed to target monocytes and neutrophils in acute and chronic inflammation models, which could be translated to MDSC-targeting in cancer, will be discussed.

## *5.1. Targeting monocytes and neutrophils*

A few works have reported a partially selective targeting of inflammatory (Ly6C$^{high}$) monocytes by different nanocarrier formulations in mouse models of inflammatory diseases. It is worth to note that M-MDSCs expanded in mouse tumor models bear phenotypic and morphologic similarities with Ly6C$^{high}$ inflammatory monocytes[10]. A current view is that M-MDSCs actually represents, at least in part, a pathological functional state of inflammatory monocytes, which acquire tumor-induced immunosuppressive functions. Similarly, PMN-MDSC may represent an altered functional state of normal granulocytes, as further discussed in paragraph 1. Therefore, strategies developed to target inflammatory monocytes or neutrophils in model of acute and chronic inflammation are also likely to found application in M-MDSC and PMN-MDSC targeting in tumor models.

Leushener et al. reported a 70-80 nm PEGylated lipid nanoparticle with a preferential internalization by Ly6C$^{high}$ inflammatory monocytes, although also other myeloid subsets in blood and lymphoid organs (including Ly6C$^{low}$ non-inflammatory monocytes, granulocytes, DCs and macrophages) showed particle uptake[146]. Such delivery system had been selected among several other prototypes based on its strong ability to deliver siRNA molecules, following a high throughput *in vitro* and *in vivo* screening procedure[147]. In the work by Leushner et al. this optimized RNA delivery system was employed to deliver a siRNA specific for the CC-chemokine receptor type 2 (CCR2), which mediates Ly6C$^{high}$ monocyte recruitment to inflammation sites[146] Of note, this signaling axis is likely involved also in the recruitment of human CD14$^{+}$CD16$^{-}$ monocytes, which share phenotypic features and homing potential with mouse Ly6C$^{high}$ inflammatory monocytes[148]. CCR2-specific siRNA delivery resulted in the successful down-regulation of the target gene in Ly6C$^{high}$ monocytes, reduced mobilization and recruitment of these cells, and attenuation of pathological symptoms in multiple disease models in which the intense and prolonged monocyte activation has a pathologic impact[146]. Notably, reduced inflammatory monocyte recruitment resulted in an attenuation of myocardial ischemia-reperfusion injury in a mouse model of myocardial infarction, reduced plaque size in an atherosclerosis model, and improved the acceptance of pancreatic islets allograft in diabetic

mice. In mice bearing EL4 subcutaneous lymphomas, prolonged siRNA administration, started as soon as tumors were palpable, resulted in the reduction of monocyte-derived tumor macrophages and delayed tumor growth[146]. More recently, another work reported a different drug delivery nanosystem formulated from poly(lactic-co-glycolic) acid (PLGA) polymer with a size around 200 nm, which was uptaken by circulating and spleen monocytes with higher efficiency as compared with neutrophils[149]. Such system was employed to deliver the statin drug pitavastatin to inflammatory monocytes, resulting in reduced MCP-1 (CCR2 ligand) expression and macrophage infiltration in atherosclerotic plaques, smaller plaque size, and decreased incidence of plaque destabilization and rupture in a mouse model of atherosclerosis[149].

Small (30 nm) PEGylated nanoparticles injected intradermally were reported to efficiently travel through the lymphatics, reach systemic blood circulation, and accumulate in monocytes in blood and multiple organs[150]. Macrophages were the secondly most targeted population, while other immune cells including T and B lymphocytes, granulocytes and DC subsets had comparatively less particle internalization, except for isolated populations residing in specific sites. The same particles, when administered to mice bearing subcutaneous lymphomas, showed propensity to accumulate in M-MDSCs in both the tumor and lymphoid organs[150]. This observation further supports the concept discussed above, that nanocarriers with preferential uptake by monocytes are also likely suitable to target M-MDSCs in tumor models.

Although most efforts to selectively target myeloid cells have been done using nanocarriers with enhanced uptake by DCs or monocyte/macrophages, also nanocarrier with granulocyte-targeting proprieties have been reported. 300 nm PEGylated nanoparticles with cylindrical shape were found to strongly accumulate in blood and spleen granulocytes in healthy BALB/c mice, while in mice with a different genetic background (C57BL/6) the same particles were mostly uptaken by monocytes and macrophages[131](this work is discussed more extensively in paragraph 4.2). A recent work by Wang et al. described the use of albumin-based 100 nm nanoparticles to target activated neutrophils adhering to vessels walls at sites of local TNF-α-induced inflammation[151,152]. In this model either non-activated circulating neutrophils or activated monocytes adhering to inflamed vessels showed minimal nanoparticle internalization. Nanoparticles loaded with piceatannol, a pharmacologic inhibitor of Syk (a kinase involved in regulation of neutrophil adhesion and migration), reduced neutrophil infiltration in lungs in a model of LPS-induced acute lung injury, and showed better efficacy as compared to the free drug[152]. Particle uptake was shown to be partially dependent on Fcγ-RIII expression on activated neutrophils[152]. According to this work, neutrophil ability to uptake opsonized nanoparticles may

be dependent on Fcγ receptor upregulation upon inflammatory stimuli, while steady-state neutrophils have reduced ability to recognize and internalize circulating particles.

## *5.2. Targeting MDSCs*

Along with nanocarriers targeting monocytes and neutrophils in healthy mice or non-tumor disease models, specific nanotechnology-based MDSC targeting strategies have been developed and evaluated in tumor models.

M-MDSC apoptosis was induced using RNA aptamers specifically blocking the IL-4 receptor α (IL-4Rα/CD124)[153]. IL4Rα-targeting aptamers preferentially bound to M-MDSCs and TAMs in mouse tumors and to M-MDSCs in the spleen[153], which bear an higher expression of the targeted receptor as compared to granuloytic cells[25]. Cytokine binding to the IL-4Rα mediates STAT6 activation, resulting in the upregulation of ARG-1 and increased immunosuppressive functions of MDSCs and TAMs[10]. The IL-4/STAT6 pathways seems to mediate also pro-survival signals in MDSCs, since its inhibition by IL-4Rα blocking aptamers caused increased MDSC apoptosis. Of note, MDSC and TAM targeting by IL4Rα-blocking aptamers was associated to an increased number of tumor-infiltrating T cells and a delayed tumor growth in a 4T1 mammary carcinoma model[153].

A nanoparticulated adjuvant containing gangliosides and bacterial components, termed very small size proteoliposomes (VSSPs)[154], was found to induce MDSCs maturation in mouse tumor models[155]. Notably, the use of VSSPs was shown both to modulate the phenotype of splenic MDSCs and reduce their ability to suppress T cytotoxic cell activation[155].

Together with already reported MDSC-targeting nanosystems, many other nanotechnology-based approaches can be envisaged, based on the encapsulation of different drugs that have been proved to deplete or functionally modulate MDSCs. Indeed, using nanocarriers to increase drug delivery to immunosuppressive myeloid cells may allow reaching immunomodulatory effects with higher selectivity, enhanced potency, and lower off-target toxicity.

Among candidate drugs, some chemotherapeutic drugs have a known activity on MDSCs at very low doses, even in absence of a directed tumor cytotoxicity; the list includes sunitinib, sorafenib, bortezomib, gemcitabine, fludarabine, 5-fluorouracyl[21,156] and docetaxel[157]. In addition, trabectedin, a drug recently approved for cancer treatment, was shown to induce a selective monocyte/macrophage apoptosis in multiple mouse tumor models and in sarcoma patients, including mouse splenic M-MDSCs[53].

A different drug candidate is the *all-trans*-retinoic acid (ATRA), a derivative of vitamin A, which is currently primarily employed in the treatment of acute myeloid leukemia. This drug has long been known to promote the differentiation of MDSCs into mature DCs, macrophages and granulocytes[158]. Strikingly, in a pilot study on metastatic renal cell carcinoma, patients having high plasma levels of ATRA after oral administration reported a decrease in circulating immature myeloid cells as compared to pre-treatment values[159]. In the same patients, circulating mononuclear cells displayed an improved ability to stimulate T cell activation *in vitro*[159]. However, ATRA administration present pharmacological issues. Notably, treatment with ATRA results in a substantial drop in plasmatic drug levels following chronic administration, due to multiple factors including induced drug enzymatic hyper catabolism and decreased intestinal absorption[160]. Liposomal and polymeric micelle formulations of ATRA, administered intravenously, were shown to maintain higher ATRA plasma levels as compared with oral or intravenous administration of the free drug[161,162]. ATRA delivery nanosystems may thus be appealing both as therapeutics for the treatment of acute myeloid leukemia and immunomodulating agents to target MDSCs in solid tumors.

In addition, the relief of MDSC-mediated immunosuppression has been achieved in preclinical models by employing drugs that exert a double inhibitory effect on iNOS and ARG1, such as phosphodiesterase-5(PDE5) inhibitors[98], nitroaspirin[163] and AT38[40]. Sildenafil, a PDE5 inhibitor, was reported to reduce iNOS and ARG1 expression, although the pharmacological mechanism of inhibition was not deeply investigated[98]. In mouse model, Sildenafil reduced tumor-induce immunosuppression and potentiated the efficacy of ACT treatments[98].

Nitroaspirin is a modified aspirin molecule, covalently linked to a NO-releasing group. Mechanistically, nitroaspirine activity on MDSCs involves both the NO-donor group and the salicylic portion of the drug. The NO release exerts a negative feedback inhibition on both iNOS activity and expression, while the acetylsalicylic acid is thought to interfere with the signaling pathways that induce ARG1 upregulation[163]. Remarkably, nitroaspirin was shown to act synergistically with anti-cancer vaccination approaches, resulting in an extended mouse survival[163].

AT38 was developed by introducing chemical modifications in the nitroaspirin molecule in order to enhance its pharmacological activity on MDSCs[40]. AT38 administration to tumor-bearing mice strongly reduced the production of peroxynitrite in tumors, thus reducing the nitration status of CCL2 and favoring T cytotoxic lymphocyte recruitment by this chemokine[40]. The use of nanocarriers to enhance the accumulation of these drugs in tumors and promote their uptake by MDSCs might allow to further improve treatment efficacy.

## *5.3. Targeting TAMs*

Liposomes have long been employed as delivery vehicles to target macrophages. General interactions between delivery nanosystems and macrophages, as well with other immune cells, have been described in detail in paragraph 4.2. In addition, liposome composition and surface charge may specifically influence particle uptake by macrophages. Notably, the presence of negatively charged phospholipids as phosphatidylserine and phosphatidylglycerol is known to enhance liposome internalization by macrophages, as compared with neutral liposomes, at least in part by engagement of scavenger receptors on macrophage membrane[164].

Liposomes loaded with bisphosphonates, as clodronate, have been used to deplete macrophages since the end of the 80's, by exploiting the preferential uptake of liposomes by these cells[165]. Remarkably, TAM depletion by clodronate-loaded liposomes was repeatedly shown to exert antitumor effects by reducing tumor growth, angiogenesis and metastatization in murine cancer models[166-170].

Although macrophages are naturally prone to bind and internalize liposomes and other nanocarriers, the use of active targeting strategies may allow achieving a more potent and specific macrophage targeting. Nanocarrier mannosilation, i.e. surface decoration with mannoside groups recognized by the mannose receptor (MR, CD206), was reported to improve macrophage targeting, both *in vitro* and *in vivo*[164]. MR ligands are particularly suitable for TAM targeting, since this receptor is overexpressed by M2-like TAMs as compared with M1 macrophages[61] (see paragraph 2). Mannosylated nanoparticles equipped with an acid-sensitive PEG shell were reported to preferential target TAMs, with reduced accumulation in liver and spleen[171]. In this system, PEG-sensitive molecules were spontaneously hydrolyzed in the acidic tumor microenvironment, thus exposing the MR targeting ligands[171].

A single domain antibody derived from heavy-chain antibodies found in Camelids (termed "nanobody") with MR specificity, was generated by Mohavedi and coworkers[172]. This nanobody was found to accumulate in subcutaneous mouse tumor model, through specific binding on MR expressed on stromal cells, mainly consisting of TAMs[172]. The MR-specific nanobody was successfully employed to image TAMs *in vivo*[172] and might be used to functionalize drug or nucleic acid delivery nanosystem to enhance TAM targeting.

A second receptor overexpressed on M2-like TAMs is the hemoglobin scavenger receptor (CD163)[61]. Surface functionalization of liposomes with anti-CD163 antibodies was shown to increase the efficacy of macrophage targeting *in vitro*[173], although *in vivo* efficacy was not evaluated.

Porous silicon nanoparticles decorated with anti-Ly6C antibodies were used to target Ly6C expressing cells in ortothotopic pancreatic cancer xenografts in mice, including endothelial cells and monocyte/macrophages[174]. *In vivo,* fluorescently labeled Ly6C-targeting particles exhibited preferential intra-tumor accumulation with respect to other organs, and co-localized with target stromal cells[174].

TAMs were also targeted using nanoparticle encapsulating hydrazinocurcumin (HC), a synthetic analog of the polyphenol compound curcumin, which exert an inhibitory activity on STAT3 phosphorilation[175]. HC-nanoparticles were found to be able to re-educate M2-like macrophage towards a M1-like phenotype *in vitro*. Moreover, treatment of mice bearing 4T1 mammary carcinoma with these particles resulted in the reduction of tumor growth, angiogenesis and lung metastasis formation, possibly due to a double inhibitory effect on STAT3-dependent pro-tumor pathways in cancer cells and STAT3-mediated M2 polarization in TAMs[175].

Besides molecules already reported to be coupled with nanocarriers, also other active targeting strategies may be envisaged based on recently described peptides and antibodies with macrophage specificity. A M2macrophage-targeting peptide, named M2pep, was identified to bind preferentially to M2-like macrophages rather than M1-like macrophages and DCs *in vitro* and target TAMs, but not liver and spleen macrophages *in vivo*[176].

Remarkably, an anti CSF-1R antibody was recently developed and pre-clinically and clinically evaluated as anticancer therapeutic agent[177]. Such antibody binds to the CSF-1R (CD115) that is a key regulator of macrophage survival, differentiation and migration[178]. Blocking the CSFR-1 receptor by antagonist antibodies, with mouse or human specificity, strongly reduced tumor-infiltrating macrophages in mouse tumor models and in human tumors of different histological types[177]. The use of these antibodies might also be extended to the functionalization of macrophage-directed nanosystems, possibly allowing potentiating the effects obtained by the anti CSF-1R antibody alone.

In addition to all the reported TAM-directed strategies, it must be pointed out that therapeutic approaches aimed at killing monocytes in blood, lymphoid organs and tumor sites, or intended at preventing their mobilization and recruitment to tumors, ultimately result in a reduced TAM accumulation. Indeed, CCR2 RNAi silencing by siRNA-delivering nanoparticle, by blocking monocyte recruitment through the CCL2/CCR2 signaling axis, caused an impaired accumulation of tumor-infiltrating macrophages[146](see also paragraph 5.1). The chemotherapeutic drug trabectedin, which was reported to selectively trigger apoptosis pathways on mouse and human circulating monocytes, significantly reduced TAM frequency in both mouse tumors and human sarcoma specimens[53].

# Aim

Since the discovery of the immunosuppressive and tumor-promoting function of myeloid cells, including myeloid-derived suppressor cells (MDSCs) and tumor associated macrophages (TAMs), a number of different strategies either to eliminate or functionally modulate these cells have been investigated. Among MDSC-targeting strategies, low dose chemotherapy with selected drugs has a considerable interest due to its simplicity and the possibility of a rapid translation to the clinic. The use of biocompatible nanosystems to encapsulate and deliver chemotherapeutics to tumor cells was shown to reduce toxicity and increase drug accumulation in the tumor site. Using such nanocarriers to increase drug delivery to immunosuppressive myeloid cells, besides tumor cells, is a less explored approach, which might allow reaching immunomodulatory effects with higher selectivity, enhanced potency, and lower off-target toxicity.

In addition to cell depletion by cytotoxic drugs, it is possible to modulate tumor-conditioned myeloid cells by switching off key genes controlling either differentiation or function of these cells. The impact of such approach has been widely demonstrated using mouse knockout models. However, its translation into therapeutic strategies requires the efficient *in vivo* delivery to myeloid cells of short RNA molecules (as siRNAs, shRNAs or miRNAs) able to downregulate target gene expression by RNA interference mechanisms. The use of nanosystems for RNA delivery can be advantageous to obtain potent *in vivo* gene regulation, due to the improved stability, increased circulation times and enhanced targeting efficiency that RNA-nanocarrier complexes may provide with respect to naked RNA.

In the present work, we aimed at developing new approaches to target immunosuppressive and tumor-promoting myeloid cells in cancer, by taking advantage of nanosystems for drug and nucleic acid delivery. To this aim, we investigated the immunomodulatory effects of low dose chemotherapy with a modified gemcitabine molecule encapsulated into lipid nanocapsules. Moreover, we also exploited a nanotechnology-based tool for *in vivo* gene silencing suitable to modulate the expression of relevant target genes in myeloid cells.

This work was carried out in the framework of a project founded by the European Community grant *Euronanomed* and was based on the collaboration between our laboratory and two research groups, which were responsible for the synthesis of delivery nanosystems, namely the group of Jean Pierre Benoit (LUNAM Université , Micro et Nanomédecines Biomimétiques, *INSERM – U1066 IBS-CHU,* F-49933 Angers, France) and of Maria Josè Alonso (Dept. Pharmacy and Pharmaceutical Technology and Center for Research in Molecular Medicine and Chronic Diseases, Campus Vida, Universidad de Santiago de Compostela, Spain).

# Results

## Biodistribution, pharmacokinetic, and cell uptake of lipid nanocapsules (LNCs)

Lipid Nanocapsules (LNCs) were prepared by a patented method, originally developed in the laboratory of J.P. Benoit and based on a phase inversion temperature process[179]. These nanocapsules were composed of an oily core surrounded by a tensioactive rigid layer containing polyethylene glycol (PEG) chains, and had a size between 65 and 55 nm.

We first characterized the *in vivo* biodistribution (BD), pharmacokinetic (PK) and cell targeting proprieties of LNCs, in order to define whether this delivery system was suitable to efficiently reach target organs (spleen and tumor) and cells (MDSCs and TAMs). For tracking purposes, we initially used LNCs loaded with the fluorescent dye DiD (DiD-LNCs) without any drug cargo. DiD dye was chosen due to its amphiphilic nature, which allows the dye to be trapped in the surfactant shell of LNCs and prevents its release, unless the nanocarrier is broken down after cell uptake[180]. LNC BD and PK proprieties were characterized either after intravenous (IV) or subcutaneous (SC) injection. The SC route was considered since SC injection of nanoparticulated formulations has been associated to the formation of subcutaneous depots from which the drug is slowly absorbed in the systemic circulation, resulting in a slower clearance and a prolonged systemic exposure to low drug doses[181,182]. A small size (below 100 nm) was shown to favor nanoparticle absorption by the lymphatic drainage of the injection site, a propriety mostly exploited for the design of nanoparticulated vaccines[150,183,184]. Interestingly, small (30 nm) PEGylated nanoparticles injected intradermally were reported to travel efficiently through the lymphatics, reach systemic blood circulation, and accumulate in monocytic (M)-MDSCs in the tumor and secondary lymphoid organs[150]. Due to their small size, LNCs were thus expected to have good lymphatic absorption proprieties through the SC route.

BD and PK experiments were performed in healthy mice. LNCs loaded with the fluorescent dye DiD (free of the drug cargo) were injected either SC or IV and a semi-quantitative measurement of DiD fluorescence in plasma and explanted organs was performed. This semi-quantitative analysis allowed us to compare LNC accumulation in the same organ at sequential time points and upon either SC or IV administration route. However, due to the different photon absorption properties of each organ, a direct comparison of DiD fluorescence signal among different organs was not possible by this technique.

Upon IV administration, LNCs rapidly distributed to most organs (fig. 1A). In comparison, SC injection resulted in a weaker DiD signal at earlier time points (1-8 hours), except for lymph nodes near the injection site (axillary, cervical and brachial lymph nodes), which were likely reached by direct lymphatic drainage (fig. 1B). At later time points (24-96 hours), SC-injected LNCs had a distribution pattern similar to IV-injected LNCs, characterized by a substantial accumulation in the liver and spleen at 24-48 hours, which decreased at 96 hours, and a sustained presence in lymph nodes over time (fig. 1C and D). Of note, at 24 hours DiD fluorescence in the spleen tended to be higher after IV injection than after SC injection, while at 48 hours DiD signal in spleens was comparable after either IV or SC administration (at both time points differences between IV and SC groups were not statistically significant).

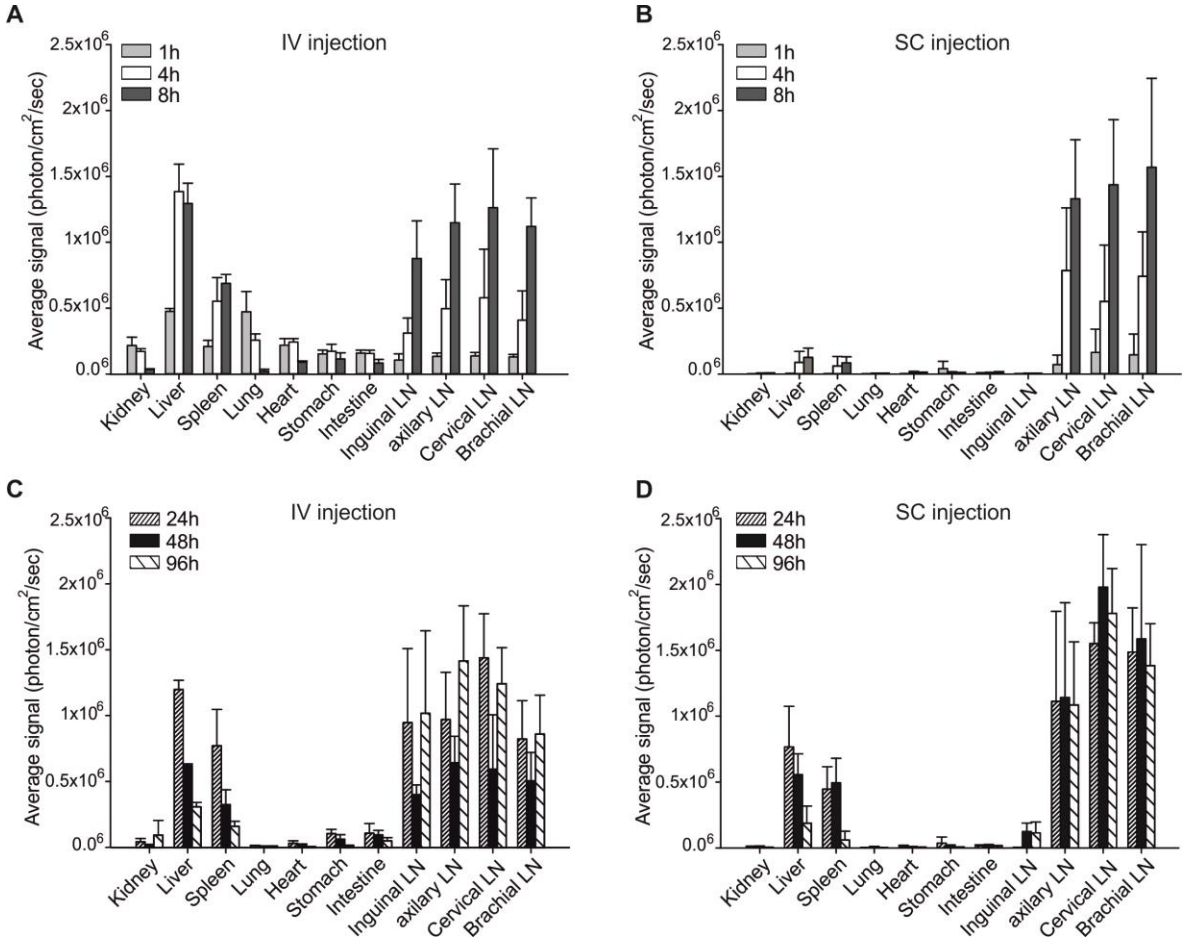


**Figure 1. Biodistribution of DiD-loaded LNCs in healthy mice**.

Healthy, nude mice were injected with DiD-loaded LNCs either intravenously (IV, panel **A** and **C**) or subcutaneously (SC, panel **B** and **D**). Average DiD fluorescence signal in explanted organs at different time points is shown. At 1h, 4h and 8h, differences in DiD fluorescence between IV and

SC groups were statistically significant for kidney, liver, spleen, lung, heart, stomach, intestine and inguinal LNs ($p<0.05$, Student's t test). At 24h, 48h and 96h, differences in DiD signal in the spleen between IV and SC groups were not statistically significant ($p>0.05$, Student's t test). Data are reported as means ± SD; n=5 mice per group.

Pharmacokinetic analysis revealed a far lower plasmatic exposure of SC-injected LNCs compared to IV-injected (fig. 2), which resulted in a lower area under the curve (AUC) associated to the SC route as compared with the IV route (10.94 µg/ml/h and 174.2 µg/ml/h, respectively). Moreover, IV-injected LNCs were cleared more rapidly from the organism than SC-injected LNCs, since calculated half-life ($t_{1/2}$ elimination) in plasma was 19 hours and 32 hours, respectively (fig. 2).

In summary, BD and PK studies showed that LNCs are slowly and probably incompletely absorbed in the blood circulation upon SC administration. The SC route is also associated with a slower clearance from the organism, possibly due to a sustained drug absorption from a subcutaneous depot over time, which compensates for LNC elimination. Importantly, SC administration avoids a high plasmatic exposure of nanocapsules and the consequent accumulation in off-target organs at early time points (1-8 hours). Moreover, despite the slow LNC absorption after SC administration, LNCs exhibited comparable accumulation levels in the spleen at 48 hours after either IV or SC injection.

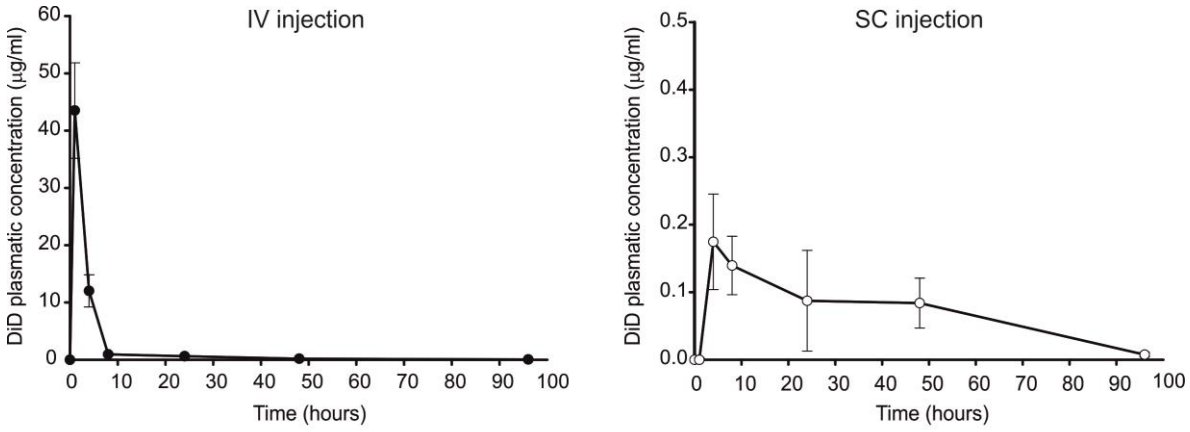


| | $T_{max}$ (h) | $C_{max}$ (µg/ml) | $t_{1/2}$ distribution (h) | $t_{1/2}$ elimination (h) | AUC (µg/ml/h) |
|---|---|---|---|---|---|
| LNC IV | - | - | 1.29 | 19 | 174.2 |
| LNC SC | 4 | 0.24 ± 0.2 | N.D | 32 | 10.94 |

**Figure 2. DiD plasmatic concentrations following injection and calculated pharmacokinetic parameters for DiD-loaded LNCs**.

Healthy, nude mice were injected with DiD-loaded LNCs either intravenously (IV) or subcutanously (SC) and blood samples were collected at sequential time points (1h, 4h, 8h, 24h, 48h, and 96h ). Data are reported as means ± SD; n=5 mice per group

In order to assess whether LNCs were able to reach the tumor site after both IV and SC injection, we injected mice bearing established, EG7-OVA subcutaneous tumors with DiD-LNCs. To assure that LNCs passed through the systemic circulation (and not just by diffusion in nearby tissues) before reaching the tumor mass, SC injection was performed on the opposite flank with respect to tumor injection site. DiD fluorescence was detected on fixed tissue sections by confocal microscopy. Figure 3 shows representative images of spleen and tumor sections and quantification of DiD mean fluorescence intensity (MFI), 24 hours after either SC or IV LNC injection. Consistently with biodistribution data on healthy mice, a stronger DiD signal was detected in the spleen upon IV injection compared to SC injection at the 24 hour time point. IV administration resulted in a more marked DiD accumulation within the tumor mass, although DiD fluorescence was detectable also after SC LNC injection. In the spleen, DiD signal was primarily detected in close proximity of vessel-like structure and in the red pulp, while lymphoid follicles were largely DiD negative.

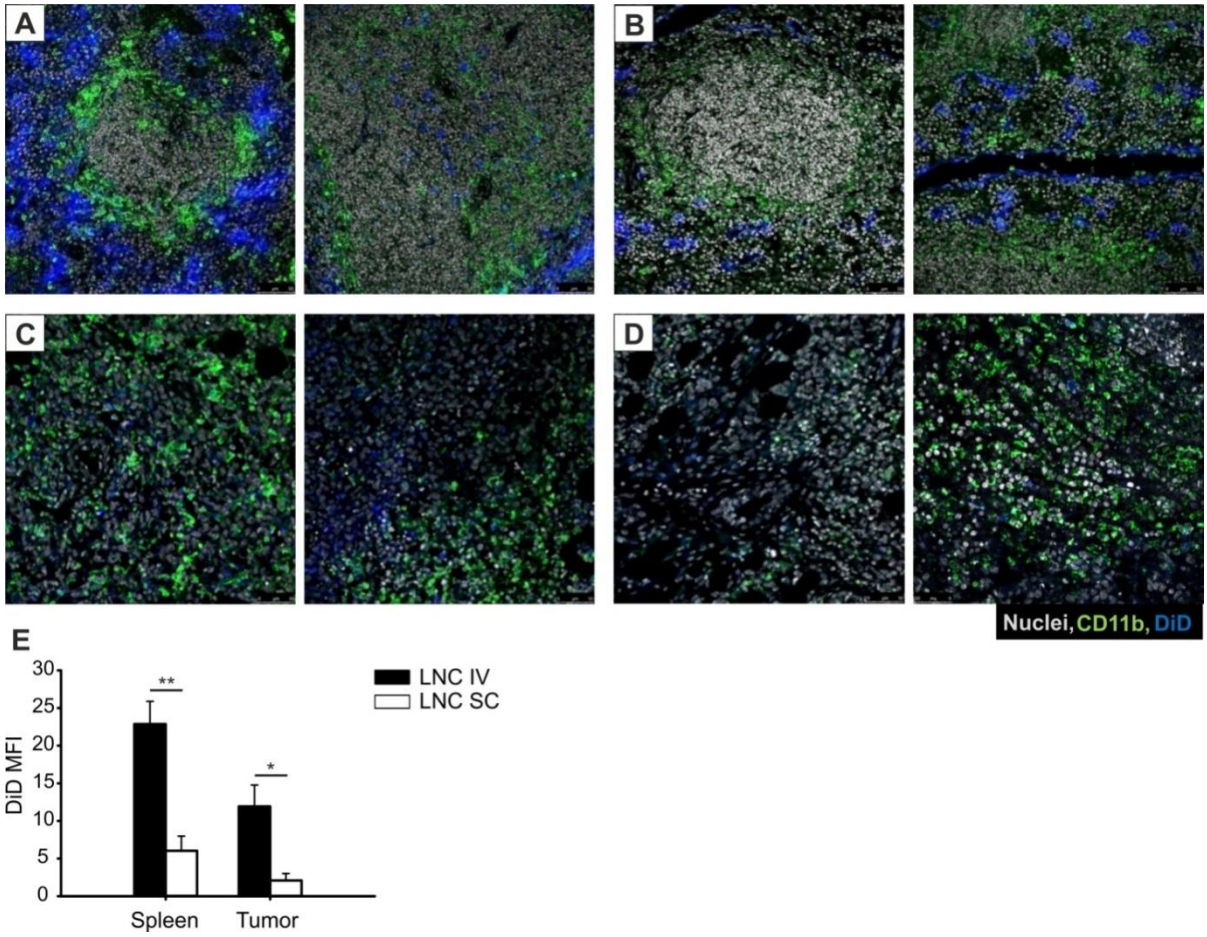


**Figure 3. Distribution of DiD-loaded LNCs in spleens and tumors of EG7-OVA tumor-bearing mice.**

**A,B,C,D.** Representative confocal microscopy images of tissue sections at 24 hours from DiD-loaded LNC (DiD-LNCs) intravenous (IV) or subcutaneous (SC) injection in C57BL/6 mice bearing ~50 $mm^2$ EG7-OVA tumors**.** SC injection was performed on the opposite flank with respect to tumor mass. Lymphoid follicles in the spleen are identified as zones with high nuclei density surrounded by $CD11b^+$ myeloid cells. Nuclei in gray (DAPI staining), CD11b in green, DiD in blue. 40x magnification **A.** Spleen after DiD-LNCs IV injection. **B.** Spleen after DiD-LNCs SC injection. **C.** Tumor after DiD-LNCs IV injection. **D.** Tumor after DiD-LNCs SC injection. **E.** Mean Fluorescence intensity (MFI) of DiD in spleens and tumor sections, calculated on a set of randomly selected field per section. Means ± SE, n= 3 mice per group. *p<0.05 **p<0.01, Student's *t*-test

We subsequently evaluated whether LNCs were differentially uptaken by distinct immune cell populations. To this aim, mice bearing EG7-OVA tumors were SC injected with DiD-LNCs and the percentage of $DiD^+$ cells within splenic and tumor-infiltrating cells was determined by flow cytometry. Myeloid cell populations in the spleen and tumors were defined as described in figure 4. The greatest LNC internalization was observed in tumor-infiltrating monocytic (M-)

MDSCs and macrophages and in splenic M-MDSCs (fig. 5A). Lower percentages of DiD$^{+}$ cells were found within polymorphonuclear/granulocytic (PMN-) MDSCs in the tumor and spleen, and F4/80$^{high}$ red-pulp macrophages and dendritic cells (DCs) in the spleen. The uptake of DiD-LNCs by T CD4$^{+}$ and T CD8$^{+}$ cells was negligible.

LNCs were not fully selective for myeloid cells, since they were also uptaken by CD11b$^{-}$ cells in the tumor, possibly including stromal cells and tumor cells (fig. 5B). However, the immune cell uptake pattern was promising and prompted us to investigate the use of LNCs as tool to target immunosuppressive monocytic/macrophagic cells in the spleen and tumor site.

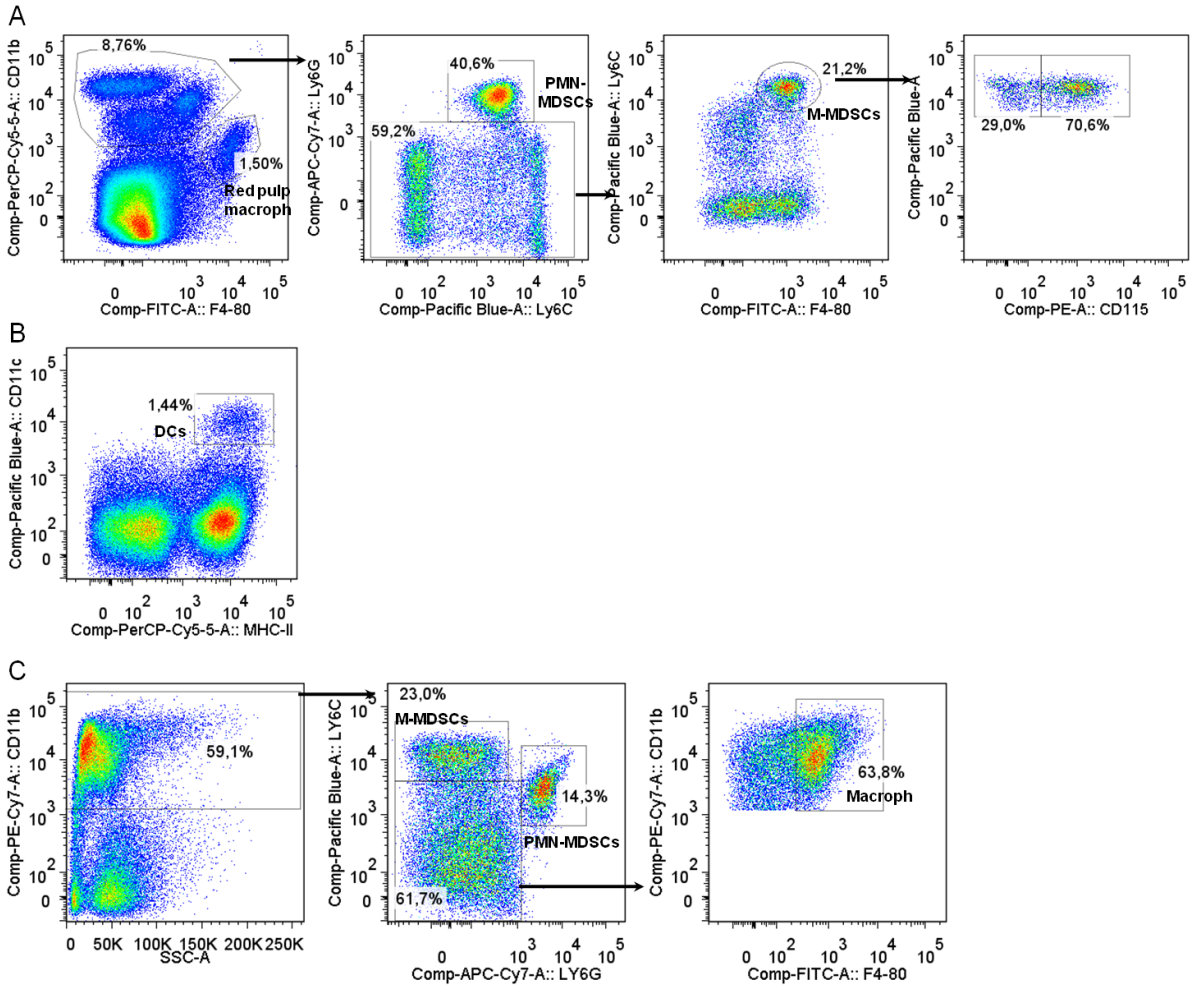


**Figure 4. Gating strategy for the identification of myeloid cell populations in the spleen and tumor.**

**A**. Dot plots showing the gating of red pulp macrophages (CD11b$^{low/neg}$ F4/80$^{high}$), polymorphonuclear/granulocytic (PMN-) MDSCs (CD11b$^{+}$Ly6G$^{+}$Ly6C$^{int}$) and monocytic (M-) MDSCs (CD11b$^{+}$Ly6G$^{-}$ Ly6C$^{high}$) in the spleen. M-MDSCs are also F4/80$^{low}$, and partially express the CD115 marker. **B.** Gating of DCs in the spleen (CD11c$^{+}$MHCII$^{+}$). **C.** Gating of PMN-MDSCs

(CD11b$^+$Ly6G$^+$Ly6C$^{int}$), M-MDSCs (CD11b$^+$Ly6G$^-$Ly6C$^{high}$) and macrophages (CD11b$^+$Ly6G$^-$ Ly6C$^{low/-}$ F4/80$^+$) in the tumor. All analysis were performed after selection of living single cells by morphologic gating, doublets exclusion and dead cell exclusion by LIVE/DEAD® dye staining. Reported dot plots refer to spleens and tumors of C57BL/6 mice bearing ~50 mm$^2$ EG7-OVA tumors.

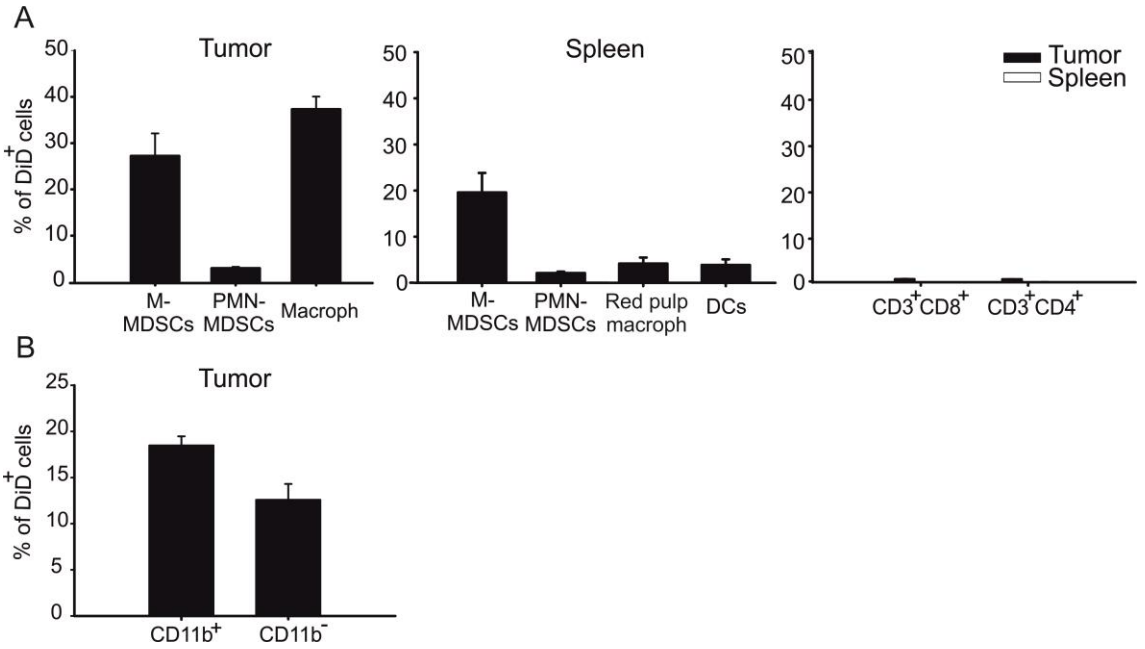


**Figure 5. Uptake of DiD-loaded LNCs by splenic and tumor-infiltrating cell populations**.
LNCs were injected SC, on the flank opposite to tumor mass, in C57BL/6 mice bearing EG7-OVA tumors; mice were sacrificed 24 hours later**. A.** Percent of DiD$^+$ cells within indicated myeloid cell populations and within T lymphocytes (CD3$^+$CD8$^+$ and CD3$^+$CD4$^+$ cells). **B.** Percent of DiD$^+$ cells within CD11b$^+$ (myeloid cells) and CD11b$^-$ cells in the tumor. Means± SE, n=4 mice.

## GemC12-loaded LNCs selectively deplete monocytic MDSCs and show improved efficacy over gemcitabine hydrochloride

LNCs were loaded with a modified form of gemcitabine, obtained by adding a single 12-carbon (C12) alkyl chain to the amine group of gemcitabine molecule. This modified gemcitabine, termed gemcitabine-C12 (GemC12), was protected from inactivation by deamination, thus improving *in vivo* stability, and had an increased lipophilicity that allowed encapsulation into LNCs[185]. Free gemcitabine hydrochloride (GemHCl) was previously reported to cause the depletion of splenic and tumor-infiltrating CD11b$^+$Gr1$^+$ myeloid cells in different mouse tumor

models, after administration of a drug dose ranging from 50 to 120 mg/kg[21,156,186-188]. We treated mice bearing established EG7-OVA tumors with a single dose of 11 mg/kg GemC12 loaded into LNCs (LNC-GemC12), a dosage at which free GemHCl was not expected to cause significant toxicity on myeloid cells. Such drug dose was chosen with the intent of disclosing the increased efficacy associated with the use of LNC-GemC12 compared to free GemHCl.

Mice were treated with 11 mg/kg LNC-GemC12, either injected IV or SC (on the flank opposite to tumor mass), or received an equal dose of GemHCl IV. LNC-GemC12 administration resulted in a substantial reduction of M-MDSC in the tumor and spleen after 24 hours from treatment. Other myeloid subsets showed no significant variations, except for a slight tendency of tumor PMN-MDSC to increase, likely compensating for the loss of M-MDSCs, and a minor decrease in DCs within the spleen (fig. 6). Unexpectedly, also GemHCl at the 11 mg/kg dose significantly depleted monocytic cells, while PMN-MDSCs and macrophages were not reduced (fig. 6). Conversely, higher gemcitabine doses are known to significantly decrease both monocytic and granulocytic MDSCs, as previously reported[21,156]. None of the given treatments resulted in a significant reduction of either splenic or tumor-infiltrating T cells ($CD3^+CD8^+$ and $CD3^+CD4^+$ cells, fig. 6). Remarkably, the strongest M-MDSC depletion was observed in mice treated with SC-injected LNC-GemC12, possibly depending on the sustained release proprieties identified for LNCs administered SC.

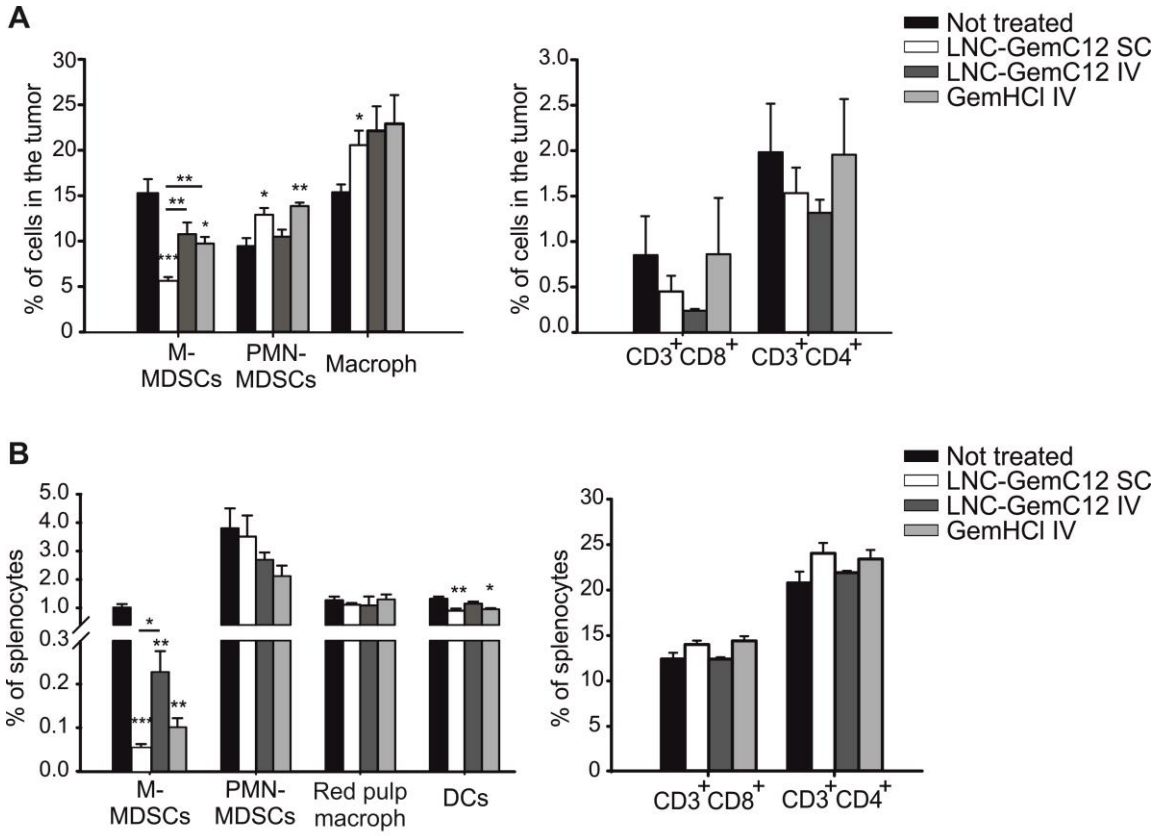


**Figure 6. Subcutaneously-administered, low dose LNC-GemC12 strongly deplete spleen and tumor-infiltrating M-MDSCs.**

Data are presented as frequency of myeloid cell subsets and T cells ($CD3^+CD8^+$ and $CD3^+CD4^+$ cells) in the tumor (**A**) and in the spleen (**B**) after 24 hours from the subcutaneous (SC) or intravenous (IV) administration of indicated treatments. Means± SE, n=4 mice per group.*p<0.05 **p<0.01, Student's *t*-test. Statistical comparisons are between each treatment group and the untreated controls, unless differently indicated.

This observation prompted us to investigate further the immunomodulatory proprieties of SC-injected LNC-GemC12. To this aim, we measured the frequency of different splenic and tumor-infiltrating myeloid cell subsets at sequential time points following administration of LNC-GemC12, GemHCl or free GemC12 solutions (11 mg/kg). To exclude biases between LNC-GemC12 and free drugs related to the administration route, all treatments were given SC, on the side opposite to tumor mass. At the time of sacrifice, tumor sizes were comparable among the different groups (fig. 7D), thus excluding the possibility of differences in myeloid cell expansion due to a delayed tumor growth following drug administration. Within the tumor site, M-MDSCs were strongly reduced at 24 and 48 hours from LNC-GemC12 administration (fig. 7A). In addition, GemC12 and GemHCl decreased M-MDSC frequency in the tumor after 24 hours from drug injection, although to a less extent as compared with LNC-GemC12. Remarkably, M-MDSCs

recovered more rapidly in GemC12 and GemHCl-treated mice than in the LNC-GemC12 group and reached comparable levels to untreated mice at the 48-hour time point (fig. 7A). In all treatment groups, normal M-MDSC frequency in the tumor was completely restored after 72 hours following drug injection. PMN-MDSCs exhibited no significant variations over the considered time points, while tumor macrophages had a slight tendency to increase at the later time points, notably in the GemHCl group (fig. 7A).

M-MDSC frequency variations in the spleen mirrored the effects observed among tumor-infiltrating M-MDSCs. At 24 hours, M-MDSCs were reduced in all treatment groups, while they faster recovered after GemC12 and GemHCl administration, as compared to the LNC-GemC12 group (fig. 7B). Interestingly, when splenic M-MDSC population was analyzed according to CD115 marker expression, the administered treatments were found to exert a greater impact on $CD115^+$ cells as compared to the $CD115^-$ fraction. At the 24 hour time point, the $CD115^+$ subset had an average 7.7, 5.2 and 5.6–fold decrease in the LNC-GemC12, GemHCl and GemC12 groups, respectively, as compared with the control untreated group (fig. 7C). At the same time point, the $CD115^-$ subset displayed a milder variation, since average fold-decreases in the same groups were 2, 2.2 and 2.4, respectively (fig. 7C). Moreover, at the 48 hours time point, mice treated with LNC-GemC12 still had a significant reduction of $CD115^+$ cells, but not of the $CD115^-$ subset. Such observation might suggest the existence of two M-MDSC subsets differing for CD115 expression, with distinct sensitivity to gemcitabine cytotoxic activity.

Only in the GemHCl group PMN-MDSCs were also significantly reduced after 24 hours from drug injection (fig. 7B), supporting the lower selectivity of free GemHCl for monocytic cells with respect to LNC-GemC12. In all treated animals, spleen PMN-MDSCs were significantly decreased at the 72 hours time point (fig. 7B). Such delayed PMN-MDSC reduction might be interpreted as a secondary effect of spleen M-MDSC depletion, since this latter population has been reported to include precursor cells with the ability to differentiate in both monocytes/macrophages and granulocytic cells[21]. However, further studies are required to demonstrate rigorously this hypothesis. T cell frequencies in both the spleen and the tumor were not decreased in all considered time points (data not shown).

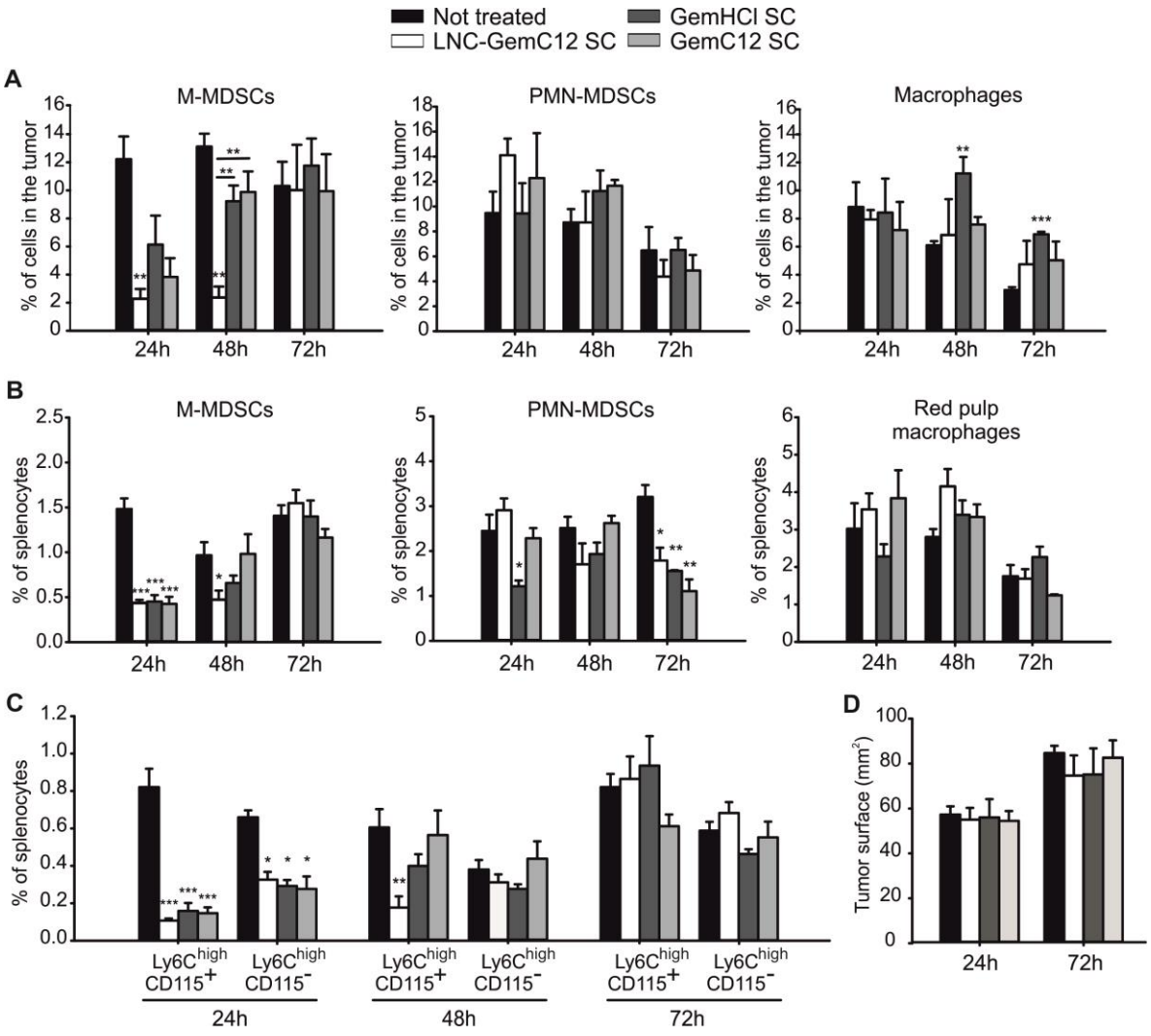


**Figure 7. Low dose LNC-GemC12 administration results in an enhanced and prolonged M-MDSC depletion**.

**A.** Frequency of M-MDSCs, PMN-MDSCs and macrophages in the tumor at 24, 48 and 72 hours from the administration of indicated treatments. **B.** Frequency of M-MDSCs, PMN-MDSCs and red pulp macrophages ($CD11b^{low/neg}$ $F480^{high}$) in the spleen at 24, 48 and 72 hours from the administration of indicated treatments. **C.** Frequency of $CD115^+$ and $CD115^-$ M-MDSC subsets in the spleen at the indicated time points. **D.** Tumor surface ($mm^2$) at the time of sacrifice.

All data are reported as means ± SE, n=4 mice per group.*p<0.05 **p<0.01 ***p<0.001, Student's *t*-test. Statistical comparison is between each treatment group and the untreated controls, unless differently indicated.

In summary, low dose GemC12 loaded into LNCs selectively depleted splenic and tumor-infiltrating monocytic cells with improved efficacy, both in terms of effect intensity and duration, as compared to gemcitabine hydrochloride. Moreover, in the experiment reported in figure 7 no substantial differences were observed between free GemC12 and GemHCl,

suggesting that the enhanced efficacy of LNC-GemC12 over GemHCl cannot be exclusively attributed to the use of a modified gemcitabine molecule, but rather to factors specifically related to the employed nanocarriers.

In mouse cancer models, both tumor-infiltrating and splenic $CD11b^+$ cells are known to exert immunosuppressive functions, which can be measured through *ex vivo* suppression assays[20,25]. Among different subsets, M-MDSCs were shown to be endowed with markedly stronger immunosuppressive abilities in comparison to PMN-MDSCs[20,22,44]. In addition, in a recent work from our group, the immunomodulatory activity of MDSC-depleting chemotherapy was found to primarily rely on the elimination of monocytic cells, while granulocytic cells played a minor role[21]. We hence reasoned that the selective depletion of monocytic cells using low dose LNC-GemC12 could result in the relief of MDSC-induced immunosuppression and be used for therapeutic purposes. To investigate these points, we first measured the immunosuppressive activity of tumor-infiltrating $CD11b^+$ cells after SC administration of 11 mg/kg LNC-GemC12 or GemHCl to EG7-OVA tumor bearing mice. Twenty four hours after drug administration, total $CD11b^+$ cells were isolated from tumor masses by immunomagnetic sorting and co-cultured with CFSE-labelled OTI splenocytes, in presence of the SIINFEKL ovalbumine antigenic peptide. The proliferation of antigen-activated T $CD8^+$ cells was measured based on CFSE dilution during cell replication. As shown in figure 8, $CD11b^+$ cells isolated from LNC-GemC12-treated mice had a reduced ability to suppress T cell proliferation as compared to control $CD11b^+$ cells isolated from untreated mice. Conversely, $CD11b^+$cells from mice that received GemHCl exerted a comparable suppressive activity to control $CD11b^+$ cells. The selective depletion of the monocytic MDSC subset by LNC-GemC12 was thus found to impair the overall immunosuppressive activity of tumor-infiltrating $CD11b^+$cells.

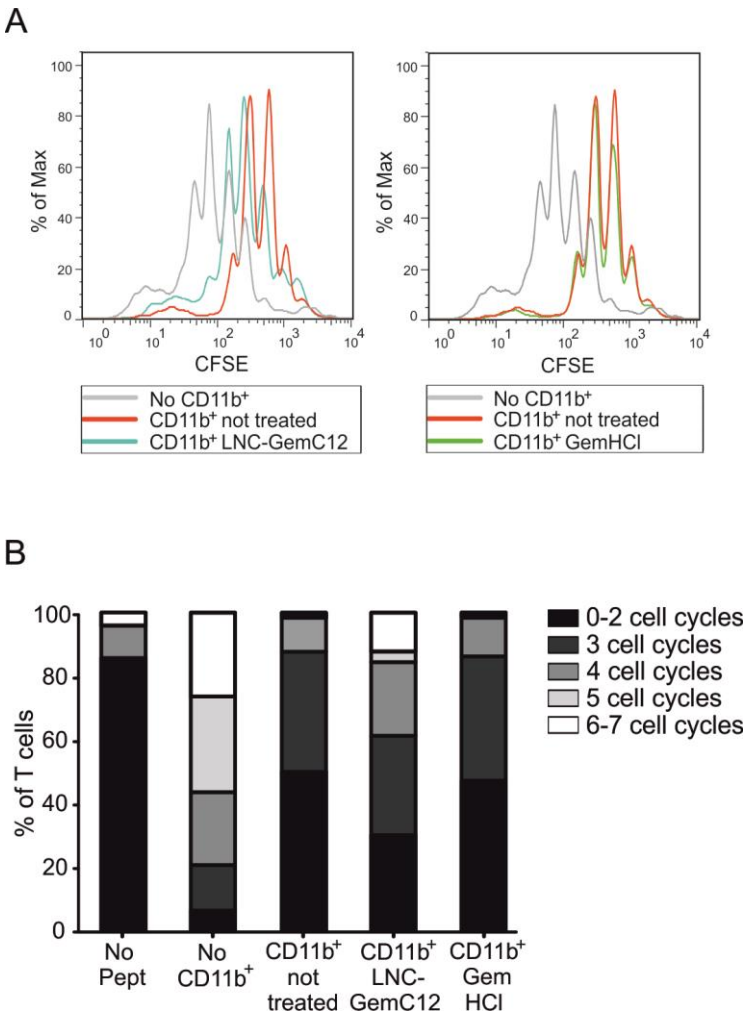


**Figure 8. Low dose LNC-GemC12 administration impairs the immunosuppressive activity of tumor-infiltrating myeloid cells.**

CD45.2$^+$ C57BL/6 mice were injected subcutaneously with either LNC-GemC12 or GemHCl when tumor surfaces reached ~50 mm$^2$, and sacrificed 24 hours later. CD45.1$^+$ OTI splenocytes were labeled with CFSE and cultured in presence of the SIINFEKL ovalbumine (OVA) peptide to induce antigen-specific activation of T CD8$^+$ cells. CD11b$^+$ myeloid cells isolated from tumor masses were added to splenocyte cultures. CFSE dilution upon T cell proliferation was measured by flow cytometry after 3 days of culture. Data for co-cultures with 24% CD11b$^+$ cells are shown

**A.** Histograms of CFSE fluorescence (% of maximum cell count *vs* fluorescence intensity) in the CD8$^+$CD45.1$^+$ gate. Control cultures without CD11b$^+$ cells (gray curve) correspond to the highest CFSE dilution, indicating maximum T cell proliferation. Other curves represent CFSE fluorescence after T cell co-culture with CD11b$^+$cells from untreated mice (red), CD11b$^+$ cells from LNC-GemC12-treated mice (blue), and CD11b$^+$ cells from GemHCl-treated mice (green). **B.** T cell proliferation is expressed as fraction of T cells that underwent the indicated number of cell cycles based on CFSE dilution. In control cell culture without OVA peptide (No pept) T cell proliferation was minimal, indicating absence of non-specific T cell activation. All other conditions refer to T cells activated in presence of their cognate peptide. The graph represents T cell proliferation in

cell cultures without $CD11b^+$ cells (No $CD11b^+$) or with $CD11b^+$ cells from not treated mice, mice treated with LNC-GemC12 or mice treated with GemHCl. Representative graph from one of two repeated experiments.

## Preconditioning with low dose LNC-GemC12 improves mouse survival following adoptive T cell therapy

The relief of tumor-induced immunosuppression is known to improve the efficacy of passive immunotherapy strategies, including the adoptive transfer of tumor-specific T cells (adoptive T cell therapy, ACT)[21,40,98], by creating a more favorable environment for T cell recruitment, proliferation and function. We hence wondered whether M-MDSC depletion by low dose LNC-GemC12 administration could be used to precondition tumor-bearing mice prior to ACT in order to enhance mouse survival.

Since LNC-GemC12-mediated M-MDSC depletion had a maximum 48h duration, we investigated whether repeated LNC administrations after T cell transfer could be used to extend the time window of attenuated immunosuppression and enhance T cell expansion upon adoptive transfer. Three different LNC administration schedules were tested in combination with ACT. The frequency of transferred T cells in lymph nodes and tumor masses and the IFNγ production upon antigen re-stimulation were evaluated as predictive parameters for therapy efficacy. ACT protocol consisted in the IV infusion of *in vitro* pre-activated T cells specifically recognizing the ovalbumin (OVA) model antigen expressed by EG7-OVA tumor cells. The frequency of overall $CD8^+CD45^+$ cells and $CD8^+CD45^+IFN\gamma^+$ cells in both lymph nodes and tumors was dramatically reduced when mice were treated with one or two LNC injection after T cells infusion (schedules II and III, fig. 9), as compared to mice receiving either ACT alone or one single LNC-GemC12 dose prior to ACT (schedule I, fig. 9). This result indicated the existence of a deleterious effect of LNC-GemC12 administration in the days immediately following T cell infusion, likely due to a direct drug cytotoxicity on transferred T cells. Conversely, following one single LNC-GemC12 injection 24 hours before ACT (schedule I, fig 9.), the frequency of overall and IFNγ-producing $CD8^+CD54.1^+$ T cells was not reduced in lymph nodes and tended to increase in tumors, as compared with control mice receiving ACT alone, although statistical significance was not reached. Of note, in mice receiving ACT alone or ACT plus single dose LNC-GemC12, tumor-infiltrating $CD8^+CD54.1^+$ T cells produced IFNγ even without re-stimulation with their cognate peptide, thus suggesting that these cells were already functionally activated *in vivo* (fig.9).

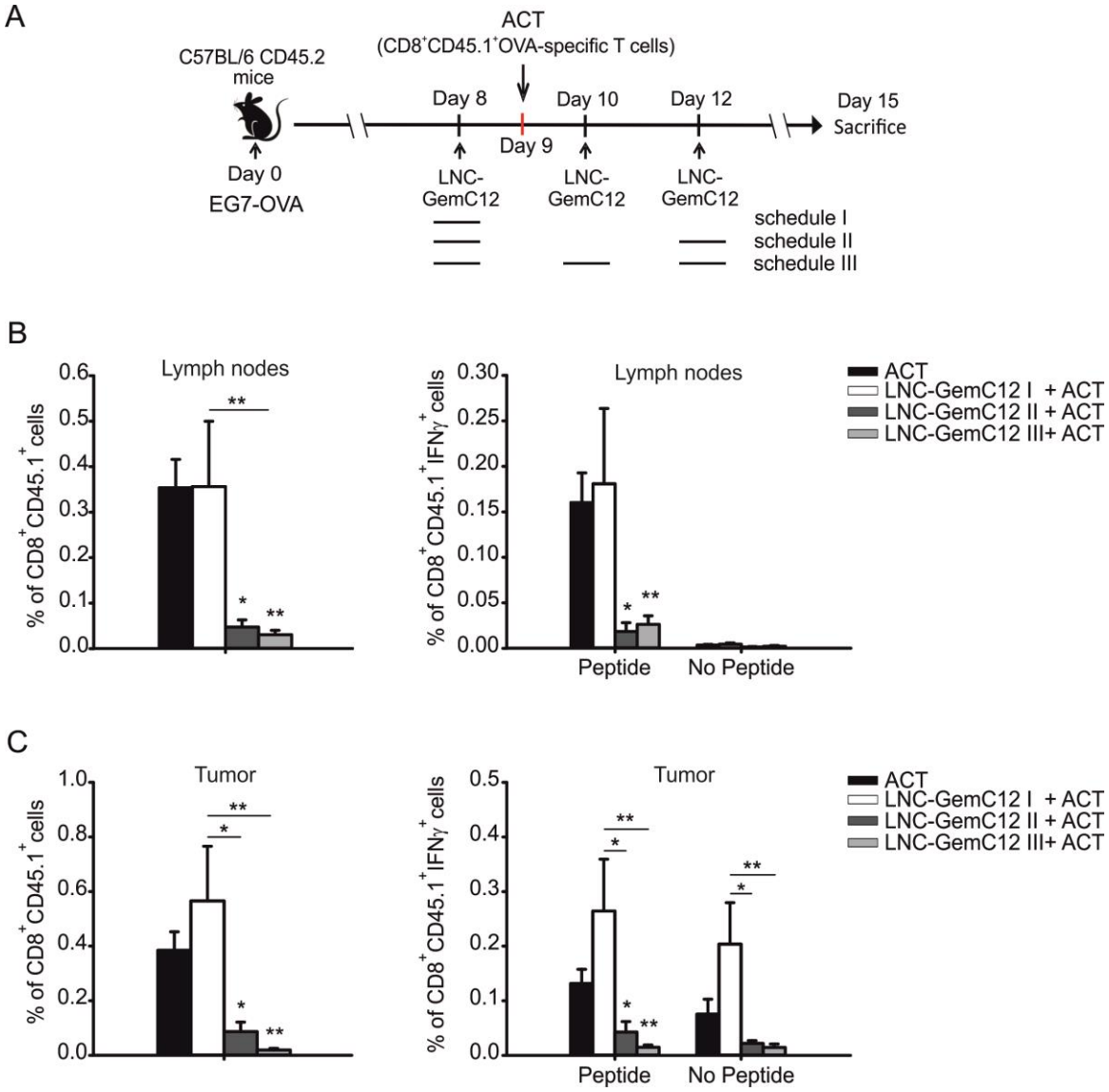


**Figure 9. Evaluation of three different schedules of LNC-GemC12 administration in combination with adoptive T cell therapy (ACT).**

**A.** LNC-GemC12 (11 mg/kg) was administered subcutaneously to CD45.2$^+$ C57BL/6 mice bearing EG7-OVA tumors, either at day 8 (schedule I), at day 8 and at day 12 (schedule II), or at day 8, 10 and 12 (schedule III) following tumor injection. ACT was given at day 9 and consisted in the intravenous infusion of pre-activated, OVA-specific CD8$^+$CD45.1$^+$ T cells. Mice were sacrificed at day 15 and cells from lymph nodes and tumors were cultured 16 hours, either in presence or absence of the specific OVA peptide, before flow cytometry staining. **B, C.** Percentage of CD8$^+$CD45.1$^+$ T cells and of CD8$^+$CD45.1$^+$ IFNγ$^+$ T cells in lymph nodes (**B**) and in tumors (**C**) after LNC-GemC12 treatment according to schedule I, II or III, plus ACT. Data are expressed as means ± SE, n=5 mice per group. *p<0.05 **p<0.01, Mann-Whitney Rank Sum Test. Statistical comparison is between each group and the control group receiving ACT alone, unless differently indicated.

Based on these data, we next evaluated the impact of a single LNC-GemC12 or GemHCl administration prior to T cell infusion on mice survival after ACT (schedule reported in fig. 10A). GemHCl was administered both SC, as LNC-GemC12, and IV, since the IV route currently represents the golden standard for GemHCl administration in clinic. As expected, ACT with pre-activated OVA-specific T cells, which have an extremely high affinity for the ovalbumin antigen, delayed tumor growth and significantly improved mice survival even without any preconditioning treatment (fig. 10B,C and D). However, combination of LNC-GemC12 with ACT resulted in a further reduction of tumor burden and extended survival as compared to mice receiving ACT alone (fig 10B, C and D). Remarkably, the survival of mice preconditioned with GemHCl, either administered SC or IV, did not significantly differ from that of control mice receiving only ACT. Interestingly, the therapeutic efficacy of combined GemHCl administration and ACT was better after SC rather than IV GemHCl administration, as indicated by the more pronounced tumor mass reduction in mice treated with GemHCl SC (fig.10B). This latter observation excludes that the improved efficacy of LNC-GemC12 over GemHCl could be due to the use of the SC route, instead of the more commonly employed IV route, for GemHCl administration.

Taken together, these results demonstrate that low dose LNC-GemC12 exert an immonumodulatory activity based on selective M-MDSC depletion, which can be exploited to attenuate tumor-induced immunosuppression and improve the efficacy of ACT. Of note, although also GemHCl administration at the same dose induced M-MDSC reduction, this treatment had a reduced potency in term of both intensity and duration of target cell depletion as compared with LNC-GemC12, and did not result in a survival improvement when used to precondition mice prior to ACT.

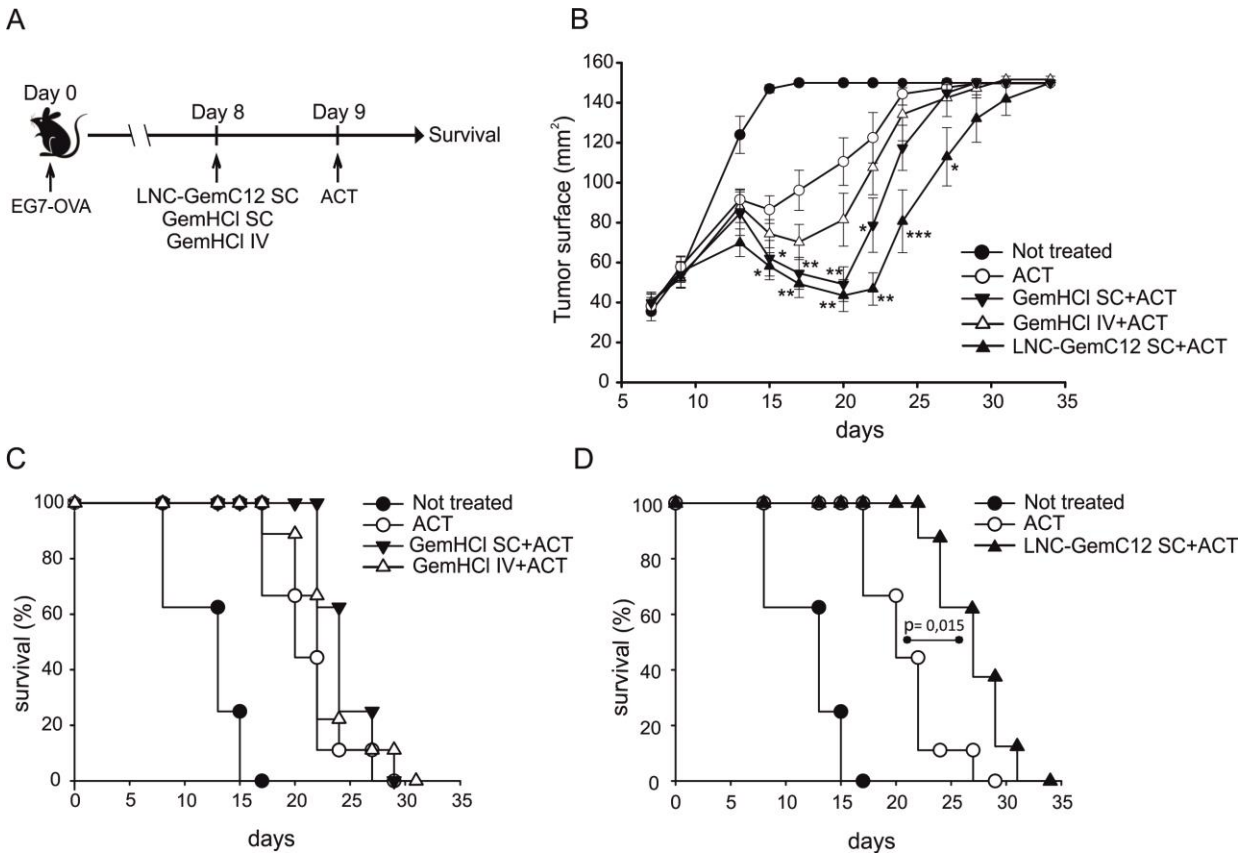


**Figure 10. Preconditioning with low dose LNC-GemC12 improves mice survival after adoptive T cell therapy (ACT).**

**A.** Therapeutic schedule: mice bearing established EG7-OVA tumors were treated either with subcutaneous (SC) LNC-GemC12, subcutaneous GemHCl or intravenous (IV) GemHCl at 11 mg/kg drug dose; 24 hours after chemotherapy, mice received an IV infusion of $0.25x10^6$ pre-activated, OVA-specific cytotoxic T cells (ACT). Tumor growth was monitored until the end-point tumor size of 150 $mm^2$, at which mice were euthanized. **B.** Tumor growth after treatment administration, expressed as tumor surface ($mm^2$) *vs* time (means± SE).n=8 mice per group. *p<0.05 **p<0.01 ***p<0.001, comparison with control group receiving ACT alone, Student's *t*-test. **C** and **D.** Overall survival curves (panel C and D refers to the same experiment). All treatments resulted in an improved survival with respect to untreated mice (p<0.001). However, only mice receiving LNC-GemC12 plus ACT had a significantly extended survival compared to mice treated with ACT alone (p= 0.015);n=8 mice per group. Statistical analysis was performed with Log-Rank test with *p*-value correction for pairwise multiple comparisons (Holm-Sidak method).

## Development of a nanosystem suitable for gene silencing in myeloid cells consisting in polyarginine nanocapsules loaded with fluorinated shRNAs

Post-transcriptional *in vivo* gene silencing based on RNA interference (RNAi) mechanisms is currently being explored for the therapy of various diseases, including cancer[137]. Naked and unmodified RNA is easily attacked by serum nucleases, rapidly cleared by renal filtration, may be immunogenic and has poor ability to cross cell membranes and reach the cytoplasm. Effective *in vivo* RNA delivery requires RNA chemical modifications and/or complexation with delivery vehicles composed of biocompatible, nontoxic materials[137]. Cationic polymers, often as component of nanocarrier formulations, are broadly used for RNA delivery since they readily bind to nucleic acids via electrostatic attractions and interact with the negatively charged glycocalyx on cell surface, thus favoring cell internalization. However, positively charged nanocarriers may also be associated with significant cytotoxicity[189] and may form aggregates in blood due to electrostatic interaction with anionic serum proteins[129].

With the intent of developing a RNA delivery system suitable to target tumor-conditioned myeloid cells, we assessed the toxicity of 4 different formulations of nanocapsules on bone marrow-derived MDSCs (BM-MDSCs). BM-MDSC differentiation was achieved through four days culture of bone marrow cells in presence of GM-CSF and IL-6 stimuli, as previously reported[99]. Nanocapsules (NCs) were added at day 0 and the ratio between viable recovered cell numbers at day 4 and plated cell numbers at day 0 was calculated as indicative parameter of NC toxicity. Formulation 1 (NC1) was a control formulation devoid of cationic polymers for nucleic acid complexation and composed of an oily core and an external hydrophilic shell of hyaluronic acid (HA). NC 2 and 3 also contained HA as one of the components and both included protamines (small, arginine-rich, proteins) as cationic polymers for nucleic acid binding. NC 2 mainly differed from NC 3 for the presence of polyethylene glycol (PEG), a widely employed biocompatible, neutrally charged polymer, as shielding component, and for the absence of succinate and sodium cholate in the formulation. NC 4 was a completely different formulation, consisting in an oily core surrounded by a surfactant layer containing PEG chains, with an outer shell of polyarginine for RNA complexation (polyarginine NCs, PolyArg NCs). As shown in figure 9, BM-MDSC differentiation in presence of NC 2 and 4 allowed a cell recovery near 100% in all the range of tested NC concentrations, while NC 1 and 3 were associated with a dramatic drop in cell recovery at higher NC concentrations.

Despite its net positive charge, NC 4 (PolyArg NCs, ζ potential +42 mV) was found to produce the lowest toxicity on BM-MDSC cultures. Moreover, PolyArg NCs did not show any tendency

towards aggregation in serum-containing media (data from M.J. Alonso laboratory, not shown). Interestingly, polyarginine is a known cell-penetrating peptide and has been reported to promote both cell internalization of delivery systems and endosomal escape[190,191]. We thus decided to investigate further PolyArg NCs as nanosystem for RNA delivery into myeloid cells.

To achieve a stronger *in vivo* gene silencing by RNAi mechanisms, we chose to load PolyArg NCs with stabilized, RNase-resistant RNA molecules, instead of conventional unmodified RNA oligos. To this aim, we set up and optimized a protocol for the *in vitro* transcription of RNase-A resistant, fluorinated short hairpin (sh)RNAs, which could be efficiently loaded onto PolyArg NCs. The workflow for fluorinated shRNA synthesis is summarized in figure 12 and further details are provided in the "Materials and methods" section. Of note, shRNA synthesis by this technique allowed to obtain consistent amounts of fluorinated RNA, suitable for *in vivo* use.

A

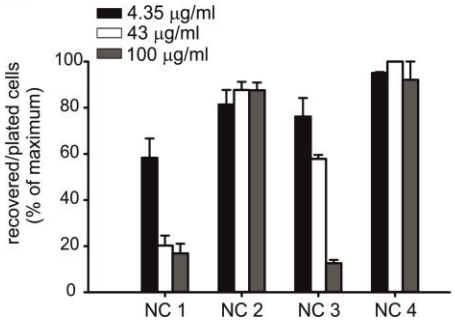


B

| | Size (nm) | ζ potential (mV) |
|---|---|---|
| NC 1 HA-nanocapsules | 130 | -36 |
| NC 2 HA-protamine nanocapsules (PEG-st) | 169 | -15 |
| NC 3 HA-protamine nanocapsules (succinate & sodium cholate) | 107 | -31 |
| NC 4 Polyarginine nanocapsules | 170 | +42 |

**Figure 11. *In vitro* cytotoxicity assessment on BM-MDSCs of nanocapsule formulations for nucleic acid delivery.**

**A**. Bone marrow cells from healthy mice were cultured for four days in presence of GM-CSF and IL-6 to induce BM-MDSC differentiation (see text and "Materials and methods" for further details). Nanocapsules were added at day 0 and the number of viable cells was determined at day 4. Data are expressed as percent ratio of recovered cell numbers at day 4 on plated cell numbers at day 0, normalized with respect to maximum cell recovery in control cell cultures without nanocapsules.
**B.** Table summarizing the tested formulations with indication of nanocapsule size and ζ potential.

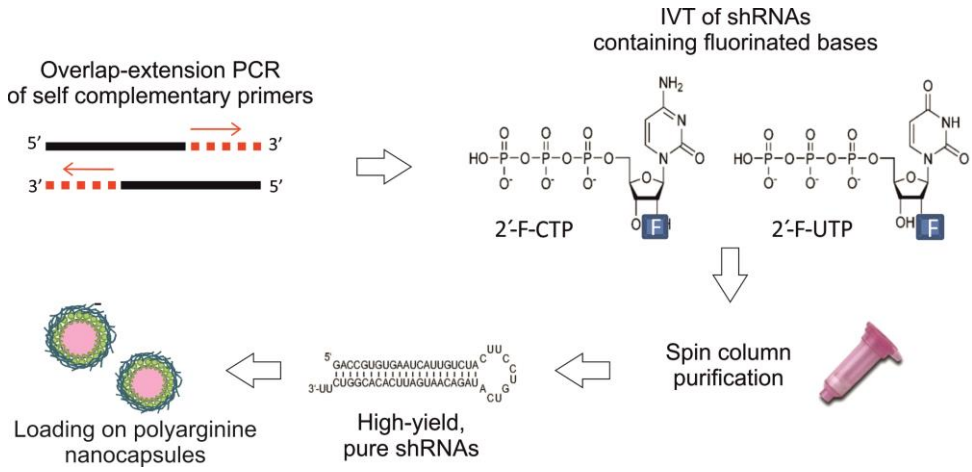


**Figure 12. Workflow for the synthesis of RNase A-resistant, fluorinated short hairpin (sh) RNAs to be loaded on PolyArg NCs.**

Specifically designed, self-annealing primers were used to obtain a dsDNA template by PCR extension. This template was then used for the *in vitro* transcription (IVT) of fluorinated shRNAs, using the Durascribe T7 transcription kit (Epicenter). The dsDNA was removed by DNAse I digestion and shRNAs were purified by spin columns and loaded onto PolyArg NCs. Further details are provided in the "Materials and methods" section.

## The shRNA-loaded polyarginine nanocapsules down-regulate C/EBPβ expression in myeloid cells *in vitro* and *in vivo*

To evaluate the efficacy of shRNA-loaded PolyArg NCs as gene silencing system, we selected a target gene with a relevant function in MDSC biology. The selected gene was the mouse CCAAT/enhancer binding protein (C/EBP)β transcription factor, which was previously shown to be required for the induction of MDSC expansion and immunosuppressive program[99.] Interestingly, C/EBPβ ablation in conditional knockout mice was reported to dramatically improve mice survival after ACT, thus supporting the relevance of C/EBPβ pathway as therapeutic target in cancer immunotherapy[99].

A shRNA with sequence complementarity to mouse C/EBPβ mRNA (shC/EBPβ) and a scrambled control shRNA (shCTRL) were designed and generated according to the protocol described in figure 12. To assess PolyArg NCs efficacy in delivering shC/EBPβ *in vitro* to myeloid cells, we trasfected an immortalized MDSC cell line (MSC1[192]) using either PolyArg NCs or a commercial trasfection reagent (Lipofectamine RNAi Max®, Invitrogen). Cells were transfected with 30 nM shRNA and harvested 24 hours later. The 30 nM shRNA concentration was chosen basing on previous titration experiments that identified this shRNA concentration as the one resulting in

the strongest sequence-specific C/EBPβ down-regulation (data not shown). As shown in figure 13, shC/EBPβ transfection with both PolyArg NCs and Lipofectamine caused a significative reduction of C/EBPβ mRNA levels.

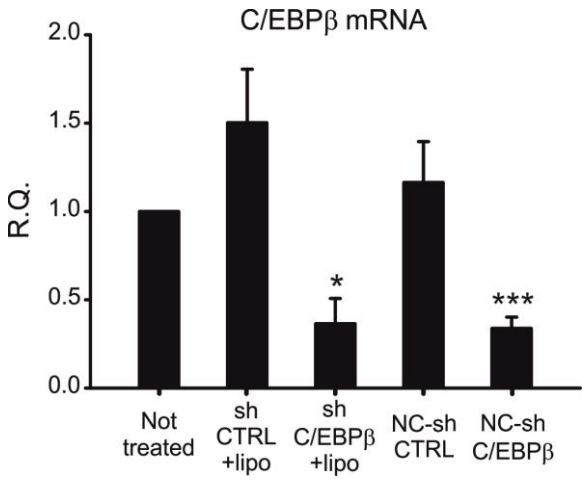


**Figure 13. PolyArg NCs loaded with C/EBPβ-targeting shRNA downregulate C/EBPβ mRNA levels in the MSC1 cell line.**

MSC1 cells were transfected with the C/EBPβ-targeting shRNA (shC/EBPβ) or a scrambled shRNA (shCTRL) either loaded on PolyArg NCs (NC-shC/EBPβ) or complexed with Lipofectamine RNAi Max® reagent (Invitrogen), and harvested 24 hours later. C/EBPβ mRNA levels were quantified by RT-qPCR and normalized with respect to an endogenous control (Rn18S). Data are expressed as relative quantification (R.Q.), normalized to non-transfected (not treated) cells. Means± SE (n=3). Statistical comparison between each group and the untreated control, *p<0.05, ***p<0.001, Student's *t*-test.

After demonstrating that shC/EBPβ-loaded NCs (NC-shC/EBPβ) were functional *in vitro,* we evaluated the *in vivo* efficacy in a mouse tumor model. The MCA203 sarcoma was selected because of the relevant C/EBPβ expression in both tumor infiltrating and splenic myeloid cells, as previously reported[99]. Mice bearing established MCA203 tumors were intravenously injected with NC-shC/EBPβ or non-loaded NCs. Treatments were started at day 11 from tumor injection when tumor surfaces were approximatively 35 $mm^2$, and repeated 3 times with 48 hours intervals (RNA dose= 20 μg/mouse/treatment, fig. 14 A). Animals were sacrificed after 48 hours from the last treatment and $CD11b^+$ myeloid cells were isolated from spleens and tumors by immunomagnetic sorting. C/EBPβ mRNA levels were significantly reduced in both splenic and tumor-infiltrating $CD11b^+$ cells in mice treated with NC-shC/EBPβ as compared to controls (fig. 14B). C/EBPβ downregulation was around 50% in splenic myeloid cells and 30% in tumor-

infiltrating myeloid cells. No evident signs of toxicity were observed during the treatment period.

To investigate whether C/EBPβ downregulation, whilst for a short time period, had an impact on tumor-associated myelopoiesis, we performed a phenotypic analysis of myeloid cell subsets in lymphoid organs (spleen and bone marrow) and at the tumor site. While our analysis revealed no differences in bone marrow and splenic myeloid populations (data not shown), a significant decrease in the frequency of tumor-associated macrophages was observed in the NC-shC/EBPβ group compared to controls (fig. 14 C). Such macrophage reduction was paralleled by a significant increase in monocytic cells (phenotypically definable as M-MDSCs), thus suggesting that C/EBPβ downregulation by RNAi might result in a partial impairment of monocyte differentiation into tumor-associated macrophages.

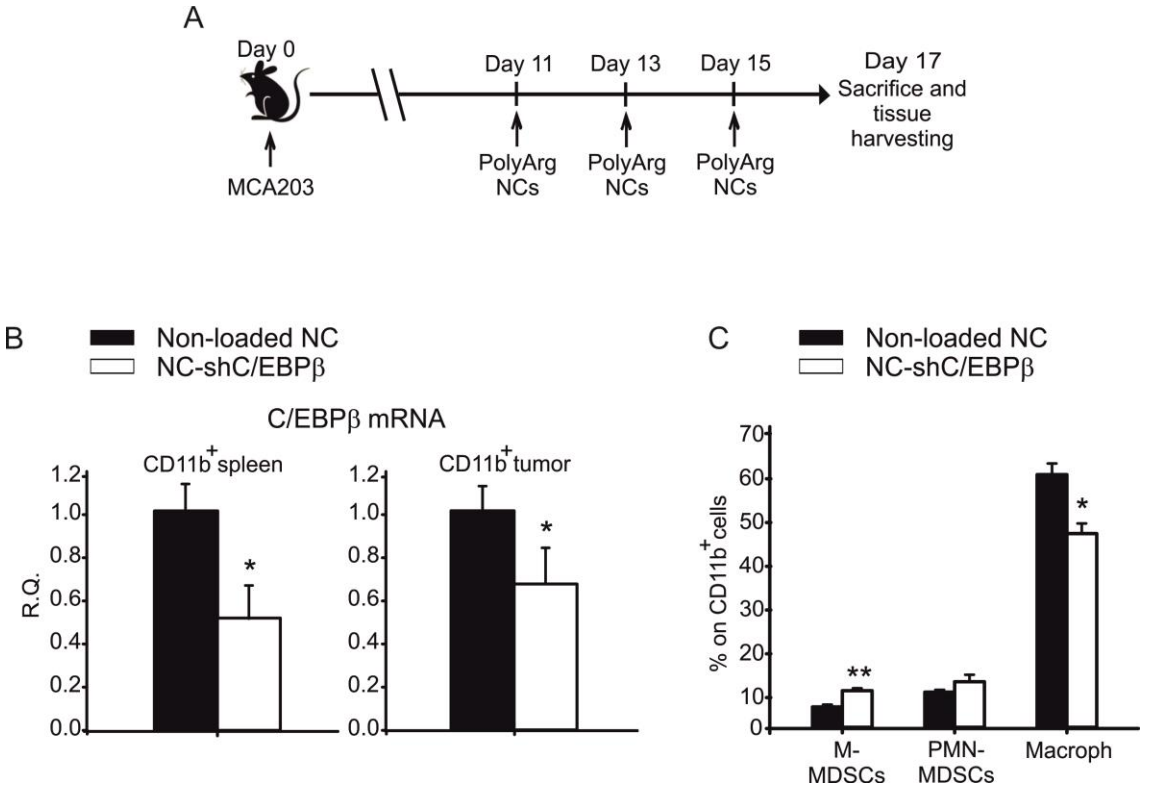


**Figure 14. PolyArg NCs loaded with C/EBPβ-targeting shRNA downregulate C/EBPβ expression *in vivo*.**

**A.** Schematic representation of the treatment schedule. C57BL/6 mice bearing MCA203 subcutanous tumors received three intravenous injection of PolyArg NCs, either unloaded or loaded with C/EBPβ-targeting shRNA (20 μg RNA/mouse/treatment). Mice were sacrificed 48 hours after the last treatment. **B.** C/EBPβ mRNA levels within $CD11b^+$ cells isolated from spleens and tumors of mice treated with either unloaded NCs or NCs loaded with the C/EBPβ-targeting

shRNA (NC-shC/EBPβ). C/EBPβ mRNA levels were quantified by RT-qPCR and normalized to an endogenous control (Rn18S). Data (means± SE) are expressed as relative quantification (R.Q.) normalized to the average cycle threshold value for the control group receiving unloaded NCs. **C.** Percentage of M-MDSCs, PMN-MDSC and macrophages on total $CD11b^+$ cells within the tumor (means± SE). Cell populations were defined according to the gating strategy reported in figure 4C. n=4 mice (unloaded NC) and n=3 mice (NC-shC/EBPβ). *p<0.05 **p<0.01 ***p<0.001, Student's *t*-test.

# Discussion

MDSC depletion or inhibition of MDSC-associated mechanisms of immunosuppression is known to improve the efficacy of cancer immunotherapy approaches in preclinical models, including ACT[21,40,98] and cancer vaccines[193]. In addition, clinical trials evaluating the efficacy of MDSC-targeted pharmacological agents, combined with either immunotherapeutics or conventional chemotherapeutics, are currently ongoing (www.clinicaltrials.gov NCT01697800; NCT02259231; NCT01803152). Due to the therapeutic interest in investigating increasingly effective approaches to reduce MDSC-mediated immunosuppression, we sought to evaluate the use of a recently developed encapsulated gemcitabine formulation, GemC12-loaded lipid nanocapsules (LNC-GemC12)[185], as MDSC targeting agent. Notably, we aimed at investigating whether low dose LNC-GemC12 can be effectively combined with ACT approaches to improve therapy efficacy.

Since the approval of the first nano-drug for cancer therapy, Doxil® (liposomal Doxorubicin) in 1995, cancer nanomedicine has received growing interest, and nanocarrier-based drug formulations have been shown to improve drug pharmacological proprieties by increasing drug stability, vascular residence, accumulation into tumor tissues and by reducing off-target toxicity[109,119]. The use of delivery nanosystems to modulate specifically immune populations is a much less explored research area, which has recently received growing attention as promising tool to improve cancer immunotherapy[145].

Remarkably, gemcitabine hydrochloride (GemHCl), the current gold standard formulation for gemcitabine, was already reported to deplete spleen and tumor infiltrating MDSCs in mouse models[21,156,186-188,194]. We hence wondered whether drug loading into lipid nanocapsules might result in a more selective and/or potent MDSC targeting and provide therapeutic advantages as compared with GemHCl.

In the present work, we considerably decreased gemcitabine dose with respect to previous reports, i.e. 50-60 mg/kg[186,188] and 120 mg/kg[21,156,187,194], in the attempt of disclosing the enhanced efficacy of LNC-GemC12 over GemHCl.

In our model, both low dose (11 mg/kg) LNC-GemC12 and GemHCl depleted M-MDSC subsets in the spleen and tumor, while leaving unchanged or minimally affecting the frequency of other immune cell subsets, including PMN-MDSCs, macrophages, DCs, and T lymphocytes. Conversely, a 120 mg/kg GemHCl dose was previously reported to cause substantial and comparable depletion of both M- and PMN-MDSCs in mouse tumor models[21,156]. Remarkably, in our experiments tumor-infiltrating M-MDSCs were more drastically decreased following LNC-

GemC12 subcutanous (SC) administration as compared with intravenous (IV) LNC-GemC12 injection or either IV or SC GemHCl administration, as shown in figure 6 and 7. Moreover, when we monitored myeloid cell frequency variations at sequential time points, SC LNC-GemC12 administration was found to produce a more durable M-MDSC depletion in the tumor than SC GemHCl.

More importantly, LNC-GemC12 treatment was associated with an attenuation of tumor-infiltrating MDSC suppressive function toward T cells (as shown in figure 8), and to an improved mouse survival when combined with an ACT protocol (data reported in figure 10). Conversely, GemHCl administration at the same dose did not result in a modulation of MDSC suppressive function nor in a survival advantage in the combined treatment schedule with ACT.

The selective depletion of M-MDSCs using very low drug doses is a potentially attractive immunomodulatory strategy, due to the strong immunosuppressive function of this cell subset in cancer. Indeed, in multiple tumor models M-MDSCs were found to be more potent suppressors of T cell response when compared with PMN-MDSCs [20-22,25,44].

In addition, in a previous work by our group, the relief of MDSC-induced immunosuppression following 5-fluorouracile (5-FU) chemotherapy was shown to be mainly dependent on the elimination M-MDSCs, while PMN-MDSCs played a minor role[21]. Strikingly, in this latter work the adoptive transfer of M-MDSCs, but not of PMN-MDSCs, resulted in the neutralization of the beneficial effect of mouse preconditioning with 5-FU in an ACT schedule[21].

The higher sensitivity of M-MDSCs, as compared to other myeloid cell subsets, to low dose gemcitabine may have different possible explanations. First, since gemcitabine activity relies on the inhibition of DNA replication, the greater gemcitabine cytotoxicity on M-MDSCs might be, at least in part, related to a higher proliferative status of these cells. Consistently with this hypothesis, we previously showed that spleen $Gr1^{int}$ and $Gr1^{low}$ myeloid cell subsets, mainly including M-MDSCs, bear an higher proliferative activity as compared with $Gr1^{high}$ cells (PMN-MDSCs)[21]. Besides, other possible mechanistic explanations may be envisaged. Interestingly, the anti-cancer drug trabectedin was reported to selectively trigger cell apoptosis in monocytes, but not in granulocytes and lymphocytes[53], thus displaying a cell-targeting pattern resembling that of low-dose gemcitabine reported in our work. The increased susceptibility to trabectedin of both human and mouse monocytes was shown to depend on the higher expression of TRAIL death receptors in these cells, which mediated the cleavage of caspase-8 and the activation of the extrinsic apoptotic pathway[53]. In addition, in a recent work by Haverkamp et al., the development of monocytic and granulocytic MDSC subsets was shown to be dependent on the continuous inhibition of different apoptotic pathways, notably the caspase-8 dependent

extrinsic pathway in M-MDSCs, and the mitochondrial intrinsic pathway in PMN-MDSC[44]. It is hence possible that monocytic and granulocytic MDSCs may be intrinsically prone to cell death through the activation of distinct apoptotic pathways, and therefore different drugs triggering the same cell death pathway might cause the preferential depletion of one myeloid subset rather than the other. This kind of mechanism could be hypothesized also for gemcitabine, and might, at least in part, explain the higher sensitivity of M-MDSCs to low drug doses. To clarify this hypothesis, a molecular analysis of cell death signalling pathways activated in different myeloid populations upon gemcitabine exposure needs to be performed, and will be subject to future investigations in our laboratory.

The enhanced sensitivity to gemcitabine activity of MDSC population compared to T lymphocytes might have further mechanistic explanations. First, since the activation and proliferation of T lymphocytes in cancer is known to be restrained by multiple tumor-induced mechanisms (see paragraphs 1-3 in the introduction), T lymphocytes are possibly poorly sensitive to the gemcitabine pharmacologic action due to their low proliferation state. Indeed, when LNC-GemC12 was administered following the transfer of pre-activated cytotoxic lymphocytes (CTLs) in ACT experiments, the treatment had a negative impact on transferred CTLs, possibly because these cells have a high proliferative potential in the days immediately following the adoptive transfer. Moreover, in a work by Vincent et al. the higher sensitivity of MDSCs to 5-FU with respect to other spleen immune cells (including T and B lymphocytes, NK cells and DCs) was mechanistically related to a lower expression of thymidylate synthase (TS), the enzyme inhibited by 5-FU[156]. TS has also been linked to gemcitabine cytotoxic activity[195] and TS expression was shown to positively correlate with gemcitabine resistance in multiple pancreatic cancer cell lines, while TS inhibition increased cancer cell sensitivity to the drug[196]. Based on these observations, MDSCs' high sensitivity to gemcitabine cytotoxicity might be, at least in part, related to a reduced TS expression, as previously reported for 5-FU.

In the present work, we showed that LNC-GemC12 is a M-MDSC depleting agent more potent than GemHCl. The improved efficacy of LNC-GemC12 over GemHCl might be in principle due to the use of a modified gemcitabine molecule, covalently linked to a C12 alkyl chain (GemC12)[185]. Indeed, GemC12, as well as other lipophilic gemcitabine compounds bearing long carbon chains linked to the 4' amino group, are known to improve gemcitabine stability due to drug protection from inactivation by cellular deaminases[197]. However, when we compared M-MDSC depletion produced by GemHCl and by a free GemC12 solution, no substantial differences were observed. This result suggests that most of LNC-GemC12 enhanced efficacy relies on the lipid nanocapsule component. GemC12 encapsulation into LNCs might enhance drug potency by multiple

mechanisms, including increased drug stability, enhanced distribution to the tumor tissue and preferential accumulation in monocytic cells, which are singularly discussed below.

Lipid nanocapsules (LNCs) developed by the JP. Benoit group were previously used to encapsulate other chemotherapeutic agents, including etoposide, paclitaxel and docetaxel, resulting in formulations with different sizes but always ≤ 100 nm[179]. Their size and the presence of a PEG shell make LNCs suitable to accumulate in tumors by the EPR[179] effect, according to the criteria extensively discussed in the introduction (paragraph 4.1,4.2.). Briefly, these criteria include: I) a size above the glomerular filtration limit in the kidneys (8 nm) and below the exclusion limit for extravasation across the hyper-permeable tumor vasculature (estimated around 200 nm); and II) the presence of hydrophilic and neutral coating (e.g. a PEG shell), which reduces non-specific absorption of serum protein and prevent an excessive rate of opsonization and clearance by cells of the immune system, thus extending vascular residence times[109].

In addition, the more intense depletion of M-MDSCs associated to LNC-GemC12 administration may also depend on an increased uptake of encapsulated GemC12 as compared to free gemcitabine by these cells. This latter hypothesis is supported by the immune cell uptake studies performed with DiD-loaded LNCs, shown in figure 5. In these experiments LNCs with the same size and structure as LNC-GemC12, but loaded with the DiD fluorescent dye, were found to preferentially target M-MDSCs in the spleen and M-MDSCs and macrophages in the tumor. As extensively discussed in the introduction (paragraph 4.2), circulating nanoparticles bind serum immunoglobulins by non-specific interactions and activate complement pathways, at a variable extent depending on particle size, charge and composition[123,124]. The reason why in our model monocytes/macrophages internalize LNCs more efficiently than other phagocytic cell populations, as DCs and granulocytic cells, is still not clear. Previous studies have already reported similar monocyte targeting properties of small (below 100 nm) PEGylated nanoparticle formulations, evaluated either in healthy mice, inflammatory disease models, or tumor models[146,150]. Based on these similarities, we could hypothesize than monocytic cells, including M-MDSC, are more prone to bind particle bearing physico-chemical features shared by these different formulations, as small size and PEGylation, with respect to other myeloid cell subsets. Interestingly, in a study evaluating the uptake of 100 nm albumin nanoparticles by neutrophils in an acute inflammation model, only activated neutrophils adhering to vessels walls, but not resting circulating neutrophils, were able to uptake the nanoparticles[152]. Moreover, nanoparticle internalization by activated neutrophils was shown to depend at least in part on FcγR up-regulation under inflammatory stimuli[152]. Based on this study, one possibility is that the poor LNC uptake by PMN-MDSC observed in our model might be related to a low expression of

FcγR and/or complement receptors by these cells that prevents an efficient binding and uptake of opsonized-circulating nanoparticles. However, specific studies should be performed in order to demonstrate this hypothesis.

In the present work, we found that the SC administration of LNC-GemC12 was associated to a significantly enhanced depletion of both spleen and tumor-infiltrating M-MDSCs as compared with the IV administration. According to biodiostribution (BD) and pharmacokinetic (PK) studies on healthy mice (reported in figures 1 and 2), DiD-loaded LNCs are slowly absorbed in blood circulation following SC injection and reach peak accumulation in peripheral tissues, notably in liver and spleen, 24-48 hours following their administration. Lymph nodes near the injection site constitute an exception to this distribution pattern, since they are likely reached by direct lymphatic drainage. This *in vivo* behavior is typically observed for nanocarrier formulations that form local depots upon SC or intradermic administration, resulting in a gradual and sustained release of the nanocarrier and/or its cargo in the systemic circulation[181,182,198]. In addition, when we measured the distribution of DiD-loaded LNCs in the spleen and tumor tissue sections 24 hours following LNC injection (shown in figure 3), a significantly higher DiD signal was measured in mice receiving IV administration as compared to SC-treated mice, in both organs. All these data indicate that greater DiD concentrations are reached in spleen and tumors following IV injection of LNCs, as compared to SC, at least at time points ≤24 hours. However, a significantly enhanced M-MDSC depletion in both organs was reported in mice treated with SC LNC-GemC12. Based on these data, the lower maximum drug concentration reached in peripheral tissues after SC nanocarrier administration as compared to IV, should be equally sufficient to trigger cell death pathways in M-MDSCs. In addition, since gemcitabine is known to be rapidly transformed by cellular enzymes[197], the slow but sustained LNC absorption from the SC injection site might continuously supply target tissue with a low drug dose, compensating its catabolic inactivation. In this way, the SC route might result in a lower but prolonged exposition of target tissues to the active drug form.

Interestingly, a series of clinical studies compared the standard, 30-minute gemcitabine IV infusion *versus* a prolonged infusion at a low fixed-dose rate. This latter drug infusion mode was found to be associated with higher levels of the active gemcitabine metabolite in blood mononuclear cells and leukemic cells[199], and with clinical benefits in pancreatic cancer patients[200]. The pharmacological basis of this phenomenon is that slower infusion rates allow to keep for longer periods a drug plasmatic concentration that saturates cell enzymes involved in drug conversion in its active metabolite. Conversely, the standard 30 min infusion of 1000-1250 mg/m$^2$ results in a drug plasmatic concentration exceeding this saturation limit [199].

We could hypothesize that the SC administration, being associated to a gradual drug absorption in the systemic circulation, might mimic a prolonged infusion schedule and hence result in an enhanced accumulation of the drug active form in target cells, as compared with the IV administration of a drug bolus. This possibly applies to both LNC-GemC12 and free drug solutions administered SC, although drug encapsulation in nanocarriers likely results in enhanced sustained release, as suggest by our data. The above considerations might also explain why GemHCl administration by the SC route showed a slightly better efficacy as compared to GemHCl IV in our immunotherapy schedule (shown in figure 10). However, a specific pharmacokinetic analysis of GemHCl using the employed drug dose, administration routes and mouse model should be performed in order to test these hypothesis.

Remarkably, in the present study we demonstrated that a very low dose (11 mg/kg) of encapsulated gemcitabine could be used to attenuate MDSC-induced immunosuppression and improve mice survival after CTL adoptive transfer. Of note, this low dose is not expected to cause any significant toxicity, since toxic effects in mice are usually reported only with higher gemcitabine doses[201] or prolonged exposition to low drug doses [202]. From a translational point of view, the present findings suggests that the use of encapsulated chemotherapeutic agents may allow reaching meaningful immunomulatory effects at lower drug doses than conventional chemotherapeutics. Specifically, LNC-GemC12 may provide better efficacy as compared to GemHCl, as MDSC-targeted agent. Monocyte/macrophage-targeting proprieties of LNC-GemC12 needs to be confirmed on human immune cells. If the unveiled targeting pattern is established, human cancers associated with the expansion of monocytic MDSC subsets[27] might primarily benefit from LNC-GemC12 immunomodulatory activity.

Gemcitabine is already being evaluated in a phase I clinal trial as MDSC-depleting agent to potentiate the efficacy of a DC-based vaccine (www.clinicaltrials.gov; NCT01803152). Of note, the population recruited in this trial is composed of advanced sarcoma patients, refractory to conventional therapies, in which the drug is not expected to have a substantial direct cytotoxicity on tumor cells and is exclusively used as immunomodulatory agent. Data obtained in the present work further support gemcitabine use in combination with ACT schedules, besides cancer vaccines.

Preconditioning regimens based on chemotherapy (fludarabine/cyclophosphamide) plus total body irradiation are currently employed to increase patient response to ACT[95]. These regimens are known to favor the expansion and function of transferred CTLs by multiple mechanisms (see paragraph 3.2 in the introduction), including the elimination of endogenous immunosuppressive cells[3]. The major drawback of preconditioning regimens currently employed in clinical setting, is

the potential of severe toxicity, which limits this therapy to highly selected patients with a good performance status and normal organ function[100,101]. The development of more effective and widely applicable ACT based approaches is therefore dependent on supporting treatments aimed at reducing tumor-associated immunosuppression with good efficacy and low toxicity. Although further investigation of LNC-GemC12 immunomodulatory activity in other tumor models is needed to consolidate the present findings, here we provide a rationale to consider the use of encapsulated drug formulations, instead of conventional chemotherapeutic drugs, in cancer immunotherapy approaches and notably in the modulation of immunosuppressive myeloid cells.

In addition to its immunomodulatory activity, LNC-GemC12, administered at higher doses and/or for longer time periods, is also expected to have a direct anti-tumor activity and cause tumor regression or tumor growth delay, possibly with superior efficacy over GemHCl. This evaluation is currently ongoing in our laboratory. In this setting, both MDSC depletion and direct tumor-cytotoxiciy may contribute to control tumor progression. Moreover, the prolonged depletion of monocytic cells by chronic LNC-GemC12 or GemHCl administration is ultimately expected to cause the reduction of monocyte-derived TAMs, an effect that was not observed after a single LNC-GemC12 injection. It is likely that the full potential of LNC-GemC12 use in cancer therapy is still not fully disclosed, for both conventional cancer therapy and immunotherapy.

In the second part of the present work, we evaluated a nanosystem platform for *in vivo* RNA delivery, which represents an additional tool to modulate selectively cancer-associated myeloid populations. Based on a preliminary *in vitro* toxicity screening (shown in figure 11) and physico-chemical characterization (data of MJ Alonso laboratory, not shown) of different nanocarrier prototypes, we selected a formulation of polyarginine-coated nanocapsules (PolyArg NCs) for further investigation. Besides the good toxicity and stability profile, this formulation was also interesting since polyarginine is a known cell-penetrating peptide, able to promote both cell internalization of RNA delivery systems and endosomal escape[190,191].

In order to evaluate the efficiency of this system in delivering RNA molecules and downregulate genes by RNAi mechanisms, we selected a relevant target gene, i.e. mouse CCAAT/enhancer binding protein (C/EBP)β transcription factor. C/EBPβ is known to regulate "emergency" granulopoyesis under inflammatory conditions, as those induced by cytokine storm or fungal infections, as opposed to C/EBPα, wich is instead required for steady-state but not for emergency granulopoiesis[203]. A new function for the C/EBPβ transcription factor was previously reported by our group, since this factor was shown to play a critical role in MDSC biology[99]. C/EBPβ expression, in fact, controlled MDSC expansion and acquisition of immunosuppressive

function in both *in vivo* tumor-induced mouse MDSCs and *in vitro* differentiated mouse and human MDSCs. Remarkably, C/EBPβ genetic ablation in conditional knockout mice dramatically improved mice survival after ACT, thus supporting the relevance of C/EBPβ pathway as therapeutic target in cancer immunotherapy[99].

Based on these previous findings, the therapeutic silencing of C/EBPβ by RNAi might be employed to potentiate the efficacy of ACT. In the present work we showed that PolyArg NCs loaded with a C/EBPβ-specific fluorinated shRNA significantly downregulated target gene expression *in vitro*, and we provided an initial validation of its efficacy *in vivo*. With the employed treatment schedule (20 μg RNA/mouse x 3 doses), we achieved about 50% and 30% reduction of C/EBPβ mRNA levels in myeloid populations ($CD11b^+$) of the spleen and tumor, respectively. Such difference in C/EBPβ downregulation efficiency might reflect a stronger PolyArg NC accumulation in the spleen with respect to tumors and/or a stronger uptake by splenic myeloid populations, although specific biodistribution and uptake studies remains to be performed.

The level of target gene downregulation, at least in the spleen, might be in principle biologically relevant, since mRNA downregulation levels around 50% have been reported to be associated with functional effects in the literature[144,146]. However, with the intent of reaching a stronger C/EBPβ downregualtion in the spleen and especially in the tumor, different shRNA-loaded PolyArg NC administration schedules, with increased RNA doses per mouse and treatment frequency, are currently being evaluated.

Interestingly, in our model C/EBPβ modulation was associated with a decreased frequency of TAMs, paralleled by a significant increase in monocytic cells (phenotypically resembling M-MDSCs). This pattern of altered myeloid cell frequencies is suggestive of an impaired monocyte differentiation into TAMs following C/EBPβ down-regulation. Our group recently reported a regulatory circuit controlling TAM differentiation, dependent on the microRNA miR-142-3p[204]. miR-142-3p downregulation was required for the *in vitro* differentiation of immunosuppressive macrophages and its enforced expression in the bone marrow, through the generation of mouse bone marrow chimeras, was associated with reduced macrophage numbers in lymphoid organs and tumor masses of tumor-beating hosts[204]. Remarkably, the regulatory activity of miR-142-3p involved the modulation of C/EBPβ isoform expression by direct binding of miR-142-3p to the C/EBPβ mRNA, resulting in a significantly reduced expression of the activating C/EBPβ isoform LAP*[204]. This reported link between C/EBPβ modulation and tumor-induced macrophage differentiation seems to support further the hypothesis of an impaired TAM differentiation

following C/EBPβ silencing by shRNA-loaded PolyArgNCs. However, further experiments are needed to demonstrate it.

The development of therapeutic agents able to specifically reduce the expansion of TAM pool, which is known to be endowed with multiple pro-tumor functions[70], and/or to reduce MDSC-mediated immunosuprression is currently object of great research efforts in the field of cancer immunotherapy. Our nanotechnology-based tool to modulate C/EBPβ transcription factor could allow reaching these kind of immunomodulatory effects, and will be therfore further investigated by our group.

# Materials and methods

## Mice

C57BL/6 (WT), congenic CD45.1 ($Ly5^+$) mice and OT-I transgenic mice (C57BL/6-Tg $(TcraTcrb)^{1100Mjb}$/Crl) were purchsed from Charles River Laboratories (Italy) and maintained under specific pathogen-free conditions in the animal facilities of the Istituto Oncologico Veneto (Padova, Italy). OT-I/CD45.1 F1 mice were obtained by crossbreeding OT-I and CD45.1 mice. Female C57BL/6 (WT) and female/male CD45.1 OT-I transgenic mice were used between 8 and 12 weeks of age. For pharmacokinetic and biodistribution studies on healthy mice, female nude SWISS mice were purchased from Harlan (Gannat, France) and maintained at the University animal facility (SCAHU) in Angers (France). Experiments involving animals were performed according to the national guidelines and approved by the local ethics committee.

## Cell lines

The EG7-OVA (aplotype H-2b) lymphoma and MCA-203 (aplotype H-2b) fibrosarcoma cell lines were obtained from the American Type Culture Collection and cultured in DMEM 10% FBS (Gibco) supplemented with 2 mM L-glutammine, 10 mM HEPES, 20 µM 2β-Mercaptoethanol, 150 U/ml streptomycin, 200 U/ml penicillin. G418 was added to EG7-OVA cell cultures to maintain transgene selection.

The MSC1 cell line was obtained by immortalizing tumor-induced splenic MDSCs[192] and cultured in RPMI medium supplemented with 10% FBS Superior (Biochrom), 2 mM L-glutammine, 1 mM Na-pyruvate, 150 U/ml streptomycin, 200 U/ml penicillin. Cultures were maintained at 37°C with 5% CO2.

## Nanocarriers

LNC-GemC12 and DiD-LNCs were prepared at the laboratory of Jean Pierre Benoit (INSERM – U1066 Institut de Biologie en Santé (IBS)-Centre Hospitalier Universitaire (CHU), Angers ,France). LNC-GemC12 and DiD-LNCs synthesis procedure is described in Moysan et al., Soft matter. 2014[185] and in Bastiat et al., J Control Release. 2013[180].

HA-nanocapsules, HA-protamine nanocapsules (PEG-st), HA-protamine nanocapsules (succinate and sodium cholate) and polyarginine nanocapsules (PolyArg NCs) were prepared in the laboratory of Maria Josè Alonso at the Center for Research in Molecular Medicine and Chronic Diseases (CIMUS), Santiago de Compostela, Spain.

All formulations were stored at +4°C , except for shRNA-loaded PolyArg NCs, which were freeze-dried soon after RNA loading and stored at -20°C.

### Preparation of cell suspensions from tumors and lymphoid organs

Mice were euthanized and spleens, tumors and axillary and inguinal lymph nodes were collected. Tumors were cut in small pieces and incubated with a digestive solution composed of collagenase IV (1 mg/ml), hyaluronidase (0.1 mg/ml), DNase (0.03 KU/ml) 37°C for 1 hour; every 10 minutes, tumors were mechanically disaggregated using a 5 ml pipette. At the end of digestion, tumor cells were collected, filtered to remove cell clumps and debris and washed in complete medium twice to remove all digestive solutions prior to subsequent use.

Spleens and lymph nodes were mechanically disaggregated and filtered with 100 μm filters.

### Cytofluorimetric analysis

Red blood cells were removed from cell suspension using a hypotonic lysis solution and cells were washed with cold PBS and incubated 10 min at +4°C with purified anti-FcγR antibody (clone 2.4G2) to minimize non-specific antibody binding. Antibodies of interest were added to cell suspensions following FcγR blocking and incubated 20 min at +4°C in the dark.

Employed antibodies were: anti-CD11b PE-Cy7 (clone M1/70), anti-CD11b PerCP-Cy5.5 (clone M1/70), anti-LY6G APC-Cy7 (clone 1A8), anti-CD11c BV421 (clone HL3), anti CD115 PE (clone AFS98) anti-I-A/I-E PerCP-Cy5.5 (clone M5/114.15.2), anti-LY6C eFluor 450 (clone HK1.4), anti-CD4 APC (clone RM4-5), anti-CD45.1PE (clone A20), anti-CD8 PerCP-Cy5.5 (clone 53-6.7), anti-CD3 FITC (clone 145-2C11)(all from eBioscience), anti-F4/80 FITC (AbDSerotec, clone CI:A3-1). Aqua LIVE/DEAD® dye (Invitogen) was used to analyze cell viability.

For intracellular staining of INF-γ the BD Citofix/Cytoperm Kit was used, according to manufacturer's instruction. INF-γ was stained using anti-INF-γ FITC (clone XMG1.2, BD)

Flow data were acquired with a BD LSRII or BD FACS Calibur instrument and analyzed with FlowJo (Tree Star, Inc.) software

### *Ex vivo* T cell suppression assay

$CD11b^+$ cells were isolated from tumors with anti-CD11b MicroBeads (Miltenyi Biotec, Germany). OT-I/CD45.1 splenocytes derived from the spleen of OT-I mice were labeled with carboxyfluorescein succinimidyl ester (CFSE, CFSE-Cell Trace Kit, Invitrogen Molecular Probe) according to manufacturer's instructions. A mixed leucocyte peptide culture (MLPC) was prepared by mixing γ-irradiated C57BL/6 splenocytes with OT-I/CD45.1 CFSE-labeled splenocytes in order to obtain 1% OT-I T $CD8^+$ lymphocytes in the final culture. MPLC culture was plated in flat-bottom 96-well plates ($0.6x10^6$ cells/well) and 1 μg/ml H-2 $K^b$-restricted OVA peptide ($OVA_{257-264}$, SIINFEKL, synthesized by JPT, Peptide Technologies, Germany) was added to the

culture to stimulate OVA-specific OT-I T $CD8^+$ lymphocytes. $CD11b^+$ cells were added at degreasing percentages with respect to MLPC culture(24%, 12%, 6%, 3% and 1,5%). Cultures were maintained at 37°C with 5% CO2 in RPMI medium supplemented with 10% FBS Superior (Biochrom), 2 mM L-glutammine, 1 mM Na-pyruvate, 150 U/ml streptomycin, 200 U/ml penicillin, 20 µM 2β-mercaptohetanol.

After 3 days of culture cells were collected, washed with cold PBS and stained with anti-CD45.1 PE (clone A20, eBioscience) and anti-CD8 PerCP-Cy5.5 (clone 53-6.7, e Bioscience). Flow data were acquired with a FACSCalibur flow cytometer (BD Biosciences) and analyzed with FlowJo (Tree Star, Inc.) software. The percentage of cells in 0 to 7 generation of proliferation was determined based on CFSE dilution within the $CD8^+CD45.1^+$ gate.

### Fluorescent immunohistochemistry (IHC)

Tumor and spleen samples were fixed in 4% Paraformaldehyde (PFA), de-hydrated through sequential passages in 20% and 30% sucrose solutions and frozen in a cryo-embedding medium (OCT, Bio-Optica, Milan, Italy). 7 µm tissue sections were prepared and stored at -20°C until usage. For IHC staining, tissue section were re-hydrated in PBS, fixed in 4% PFA for 5 minutes at room temperature (RT), incubated 1h RT with a blocking solution (PBS 10% FBS) to reduce non-specific binding, and stained overnight with rat anti-mouse CD11b-FITC (clone M1/70 eBioscience). Goat anti-rat IgG Alexa Fluor 488 (Abcam) was used as secondary antibody and incubated 3 hours at RT. Nuclear staining was performed with DAPI (Invitrogen) for 10 minutes at RT. Slices were mounted with ProLongR Gold Antifade Reagent (Invitrogen). Images were acquired with a Zeiss LSM 510 confocal microscope. MFI in the DiD channel was measured on 4-7 randomly selected fields per tissue section, and means MFI ± standard errors (SE) were calculated for tissue sections from n=3 mice per group.

### MDSC generation from bone marrow cells

Bone marrow cells were isolated from tibiae and femurs of C57BL/6 mice and red blood cells were lysed with hypotonic solution. $1,5x10^6$ bone marrow cells/well were plated in 6-well tissue culture plates (Falcon,Corning) in 2 ml of RPMI medium supplemented with 10% FBS Superior (Biochrom), 2 mM L-glutammine, 1 mM Na-pyruvate, 150 U/ml streptomycin, 200 U/ml penicillin, 20 µM 2β-mercaptohetanol. Recombinant murine GM-CSF and IL-6 (Peprotech) were added at 40 ng/ml final concentration to induce differentiation of bone-marrow derived MDSCs (BM-MDSCs), as previously reported[99]. Cultures were incubated for 4 days at 37°C with 5% CO2. Cells from the non-adherent and adherent fraction were collected by rinsing the dishes with PBS 2mM EDTA and used for flow cytometry analysis.

### *In vivo* treatments on tumor bearing mice

To establish tumors, EG7-OVA cells ($0.5x10^6$ cells/mouse) or MCA203 cells ($1x10^6$ cells/mouse) were injected subcutaneously (SC.) on the left flank of C57BL/6 mice, and tumor growth was monitored every 2 days by digital calipers.

LNC-GemC12, Gemcitabine hydrochloride and free GemC12 were administered either SC, on the right flank ,or intravenously (IV), on the tail vein. All treatments were administered at a 11 mg/kg Gemcitabine or GemC12 dose. For tracking of DiD-loaded LNCs (DiD-LNCs) by fluorescence microscopy on tissue section and by flow cytometry, mice were injected with 8.8 mg of DiD-LNCs (≈4 µg of DiD dye), corresponding to the same amount of LNC per mouse administered in experiments with LNC-GemC12. In the EG7-OVA model, treatments were administered after 8 days following EG7-OVA cell injection (tumor surface approximately 50 $mm^2$).

In experiments with shRNA-loaded polyarginine nanocarriers (PolyArg NCs), treatments were started at day 11 from MCA203 tumor cell injection, when tumor surfaces were approximately 35 $mm^2$, and repeated 3 times with 48 hours intervals (RNA dose= 20 µg/mouse/treatment).

### Adoptive T cell therapy (ACT)

ACT was administered to mice bearing EG7-OVA tumors, after 9 days from tumor cell injection. OVA specific $CD8^+CD45.1^+$ cytotoxic T lymphocytes (CTLs) were prepared by culturing OT-I/CD45.1 splenocytes in presence of 1 µg/ml $OVA_{257-264}$ (SIINFEKL) peptide and 20 IU/ml IL-2 (Novartis, Basel, Switzerland). Cell cultures were maintained 7 days before *in vivo* injection. OVA-specific CTLs were injected IV on the tail vein ($0.25x10^6$ cells/mouse).

### Pharmacokinetic and biodistribution of DiD-loaded LNCs (DiD-LNCs) in healthy mice

Pharmacokinetic and biodistribution experiments in healthy mice were performed in the in the laboratory of Jean Pierre Benoit (INSERM – U1066 Institut de Biologie en Santé (IBS)-Centre Hospitalier Universitaire (CHU), Angers ,France).

Healthy female nude SWISS mice of 9 weeks of age were injected with DiD-LNCs either subcutaneously (sc) behind the neck, or intravenously (iv) into the tail vein. Each mouse was injected with 48 mg DiD-LNCs, corresponding to 24 µg of DiD dye. At sequential time points from DiD-LNC injection (1h, 4h, 8h, 24h, 48h, 96h and 336h ) mice were sacrificed, blood was collected by cardiac puncture and organs were removed for biodistribution analysis . Plasma from each blood sample was obtained after 10 min of centrifugation at 2,000 g. DiD concentrations in plasma (encapsulated inside LNC) along time were determined using a microplate reader Fluoroscan Ascent® (Labsystems SA, Cergy-Pontoise, France) at excitation and

emission wavelengths of 646 and 678 nm, respectively. DiD concentrations in plasma were intrapolated from linear curve between 0.006 and 12 µg/mL (r2 > 0.999). Pharmacokinetic data were determined by iv bolus and extravascular non-compartmental analysis (for iv and sc administration, respectively) of the recovered systemic DiD concentration versus time using Kinetica 4.1.1 software (Thermo Fisher Scientific, Villebon sur Yvette, France). The trapezoidal calculation method was used to determine the area under the curve (AUC) during the whole experimental period (from 1 to 336 h) without extrapolation. The $t_{1/2}$ were calculated from 1 to 8 h for $t_{1/2}$ distribution and from 8 to 336 h for $t_{1/2}$ elimination.

For the biodistribution study, the organs (i.e., kidneys, liver, spleen, lung, heart, stomach, and intestine), and lymph nodes (i.e., inguinal, axillary, cervical and brachial lymph nodes) were removed and analyzed by a fluorescence CRI MaestroTM imaging system (Woburn, USA). Semi-quantitative data were obtained by setting a time exposition of 10 ms between 630 and 800 nm, unmixing the generated cube, extracting the background and drawing the regions of interest from fluorescence images (Figure 1-A). The software Maestro 2.10 (Woburn, USA) was used to calculate the average signal expressed in photon/cm²/s.

### Cell transfection

$5*10^4$ MSC1 cells/well were plated in 24-well plates (Falcon, Corning) the day before transfection.

Nacked shRNAs were transfected using the Lipofectamine RNAi Max® reagent (Invitrogen) according to manifacturer's instruction. Freeze-dryed shRNA-loaded PolyArg NCs were reconstituted in RNase free water and added to the cell culture. Cells were harvested 24 hours after transfection.

### RNA extraction and qRT-PCR

$CD11b^+$ cells were isolated from tumors ant spleens with anti-CD11b MicroBeads (MiltenyiBiotec, Germany) and total RNA was extracted using the miRNeasy Micro Kit (Qiagen) according to manifacturers' instructions. For *in vitro* experiments, TRIzol® reagent (Invitrogen) was added directly to the culture plate after medium removal, and total RNA was extracted according to the TRIzol® extraction protocol. Following TRIzol® extraction, genomic DNA contaminants were removed using the TURBO DNA-free™ Kit (Ambion).

cDNA was generated using the reverse transcriptase SuperScript II and polyd$T_{12-18}$ primers (Invitrogen). PCR and fluorescence detection were performed using the ABI 7900HT fast real-time PCR Systems in a reaction volume of 20 µl containing 1× TaqMan Universal PCR Master Mix (Applied Biosystems) and 50 ng cDNA. For quantification of mouse *Cebpb* and *Rn18s* the 1× TaqMan Gene Expression Assays Mm00843434_s1 and Mm03928990_g1 (Applied Biosystems)

were used. All measurements were performed in duplicates and were analyzed by the ΔΔCt relative quantification method: the arithmetic means of the cycle threshold (Ct) values were calculated and target gene mean Ct values were normalized to the respective endogenous control (Rn18s), and then to ΔCt value of control samples. The values obtained were exponentiated 2(−ΔΔCt) to be expressed as n-fold changes in regulation compared with the reference sample.

### Synthesis of fluorinated short hairpin (sh) RNAs

Specifically designed, self-annealing ssDNA primers were purchased from Eurofins MWG Operon and were used to obtain dsDNA by PCR extension. PCR extension was performed in a 50 µl final reaction volume containing 1x PCR buffer, 2,5 mM $MgCl_2$ , 0.2 mM dNTPs, 1 U Taq DNA polymerase (all from Invitrogen) and 20 µM ssDNA primers. A single PCR cycle was run with the following protocol: 95°C 10min, 60°C 1 min, 72°C 20min. dsDNA was purified using the Wizard® SV Gel and PCR Clean-up system (Promega) according to manufacturer's instruction.

1 ug of dsDNA was used as template to transcribe shRNA molecules in a single *in vitro* transcription (IVT) reaction, using the DuraScribe® T7 transcription kit (Epicentre). IVT reaction was run overnight at 37°C in a temperature-controlled oven. DNA template was removed by DNase I digestion and shRNAs were purified using the miRNeasy Micro Kit (Qiagen). Purified shRNAs were quantified by spectrophotometer and correct molecule length was checked by denaturing gel electrophoresis (polyacrilammide 15%, urea 7M).

Purified shRNAs were used for cell transfection experiments or shipped to the Center for Research in Molecular Medicine and Chronic Diseases (CIMUS), Santiago de Compostela, Spain for loading on PolyArg NCs. The workflow for fluorinated shRNA synthesis is graphically represented in figure 12 in the result section. ssDNA Primer sequences for the generation of the C/EBPβ-specific shRNA and control scrambled shRNA were kindly provided by Paolo Serafini (University of Miami, Department of Microbiology and Immunology, University of Miami, Miami, Florida, USA).

## Statistical analysis

Values are reported as means ± standard errors (SE). Survival experiments are reported as Kaplan-Meyer curves and significance was determined with log-rank test with *p*-value correction for pairwise multiple comparisons by the Holm-Sidak method. Student's *t*-test was performed on groups with normal distribution, as evaluated by Shapiro-Wilk normality test. For non-normal data, group comparison was performed using the Mann-Whitney Rank Sum Test. Values were considered significantly with $p \leq 0.05$ and are indicated as *$p \leq 0.05$; **$p \leq 0.01$ and ***$p \leq 0.001$.

# Abbreviations

5-FU.....5-Fluorouracile
ACT ..... Adoptive cell therapy
APC .....Antigen presenting cell
APC ..... Allophycocyanin
ARG ..... Arginase
ATRA ..... All-trans retinoic acid
BM ..... Bone Marrow
C/EBP ..... CCAAT-enhancer-binding protein
CCR2.....C-C chemokine receptor type 2
CD ..... Cluster of differentiation
CSFE .....Carboxyfluorescein diacetate succinimidyl ester
CTL ..... Cytotoxic T lymphocyte
CTLA4 ..... Cytotoxic T-Lymphocyte Antigen 4
DNA.....Deoxyribonucleic acid
DAPI ..... 4',6-diamidino-2-phenylindole
DC ..... Dendritic cell
DMEM ..... Dulbecco's Modified Eagle Medium
EDTA ..... Ethylenediaminetetraacetic acid
EGF..... Epidermal growth factor
EPR..... Enhanced permeability and retention
FBS ..... Fetal bovine serum
FSC.....Forward scatter
FITC ..... Fluorescein isothiocyanate
Foxp3 ..... Forkhead box P3
G-CSF ..... Granulocyte colony-stimulating factor
GemC12.....Gemcitabine C12
GemHCl..... Gemcitabine hydrocloride
GM-CSF .....Granulocyte-macrophage colony-stimulating factor
HEPES ..... 4-(2-hydroxyethyl)-1-piperazineethanesulfonic acid
HIF..... Hypoxia-inducible factors
HLA ..... Human leukocyte antigen

IP..... Intraperitoneal

IDO .....Indoleamine 2,3-dioxygenase

IL ..... Interleukin

INF ..... Interferon

iNOS ..... Inducible Nitric oxide synthase

IV.....Intravenous

IVT.....*In vitro* transcription

JAK ..... Janus kinase

KO .....Knock-Out

LNC.....Lipid nanocapsule

LPS ..... Lipopolysaccharide

MCA ..... Methylcholanthrene

M-CSF ..... Macrophage colony-stimulating factor

MDSC ..... Myeloid derived suppressor cell

miRNA.....microRNA

MHC ..... Major histocompatibility complex

MLPC ..... Mixed lymphocyte-peptide culture

M-MDSC ..... Monocytic-Myeloid derived suppressor cell

MMP ..... Matrix metalloproteinase

MR.....Mannose Receptor

NC.....Nanocapsule

NF-κB ..... Nuclear factor kappa-light-chain-enhancer of activated B cells

NK ..... Natural killer cell

OCT ..... Optimal cutting temperature compound

OVA ..... Ovalbumin

PBS ..... Phosphate buffered saline

PD-1..... Programmed cell death protein 1

PD-L1..... Programmed cell death protein ligand 1

PDE5 ..... Phosphodiesterase 5

PE ..... Phycoerythrin

PEG.....Polyethylene glycol

PerCPCy5.5 ..... Peridinin-chlorophyll-protein complex cyanin5.5

PMN-MDSC .....Polymorphonuclear myeloid derived suppressor cell

PolyArg.....Polyarginine

qRT-PCR.....Quantitative reverse transcriptase PCR

RNA.....Ribonucleic acid

RNAi.....RNA interference

RNS ..... Reactive nitrogen species

ROS .....Reactive Oxygen Species

RT ..... Room temperature

SC..... Subcutaneous

SCF ..... Stem cell factor

SD.....Standard deviation

siRNA.....Small interfering RNA

shRNA..... Short hairpin RNA

SSC.....Side scatter

STAT..... Signal transducer and activator of transcription

TAM ..... Tumor associated macrophage

TCR ..... T cell receptor

TGF ..... Tumor growth factor

Th.....T helper

TIL ..... Tumor infiltrating lymphocyte

TLR ..... Toll-like receptor

TNF ..... Tumor necrosis factor

Treg ..... T regulatory lymphocyte

VEGF ..... Vascular endothelial growth factor

# References


1 Hanahan, D. & Weinberg, R. A. Hallmarks of cancer: the next generation. *Cell* **144**, 646-674, doi:10.1016/j.cell.2011.02.013 (2011).

2 Schreiber, R. D., Old, L. J. & Smyth, M. J. Cancer immunoediting: integrating immunity's roles in cancer suppression and promotion. *Science* **331**, 1565-1570, doi:10.1126/science.1203486 (2011).

3 Hinrichs, C. S. & Rosenberg, S. A. Exploiting the curative potential of adoptive T-cell therapy for cancer. *Immunological reviews* **257**, 56-71, doi:10.1111/imr.12132 (2014).

4 Restifo, N. P., Dudley, M. E. & Rosenberg, S. A. Adoptive immunotherapy for cancer: harnessing the T cell response. *Nature reviews. Immunology* **12**, 269-281, doi:10.1038/nri3191 (2012).

5 Curiel, T. J. *et al.* Specific recruitment of regulatory T cells in ovarian carcinoma fosters immune privilege and predicts reduced survival. *Nature medicine* **10**, 942-949, doi:10.1038/nm1093 (2004).

6 Liu, J. *et al.* Tumor-associated macrophages recruit CCR6+ regulatory T cells and promote the development of colorectal cancer via enhancing CCL20 production in mice. *PloS one* **6**, e19495, doi:10.1371/journal.pone.0019495 (2011).

7 Adeegbe, D. O. & Nishikawa, H. Natural and induced T regulatory cells in cancer. *Frontiers in immunology* **4**, 190, doi:10.3389/fimmu.2013.00190 (2013).

8 Mellman, I. & Steinman, R. M. Dendritic cells: specialized and regulated antigen processing machines. *Cell* **106**, 255-258 (2001).

9 Gabrilovich, D. Mechanisms and functional significance of tumour-induced dendritic-cell defects. *Nature reviews. Immunology* **4**, 941-952, doi:10.1038/nri1498 (2004).

10 Gabrilovich, D. I., Ostrand-Rosenberg, S. & Bronte, V. Coordinated regulation of myeloid cells by tumours. *Nature reviews. Immunology* **12**, 253-268, doi:10.1038/nri3175 (2012).

11 Gabrilovich, D. I. & Nagaraj, S. Myeloid-derived suppressor cells as regulators of the immune system. *Nature reviews. Immunology* **9**, 162-174, doi:10.1038/nri2506 (2009).

12 Giordanengo, L. *et al.* Cruzipain, a major Trypanosoma cruzi antigen, conditions the host immune response in favor of parasite. *European journal of immunology* **32**, 1003-1011, doi:10.1002/1521-4141(200204)32:4<1003::AID-IMMU1003>3.0.CO;2-P (2002).

13 Voisin, M. B., Buzoni-Gatel, D., Bout, D. & Velge-Roussel, F. Both expansion of regulatory GR1+ CD11b+ myeloid cells and anergy of T lymphocytes participate in hyporesponsiveness of the lung-associated immune system during acute toxoplasmosis. *Infection and immunity* **72**, 5487-5492, doi:10.1128/IAI.72.9.5487-5492.2004 (2004).

14 Terrazas, L. I., Walsh, K. L., Piskorska, D., McGuire, E. & Harn, D. A., Jr. The schistosome oligosaccharide lacto-N-neotetraose expands Gr1(+) cells that secrete anti-inflammatory cytokines and inhibit proliferation of naive CD4(+) cells: a potential mechanism for immune polarization in helminth infections. *Journal of immunology* **167**, 5294-5303 (2001).

15 Delano, M. J. *et al.* MyD88-dependent expansion of an immature GR-1(+)CD11b(+) population induces T cell suppression and Th2 polarization in sepsis. *The Journal of experimental medicine* **204**, 1463-1474, doi:10.1084/jem.20062602 (2007).

16 Zhu, B. *et al.* CD11b+Ly-6C(hi) suppressive monocytes in experimental autoimmune encephalomyelitis. *Journal of immunology* **179**, 5228-5237 (2007).

17 Haile, L. A. *et al.* Myeloid-derived suppressor cells in inflammatory bowel disease: a new immunoregulatory pathway. *Gastroenterology* **135**, 871-881, 881 e871-875, doi:10.1053/j.gastro.2008.06.032 (2008).

18 Makarenkova, V. P., Bansal, V., Matta, B. M., Perez, L. A. & Ochoa, J. B. CD11b+/Gr-1+ myeloid suppressor cells cause T cell dysfunction after traumatic stress. *Journal of immunology* **176**, 2085-2094 (2006).

19 Damuzzo, V. *et al.* Complexity and challenges in defining myeloid-derived suppressor cells. *Cytometry. Part B, Clinical cytometry*, doi:10.1002/cyto.b.21206 (2014).

20 Movahedi, K. *et al.* Identification of discrete tumor-induced myeloid-derived suppressor cell subpopulations with distinct T cell-suppressive activity. *Blood* **111**, 4233-4244, doi:10.1182/blood-2007-07-099226 (2008).

21 Ugel, S. *et al.* Immune tolerance to tumor antigens occurs in a specialized environment of the spleen. *Cell reports* **2**, 628-639, doi:10.1016/j.celrep.2012.08.006 (2012).

22 Dolcetti, L. *et al.* Hierarchy of immunosuppressive strength among myeloid-derived suppressor cell subsets is determined by GM-CSF. *European journal of immunology* **40**, 22-35, doi:10.1002/eji.200939903 (2010).
23 Youn, J. I., Collazo, M., Shalova, I. N., Biswas, S. K. & Gabrilovich, D. I. Characterization of the nature of granulocytic myeloid-derived suppressor cells in tumor-bearing mice. *Journal of leukocyte biology* **91**, 167-181, doi:10.1189/jlb.0311177 (2012).
24 Bronte, V. *et al.* Identification of a CD11b(+)/Gr-1(+)/CD31(+) myeloid progenitor capable of activating or suppressing CD8(+) T cells. *Blood* **96**, 3838-3846 (2000).
25 Gallina, G. *et al.* Tumors induce a subset of inflammatory monocytes with immunosuppressive activity on CD8+ T cells. *The Journal of clinical investigation* **116**, 2777-2790, doi:10.1172/JCI28828 (2006).
26 Bronte, V. & Pittet, M. J. The spleen in local and systemic regulation of immunity. *Immunity* **39**, 806-818, doi:10.1016/j.immuni.2013.10.010 (2013).
27 Solito, S. *et al.* Myeloid-derived suppressor cell heterogeneity in human cancers. *Annals of the New York Academy of Sciences* **1319**, 47-65, doi:10.1111/nyas.12469 (2014).
28 Diaz-Montero, C. M. *et al.* Increased circulating myeloid-derived suppressor cells correlate with clinical cancer stage, metastatic tumor burden, and doxorubicin-cyclophosphamide chemotherapy. *Cancer immunology, immunotherapy : CII* **58**, 49-59, doi:10.1007/s00262-008-0523-4 (2009).
29 Huang, A. *et al.* Increased CD14(+)HLA-DR (-/low) myeloid-derived suppressor cells correlate with extrathoracic metastasis and poor response to chemotherapy in non-small cell lung cancer patients. *Cancer immunology, immunotherapy : CII* **62**, 1439-1451, doi:10.1007/s00262-013-1450-6 (2013).
30 Wang, L. *et al.* Increased myeloid-derived suppressor cells in gastric cancer correlate with cancer stage and plasma S100A8/A9 proinflammatory proteins. *Journal of immunology* **190**, 794-804, doi:10.4049/jimmunol.1202088 (2013).
31 Zhang, B. *et al.* Circulating and tumor-infiltrating myeloid-derived suppressor cells in patients with colorectal carcinoma. *PloS one* **8**, e57114, doi:10.1371/journal.pone.0057114 (2013).
32 Bronte, V. & Zanovello, P. Regulation of immune responses by L-arginine metabolism. *Nature reviews. Immunology* **5**, 641-654, doi:10.1038/nri1668 (2005).
33 Rodriguez, P. C. *et al.* Arginase I production in the tumor microenvironment by mature myeloid cells inhibits T-cell receptor expression and antigen-specific T-cell responses. *Cancer research* **64**, 5839-5849, doi:10.1158/0008-5472.CAN-04-0465 (2004).
34 Srivastava, M. K., Sinha, P., Clements, V. K., Rodriguez, P. & Ostrand-Rosenberg, S. Myeloid-derived suppressor cells inhibit T-cell activation by depleting cystine and cysteine. *Cancer research* **70**, 68-77, doi:10.1158/0008-5472.CAN-09-2587 (2010).
35 Mazzoni, A. *et al.* Myeloid suppressor lines inhibit T cell responses by an NO-dependent mechanism. *Journal of immunology* **168**, 689-695 (2002).
36 Macphail, S. E. *et al.* Nitric oxide regulation of human peripheral blood mononuclear cells: critical time dependence and selectivity for cytokine versus chemokine expression. *Journal of immunology* **171**, 4809-4815 (2003).
37 Bronte, V. *et al.* IL-4-induced arginase 1 suppresses alloreactive T cells in tumor-bearing mice. *Journal of immunology* **170**, 270-278 (2003).
38 De Sanctis, F. *et al.* The emerging immunological role of post-translational modifications by reactive nitrogen species in cancer microenvironment. *Frontiers in immunology* **5**, 69, doi:10.3389/fimmu.2014.00069 (2014).
39 Nagaraj, S. *et al.* Altered recognition of antigen is a mechanism of CD8+ T cell tolerance in cancer. *Nature medicine* **13**, 828-835, doi:10.1038/nm1609 (2007).
40 Molon, B. *et al.* Chemokine nitration prevents intratumoral infiltration of antigen-specific T cells. *The Journal of experimental medicine* **208**, 1949-1962, doi:10.1084/jem.20101956 (2011).
41 Kusmartsev, S., Nefedova, Y., Yoder, D. & Gabrilovich, D. I. Antigen-specific inhibition of CD8+ T cell response by immature myeloid cells in cancer is mediated by reactive oxygen species. *Journal of immunology* **172**, 989-999 (2004).
42 Schmielau, J. & Finn, O. J. Activated granulocytes and granulocyte-derived hydrogen peroxide are the underlying mechanism of suppression of t-cell function in advanced cancer patients. *Cancer research* **61**, 4756-4760 (2001).

43 Youn, J. I., Nagaraj, S., Collazo, M. & Gabrilovich, D. I. Subsets of myeloid-derived suppressor cells in tumor-bearing mice. *Journal of immunology* **181**, 5791-5802 (2008).

44 Haverkamp, J. M. *et al.* Myeloid-derived suppressor activity is mediated by monocytic lineages maintained by continuous inhibition of extrinsic and intrinsic death pathways. *Immunity* **41**, 947-959, doi:10.1016/j.immuni.2014.10.020 (2014).

45 Elkabets, M. *et al.* IL-1beta regulates a novel myeloid-derived suppressor cell subset that impairs NK cell development and function. *European journal of immunology* **40**, 3347-3357, doi:10.1002/eji.201041037 (2010).

46 Hoechst, B. *et al.* Myeloid derived suppressor cells inhibit natural killer cells in patients with hepatocellular carcinoma via the NKp30 receptor. *Hepatology* **50**, 799-807, doi:10.1002/hep.23054 (2009).

47 Li, H., Han, Y., Guo, Q., Zhang, M. & Cao, X. Cancer-expanded myeloid-derived suppressor cells induce anergy of NK cells through membrane-bound TGF-beta 1. *Journal of immunology* **182**, 240-249 (2009).

48 Huang, B. *et al.* Gr-1+CD115+ immature myeloid suppressor cells mediate the development of tumor-induced T regulatory cells and T-cell anergy in tumor-bearing host. *Cancer research* **66**, 1123-1131, doi:10.1158/0008-5472.CAN-05-1299 (2006).

49 Pan, P. Y. *et al.* Immune stimulatory receptor CD40 is required for T-cell suppression and T regulatory cell activation mediated by myeloid-derived suppressor cells in cancer. *Cancer research* **70**, 99-108, doi:10.1158/0008-5472.CAN-09-1882 (2010).

50 Schlecker, E. *et al.* Tumor-infiltrating monocytic myeloid-derived suppressor cells mediate CCR5-dependent recruitment of regulatory T cells favoring tumor growth. *Journal of immunology* **189**, 5602-5611, doi:10.4049/jimmunol.1201018 (2012).

51 Di Mitri, D. *et al.* Tumour-infiltrating Gr-1+ myeloid cells antagonize senescence in cancer. *Nature* **515**, 134-137, doi:10.1038/nature13638 (2014).

52 Corzo, C. A. *et al.* HIF-1alpha regulates function and differentiation of myeloid-derived suppressor cells in the tumor microenvironment. *The Journal of experimental medicine* **207**, 2439-2453, doi:10.1084/jem.20100587 (2010).

53 Germano, G. *et al.* Role of macrophage targeting in the antitumor activity of trabectedin. *Cancer cell* **23**, 249-262, doi:10.1016/j.ccr.2013.01.008 (2013).

54 Franklin, R. A. *et al.* The cellular and molecular origin of tumor-associated macrophages. *Science* **344**, 921-925, doi:10.1126/science.1252510 (2014).

55 Movahedi, K. *et al.* Different tumor microenvironments contain functionally distinct subsets of macrophages derived from Ly6C(high) monocytes. *Cancer research* **70**, 5728-5739, doi:10.1158/0008-5472.CAN-09-4672 (2010).

56 Guilliams, M. *et al.* Alveolar macrophages develop from fetal monocytes that differentiate into long-lived cells in the first week of life via GM-CSF. *The Journal of experimental medicine* **210**, 1977-1992, doi:10.1084/jem.20131199 (2013).

57 Hoeffel, G. *et al.* Adult Langerhans cells derive predominantly from embryonic fetal liver monocytes with a minor contribution of yolk sac-derived macrophages. *The Journal of experimental medicine* **209**, 1167-1181, doi:10.1084/jem.20120340 (2012).

58 Schulz, C. *et al.* A lineage of myeloid cells independent of Myb and hematopoietic stem cells. *Science* **336**, 86-90, doi:10.1126/science.1219179 (2012).

59 Qian, B. Z. & Pollard, J. W. Macrophage diversity enhances tumor progression and metastasis. *Cell* **141**, 39-51, doi:10.1016/j.cell.2010.03.014 (2010).

60 Sica, A. & Mantovani, A. Macrophage plasticity and polarization: in vivo veritas. *The Journal of clinical investigation* **122**, 787-795, doi:10.1172/JCI59643 (2012).

61 Mantovani, A., Sozzani, S., Locati, M., Allavena, P. & Sica, A. Macrophage polarization: tumor-associated macrophages as a paradigm for polarized M2 mononuclear phagocytes. *Trends in immunology* **23**, 549-555 (2002).

62 DeNardo, D. G. *et al.* Leukocyte complexity predicts breast cancer survival and functionally regulates response to chemotherapy. *Cancer discovery* **1**, 54-67, doi:10.1158/2159-8274.CD-10-0028 (2011).

63 Steidl, C. *et al.* Tumor-associated macrophages and survival in classic Hodgkin's lymphoma. *The New England journal of medicine* **362**, 875-885, doi:10.1056/NEJMoa0905680 (2010).

64 Belai, E. B. *et al.* PD-1 blockage delays murine squamous cell carcinoma development. *Carcinogenesis* **35**, 424-431, doi:10.1093/carcin/bgt305 (2014).

65 Kuang, D. M. *et al.* Activated monocytes in peritumoral stroma of hepatocellular carcinoma foster immune privilege and disease progression through PD-L1. *The Journal of experimental medicine* **206**, 1327-1337, doi:10.1084/jem.20082173 (2009).
66 Noman, M. Z. *et al.* PD-L1 is a novel direct target of HIF-1alpha, and its blockade under hypoxia enhanced MDSC-mediated T cell activation. *The Journal of experimental medicine* **211**, 781-790, doi:10.1084/jem.20131916 (2014).
67 Morandi, F. & Pistoia, V. Interactions between HLA-G and HLA-E in Physiological and Pathological Conditions. *Frontiers in immunology* **5**, 394, doi:10.3389/fimmu.2014.00394 (2014).
68 Biswas, S. K. *et al.* A distinct and unique transcriptional program expressed by tumor-associated macrophages (defective NF-kappaB and enhanced IRF-3/STAT1 activation). *Blood* **107**, 2112-2122, doi:10.1182/blood-2005-01-0428 (2006).
69 Liou, G. Y. *et al.* Macrophage-secreted cytokines drive pancreatic acinar-to-ductal metaplasia through NF-kappaB and MMPs. *The Journal of cell biology* **202**, 563-577, doi:10.1083/jcb.201301001 (2013).
70 Noy, R. & Pollard, J. W. Tumor-associated macrophages: from mechanisms to therapy. *Immunity* **41**, 49-61, doi:10.1016/j.immuni.2014.06.010 (2014).
71 Sharda, D. R. *et al.* Regulation of macrophage arginase expression and tumor growth by the Ron receptor tyrosine kinase. *Journal of immunology* **187**, 2181-2192, doi:10.4049/jimmunol.1003460 (2011).
72 Lin, E. Y. *et al.* Vascular endothelial growth factor restores delayed tumor progression in tumors depleted of macrophages. *Molecular oncology* **1**, 288-302, doi:10.1016/j.molonc.2007.10.003 (2007).
73 Lin, E. Y. *et al.* Macrophages regulate the angiogenic switch in a mouse model of breast cancer. *Cancer research* **66**, 11238-11246, doi:10.1158/0008-5472.CAN-06-1278 (2006).
74 Yeo, E. J. *et al.* Myeloid WNT7b mediates the angiogenic switch and metastasis in breast cancer. *Cancer research* **74**, 2962-2973, doi:10.1158/0008-5472.CAN-13-2421 (2014).
75 De Palma, M. *et al.* Tie2 identifies a hematopoietic lineage of proangiogenic monocytes required for tumor vessel formation and a mesenchymal population of pericyte progenitors. *Cancer cell* **8**, 211-226, doi:10.1016/j.ccr.2005.08.002 (2005).
76 Mazzieri, R. *et al.* Targeting the ANG2/TIE2 axis inhibits tumor growth and metastasis by impairing angiogenesis and disabling rebounds of proangiogenic myeloid cells. *Cancer cell* **19**, 512-526, doi:10.1016/j.ccr.2011.02.005 (2011).
77 Kessenbrock, K., Plaks, V. & Werb, Z. Matrix metalloproteinases: regulators of the tumor microenvironment. *Cell* **141**, 52-67, doi:10.1016/j.cell.2010.03.015 (2010).
78 Wyckoff, J. *et al.* A paracrine loop between tumor cells and macrophages is required for tumor cell migration in mammary tumors. *Cancer research* **64**, 7022-7029, doi:10.1158/0008-5472.CAN-04-1449 (2004).
79 Sangaletti, S. *et al.* Macrophage-derived SPARC bridges tumor cell-extracellular matrix interactions toward metastasis. *Cancer research* **68**, 9050-9059, doi:10.1158/0008-5472.CAN-08-1327 (2008).
80 Wyckoff, J. B. *et al.* Direct visualization of macrophage-assisted tumor cell intravasation in mammary tumors. *Cancer research* **67**, 2649-2656, doi:10.1158/0008-5472.CAN-06-1823 (2007).
81 Hiratsuka, S., Watanabe, A., Aburatani, H. & Maru, Y. Tumour-mediated upregulation of chemoattractants and recruitment of myeloid cells predetermines lung metastasis. *Nature cell biology* **8**, 1369-1375, doi:10.1038/ncb1507 (2006).
82 Kaplan, R. N. *et al.* VEGFR1-positive haematopoietic bone marrow progenitors initiate the pre-metastatic niche. *Nature* **438**, 820-827, doi:10.1038/nature04186 (2005).
83 Gil-Bernabe, A. M. *et al.* Recruitment of monocytes/macrophages by tissue factor-mediated coagulation is essential for metastatic cell survival and premetastatic niche establishment in mice. *Blood* **119**, 3164-3175, doi:10.1182/blood-2011-08-376426 (2012).
84 Ferjancic, S. *et al.* VCAM-1 and VAP-1 recruit myeloid cells that promote pulmonary metastasis in mice. *Blood* **121**, 3289-3297, doi:10.1182/blood-2012-08-449819 (2013).
85 Qian, B. *et al.* A distinct macrophage population mediates metastatic breast cancer cell extravasation, establishment and growth. *PloS one* **4**, e6562, doi:10.1371/journal.pone.0006562 (2009).

86 Lipson, E. J. & Drake, C. G. Ipilimumab: an anti-CTLA-4 antibody for metastatic melanoma. *Clinical cancer research : an official journal of the American Association for Cancer Research* **17**, 6958-6962, doi:10.1158/1078-0432.CCR-11-1595 (2011).
87 Hodi, F. S. *et al.* Improved survival with ipilimumab in patients with metastatic melanoma. *The New England journal of medicine* **363**, 711-723, doi:10.1056/NEJMoa1003466 (2010).
88 Zou, W. Regulatory T cells, tumour immunity and immunotherapy. *Nature reviews. Immunology* **6**, 295-307, doi:10.1038/nri1806 (2006).
89 Topalian, S. L. *et al.* Safety, activity, and immune correlates of anti-PD-1 antibody in cancer. *The New England journal of medicine* **366**, 2443-2454, doi:10.1056/NEJMoa1200690 (2012).
90 Topalian, S. L. *et al.* Survival, durable tumor remission, and long-term safety in patients with advanced melanoma receiving nivolumab. *Journal of clinical oncology : official journal of the American Society of Clinical Oncology* **32**, 1020-1030, doi:10.1200/JCO.2013.53.0105 (2014).
91 Brahmer, J. R. *et al.* Safety and activity of anti-PD-L1 antibody in patients with advanced cancer. *The New England journal of medicine* **366**, 2455-2465, doi:10.1056/NEJMoa1200694 (2012).
92 Mellman, I., Coukos, G. & Dranoff, G. Cancer immunotherapy comes of age. *Nature* **480**, 480-489, doi:10.1038/nature10673 (2011).
93 Kantoff, P. W. *et al.* Sipuleucel-T immunotherapy for castration-resistant prostate cancer. *The New England journal of medicine* **363**, 411-422, doi:10.1056/NEJMoa1001294 (2010).
94 Schwartzentruber, D. J. *et al.* gp100 peptide vaccine and interleukin-2 in patients with advanced melanoma. *The New England journal of medicine* **364**, 2119-2127, doi:10.1056/NEJMoa1012863 (2011).
95 Rosenberg, S. A. *et al.* Durable complete responses in heavily pretreated patients with metastatic melanoma using T-cell transfer immunotherapy. *Clinical cancer research : an official journal of the American Association for Cancer Research* **17**, 4550-4557, doi:10.1158/1078-0432.CCR-11-0116 (2011).
96 Wrzesinski, C. *et al.* Increased intensity lymphodepletion enhances tumor treatment efficacy of adoptively transferred tumor-specific T cells. *Journal of immunotherapy* **33**, 1-7, doi:10.1097/CJI.0b013e3181b88ffc (2010).
97 Paulos, C. M. *et al.* Microbial translocation augments the function of adoptively transferred self/tumor-specific CD8+ T cells via TLR4 signaling. *The Journal of clinical investigation* **117**, 2197-2204, doi:10.1172/JCI32205 (2007).
98 Serafini, P. *et al.* Phosphodiesterase-5 inhibition augments endogenous antitumor immunity by reducing myeloid-derived suppressor cell function. *The Journal of experimental medicine* **203**, 2691-2702, doi:10.1084/jem.20061104 (2006).
99 Marigo, I. *et al.* Tumor-induced tolerance and immune suppression depend on the C/EBPbeta transcription factor. *Immunity* **32**, 790-802, doi:10.1016/j.immuni.2010.05.010 (2010).
100 Dudley, M. E. *et al.* Adoptive cell therapy for patients with metastatic melanoma: evaluation of intensive myeloablative chemoradiation preparative regimens. *Journal of clinical oncology : official journal of the American Society of Clinical Oncology* **26**, 5233-5239, doi:10.1200/JCO.2008.16.5449 (2008).
101 Gangadhar, T. C. & Vonderheide, R. H. Mitigating the toxic effects of anticancer immunotherapy. *Nature reviews. Clinical oncology* **11**, 91-99, doi:10.1038/nrclinonc.2013.245 (2014).
102 Lamers, C. H. *et al.* Treatment of metastatic renal cell carcinoma with CAIX CAR-engineered T cells: clinical evaluation and management of on-target toxicity. *Molecular therapy : the journal of the American Society of Gene Therapy* **21**, 904-912, doi:10.1038/mt.2013.17 (2013).
103 Lamers, C. H. *et al.* Treatment of metastatic renal cell carcinoma with autologous T-lymphocytes genetically retargeted against carbonic anhydrase IX: first clinical experience. *Journal of clinical oncology : official journal of the American Society of Clinical Oncology* **24**, e20-22, doi:10.1200/JCO.2006.05.9964 (2006).
104 Morgan, R. A. *et al.* Case report of a serious adverse event following the administration of T cells transduced with a chimeric antigen receptor recognizing ERBB2. *Molecular therapy : the journal of the American Society of Gene Therapy* **18**, 843-851, doi:10.1038/mt.2010.24 (2010).
105 Grupp, S. A. *et al.* Chimeric antigen receptor-modified T cells for acute lymphoid leukemia. *The New England journal of medicine* **368**, 1509-1518, doi:10.1056/NEJMoa1215134 (2013).
106 Kochenderfer, J. N. *et al.* B-cell depletion and remissions of malignancy along with cytokine-associated toxicity in a clinical trial of anti-CD19 chimeric-antigen-receptor-transduced T cells. *Blood* **119**, 2709-2720, doi:10.1182/blood-2011-10-384388 (2012).

107 Porter, D. L., Levine, B. L., Kalos, M., Bagg, A. & June, C. H. Chimeric antigen receptor-modified T cells in chronic lymphoid leukemia. *The New England journal of medicine* **365**, 725-733, doi:10.1056/NEJMoa1103849 (2011).

108 Robbins, P. F. *et al.* Tumor regression in patients with metastatic synovial cell sarcoma and melanoma using genetically engineered lymphocytes reactive with NY-ESO-1. *Journal of clinical oncology : official journal of the American Society of Clinical Oncology* **29**, 917-924, doi:10.1200/JCO.2010.32.2537 (2011).

109 Dawidczyk, C. M. *et al.* State-of-the-art in design rules for drug delivery platforms: lessons learned from FDA-approved nanomedicines. *Journal of controlled release : official journal of the Controlled Release Society* **187**, 133-144, doi:10.1016/j.jconrel.2014.05.036 (2014).

110 Matsumura, Y. & Maeda, H. A new concept for macromolecular therapeutics in cancer chemotherapy: mechanism of tumoritropic accumulation of proteins and the antitumor agent smancs. *Cancer research* **46**, 6387-6392 (1986).

111 Carmeliet, P. & Jain, R. K. Molecular mechanisms and clinical applications of angiogenesis. *Nature* **473**, 298-307, doi:10.1038/nature10144 (2011).

112 Jain, R. K. & Stylianopoulos, T. Delivering nanomedicine to solid tumors. *Nature reviews. Clinical oncology* **7**, 653-664, doi:10.1038/nrclinonc.2010.139 (2010).

113 Barenholz, Y. Doxil(R)--the first FDA-approved nano-drug: lessons learned. *Journal of controlled release : official journal of the Controlled Release Society* **160**, 117-134, doi:10.1016/j.jconrel.2012.03.020 (2012).

114 Gabizon, A. *et al.* Prolonged circulation time and enhanced accumulation in malignant exudates of doxorubicin encapsulated in polyethylene-glycol coated liposomes. *Cancer research* **54**, 987-992 (1994).

115 Bertrand, N., Wu, J., Xu, X., Kamaly, N. & Farokhzad, O. C. Cancer nanotechnology: the impact of passive and active targeting in the era of modern cancer biology. *Advanced drug delivery reviews* **66**, 2-25, doi:10.1016/j.addr.2013.11.009 (2014).

116 O'Brien, M. E. *et al.* Reduced cardiotoxicity and comparable efficacy in a phase III trial of pegylated liposomal doxorubicin HCl (CAELYX/Doxil) versus conventional doxorubicin for first-line treatment of metastatic breast cancer. *Annals of oncology : official journal of the European Society for Medical Oncology / ESMO* **15**, 440-449 (2004).

117 Orlowski, R. Z. *et al.* Randomized phase III study of pegylated liposomal doxorubicin plus bortezomib compared with bortezomib alone in relapsed or refractory multiple myeloma: combination therapy improves time to progression. *Journal of clinical oncology : official journal of the American Society of Clinical Oncology* **25**, 3892-3901, doi:10.1200/JCO.2006.10.5460 (2007).

118 Stewart, S. *et al.* Randomized comparative trial of pegylated liposomal doxorubicin versus bleomycin and vincristine in the treatment of AIDS-related Kaposi's sarcoma. International Pegylated Liposomal Doxorubicin Study Group. *Journal of clinical oncology : official journal of the American Society of Clinical Oncology* **16**, 683-691 (1998).

119 Nichols, J. W. & Bae, Y. H. EPR: Evidence and fallacy. *Journal of controlled release : official journal of the Controlled Release Society* **190**, 451-464, doi:10.1016/j.jconrel.2014.03.057 (2014).

120 Safra, T. *et al.* Pegylated liposomal doxorubicin (doxil): reduced clinical cardiotoxicity in patients reaching or exceeding cumulative doses of 500 mg/m2. *Annals of oncology : official journal of the European Society for Medical Oncology / ESMO* **11**, 1029-1033 (2000).

121 Gradishar, W. J. *et al.* Phase III trial of nanoparticle albumin-bound paclitaxel compared with polyethylated castor oil-based paclitaxel in women with breast cancer. *Journal of clinical oncology : official journal of the American Society of Clinical Oncology* **23**, 7794-7803, doi:10.1200/JCO.2005.04.937 (2005).

122 Lundqvist, M. *et al.* Nanoparticle size and surface properties determine the protein corona with possible implications for biological impacts. *Proceedings of the National Academy of Sciences of the United States of America* **105**, 14265-14270, doi:10.1073/pnas.0805135105 (2008).

123 Nel, A. E. *et al.* Understanding biophysicochemical interactions at the nano-bio interface. *Nature materials* **8**, 543-557, doi:10.1038/nmat2442 (2009).

124 Szebeni, J., Muggia, F., Gabizon, A. & Barenholz, Y. Activation of complement by therapeutic liposomes and other lipid excipient-based therapeutic products: prediction and prevention. *Advanced drug delivery reviews* **63**, 1020-1030, doi:10.1016/j.addr.2011.06.017 (2011).

125 Dale, D. C., Boxer, L. & Liles, W. C. The phagocytes: neutrophils and monocytes. *Blood* **112**, 935-945, doi:10.1182/blood-2007-12-077917 (2008).

126 Chonn, A., Cullis, P. R. & Devine, D. V. The role of surface charge in the activation of the classical and alternative pathways of complement by liposomes. *Journal of immunology* **146**, 4234-4241 (1991).
127 Devine, D. V., Wong, K., Serrano, K., Chonn, A. & Cullis, P. R. Liposome-complement interactions in rat serum: implications for liposome survival studies. *Biochimica et biophysica acta* **1191**, 43-51 (1994).
128 Vonarbourg, A., Passirani, C., Saulnier, P. & Benoit, J. P. Parameters influencing the stealthiness of colloidal drug delivery systems. *Biomaterials* **27**, 4356-4373, doi:10.1016/j.biomaterials.2006.03.039 (2006).
129 Zhao, W., Zhuang, S. & Qi, X. R. Comparative study of the in vitro and in vivo characteristics of cationic and neutral liposomes. *International journal of nanomedicine* **6**, 3087-3098, doi:10.2147/IJN.S25399 (2011).
130 Owens, D. E., 3rd & Peppas, N. A. Opsonization, biodistribution, and pharmacokinetics of polymeric nanoparticles. *International journal of pharmaceutics* **307**, 93-102, doi:10.1016/j.ijpharm.2005.10.010 (2006).
131 Jones, S. W. *et al.* Nanoparticle clearance is governed by Th1/Th2 immunity and strain background. *The Journal of clinical investigation* **123**, 3061-3073, doi:10.1172/JCI66895 (2013).
132 Cheng, Z., Al Zaki, A., Hui, J. Z., Muzykantov, V. R. & Tsourkas, A. Multifunctional nanoparticles: cost versus benefit of adding targeting and imaging capabilities. *Science* **338**, 903-910, doi:10.1126/science.1226338 (2012).
133 Rajasekaran, A. K., Anilkumar, G. & Christiansen, J. J. Is prostate-specific membrane antigen a multifunctional protein? *American journal of physiology. Cell physiology* **288**, C975-981, doi:10.1152/ajpcell.00506.2004 (2005).
134 Hrkach, J. *et al.* Preclinical development and clinical translation of a PSMA-targeted docetaxel nanoparticle with a differentiated pharmacological profile. *Science translational medicine* **4**, 128ra139, doi:10.1126/scitranslmed.3003651 (2012).
135 Djuranovic, S., Nahvi, A. & Green, R. A parsimonious model for gene regulation by miRNAs. *Science* **331**, 550-553, doi:10.1126/science.1191138 (2011).
136 Fellmann, C. & Lowe, S. W. Stable RNA interference rules for silencing. *Nature cell biology* **16**, 10-18, doi:10.1038/ncb2895 (2014).
137 Kanasty, R., Dorkin, J. R., Vegas, A. & Anderson, D. Delivery materials for siRNA therapeutics. *Nature materials* **12**, 967-977, doi:10.1038/nmat3765 (2013).
138 Hornung, V. *et al.* Sequence-specific potent induction of IFN-alpha by short interfering RNA in plasmacytoid dendritic cells through TLR7. *Nature medicine* **11**, 263-270, doi:10.1038/nm1191 (2005).
139 Judge, A. D., Bola, G., Lee, A. C. & MacLachlan, I. Design of noninflammatory synthetic siRNA mediating potent gene silencing in vivo. *Molecular therapy : the journal of the American Society of Gene Therapy* **13**, 494-505, doi:10.1016/j.ymthe.2005.11.002 (2006).
140 Elmen, J. *et al.* LNA-mediated microRNA silencing in non-human primates. *Nature* **452**, 896-899, doi:10.1038/nature06783 (2008).
141 Lanford, R. E. *et al.* Therapeutic silencing of microRNA-122 in primates with chronic hepatitis C virus infection. *Science* **327**, 198-201, doi:10.1126/science.1178178 (2010).
142 Whitehead, K. A., Langer, R. & Anderson, D. G. Knocking down barriers: advances in siRNA delivery. *Nature reviews. Drug discovery* **8**, 129-138, doi:10.1038/nrd2742 (2009).
143 Shim, M. S. & Kwon, Y. J. Stimuli-responsive polymers and nanomaterials for gene delivery and imaging applications. *Advanced drug delivery reviews* **64**, 1046-1059, doi:10.1016/j.addr.2012.01.018 (2012).
144 Tabernero, J. *et al.* First-in-humans trial of an RNA interference therapeutic targeting VEGF and KSP in cancer patients with liver involvement. *Cancer discovery* **3**, 406-417, doi:10.1158/2159-8290.CD-12-0429 (2013).
145 Amoozgar, Z. & Goldberg, M. S. Targeting myeloid cells using nanoparticles to improve cancer immunotherapy. *Advanced drug delivery reviews*, doi:10.1016/j.addr.2014.09.007 (2014).
146 Leuschner, F. *et al.* Therapeutic siRNA silencing in inflammatory monocytes in mice. *Nature biotechnology* **29**, 1005-1010, doi:10.1038/nbt.1989 (2011).
147 Love, K. T. *et al.* Lipid-like materials for low-dose, in vivo gene silencing. *Proceedings of the National Academy of Sciences of the United States of America* **107**, 1864-1869, doi:10.1073/pnas.0910603106 (2010).

148 Geissmann, F., Jung, S. & Littman, D. R. Blood monocytes consist of two principal subsets with distinct migratory properties. *Immunity* **19**, 71-82 (2003).
149 Katsuki, S. *et al.* Nanoparticle-mediated delivery of pitavastatin inhibits atherosclerotic plaque destabilization/rupture in mice by regulating the recruitment of inflammatory monocytes. *Circulation* **129**, 896-906, doi:10.1161/CIRCULATIONAHA.113.002870 (2014).
150 Kourtis, I. C. *et al.* Peripherally administered nanoparticles target monocytic myeloid cells, secondary lymphoid organs and tumors in mice. *PloS one* **8**, e61646, doi:10.1371/journal.pone.0061646 (2013).
151 Kugelberg, E. Neutrophils: nanoparticles targeting the bad guys. *Nature reviews. Immunology* **14**, 214, doi:10.1038/nri3648 (2014).
152 Wang, Z., Li, J., Cho, J. & Malik, A. B. Prevention of vascular inflammation by nanoparticle targeting of adherent neutrophils. *Nature nanotechnology* **9**, 204-210, doi:10.1038/nnano.2014.17 (2014).
153 Roth, F. *et al.* Aptamer-mediated blockade of IL4Ralpha triggers apoptosis of MDSCs and limits tumor progression. *Cancer research* **72**, 1373-1383, doi:10.1158/0008-5472.CAN-11-2772 (2012).
154 Estevez, F. *et al.* Enhancement of the immune response to poorly immunogenic gangliosides after incorporation into very small size proteoliposomes (VSSP). *Vaccine* **18**, 190-197 (1999).
155 Fernandez, A. *et al.* Inhibition of tumor-induced myeloid-derived suppressor cell function by a nanoparticulated adjuvant. *Journal of immunology* **186**, 264-274, doi:10.4049/jimmunol.1001465 (2011).
156 Vincent, J. *et al.* 5-Fluorouracil selectively kills tumor-associated myeloid-derived suppressor cells resulting in enhanced T cell-dependent antitumor immunity. *Cancer research* **70**, 3052-3061, doi:10.1158/0008-5472.CAN-09-3690 (2010).
157 Kodumudi, K. N. *et al.* A novel chemoimmunomodulating property of docetaxel: suppression of myeloid-derived suppressor cells in tumor bearers. *Clinical cancer research : an official journal of the American Association for Cancer Research* **16**, 4583-4594, doi:10.1158/1078-0432.CCR-10-0733 (2010).
158 Kusmartsev, S. *et al.* All-trans-retinoic acid eliminates immature myeloid cells from tumor-bearing mice and improves the effect of vaccination. *Cancer research* **63**, 4441-4449 (2003).
159 Mirza, N. *et al.* All-trans-retinoic acid improves differentiation of myeloid cells and immune response in cancer patients. *Cancer research* **66**, 9299-9307, doi:10.1158/0008-5472.CAN-06-1690 (2006).
160 Regazzi, M. B., Iacona, I., Gervasutti, C., Lazzarino, M. & Toma, S. Clinical pharmacokinetics of tretinoin. *Clinical pharmacokinetics* **32**, 382-402, doi:10.2165/00003088-199732050-00004 (1997).
161 Kawakami, S. *et al.* Biodistribution characteristics of all-trans retinoic acid incorporated in liposomes and polymeric micelles following intravenous administration. *Journal of pharmaceutical sciences* **94**, 2606-2615, doi:10.1002/jps.20487 (2005).
162 Ozpolat, B., Lopez-Berestein, G., Adamson, P., Fu, C. J. & Williams, A. H. Pharmacokinetics of intravenously administered liposomal all-trans-retinoic acid (ATRA) and orally administered ATRA in healthy volunteers. *Journal of pharmacy & pharmaceutical sciences : a publication of the Canadian Society for Pharmaceutical Sciences, Societe canadienne des sciences pharmaceutiques* **6**, 292-301 (2003).
163 De Santo, C. *et al.* Nitroaspirin corrects immune dysfunction in tumor-bearing hosts and promotes tumor eradication by cancer vaccination. *Proceedings of the National Academy of Sciences of the United States of America* **102**, 4185-4190, doi:10.1073/pnas.0409783102 (2005).
164 Kelly, C., Jefferies, C. & Cryan, S. A. Targeted liposomal drug delivery to monocytes and macrophages. *Journal of drug delivery* **2011**, 727241, doi:10.1155/2011/727241 (2011).
165 Van Rooijen, N. The liposome-mediated macrophage 'suicide' technique. *Journal of immunological methods* **124**, 1-6 (1989).
166 Halin, S., Rudolfsson, S. H., Van Rooijen, N. & Bergh, A. Extratumoral macrophages promote tumor and vascular growth in an orthotopic rat prostate tumor model. *Neoplasia* **11**, 177-186 (2009).
167 Hiraoka, K. *et al.* Inhibition of bone and muscle metastases of lung cancer cells by a decrease in the number of monocytes/macrophages. *Cancer science* **99**, 1595-1602, doi:10.1111/j.1349-7006.2008.00880.x (2008).

168 Kimura, Y. N. *et al.* Inflammatory stimuli from macrophages and cancer cells synergistically promote tumor growth and angiogenesis. *Cancer science* **98**, 2009-2018, doi:10.1111/j.1349-7006.2007.00633.x (2007).
169 Miselis, N. R., Wu, Z. J., Van Rooijen, N. & Kane, A. B. Targeting tumor-associated macrophages in an orthotopic murine model of diffuse malignant mesothelioma. *Molecular cancer therapeutics* **7**, 788-799, doi:10.1158/1535-7163.MCT-07-0579 (2008).
170 Zeisberger, S. M. *et al.* Clodronate-liposome-mediated depletion of tumour-associated macrophages: a new and highly effective antiangiogenic therapy approach. *British journal of cancer* **95**, 272-281, doi:10.1038/sj.bjc.6603240 (2006).
171 Zhu, S., Niu, M., O'Mary, H. & Cui, Z. Targeting of tumor-associated macrophages made possible by PEG-sheddable, mannose-modified nanoparticles. *Molecular pharmaceutics* **10**, 3525-3530, doi:10.1021/mp400216r (2013).
172 Movahedi, K. *et al.* Nanobody-based targeting of the macrophage mannose receptor for effective in vivo imaging of tumor-associated macrophages. *Cancer research* **72**, 4165-4177, doi:10.1158/0008-5472.CAN-11-2994 (2012).
173 Etzerodt, A. *et al.* Efficient intracellular drug-targeting of macrophages using stealth liposomes directed to the hemoglobin scavenger receptor CD163. *Journal of controlled release : official journal of the Controlled Release Society* **160**, 72-80, doi:10.1016/j.jconrel.2012.01.034 (2012).
174 Yokoi, K. *et al.* Porous silicon nanocarriers for dual targeting tumor associated endothelial cells and macrophages in stroma of orthotopic human pancreatic cancers. *Cancer letters* **334**, 319-327, doi:10.1016/j.canlet.2012.09.001 (2013).
175 Zhang, X. *et al.* Hydrazinocurcumin Encapsuled nanoparticles "re-educate" tumor-associated macrophages and exhibit anti-tumor effects on breast cancer following STAT3 suppression. *PloS one* **8**, e65896, doi:10.1371/journal.pone.0065896 (2013).
176 Cieslewicz, M. *et al.* Targeted delivery of proapoptotic peptides to tumor-associated macrophages improves survival. *Proceedings of the National Academy of Sciences of the United States of America* **110**, 15919-15924, doi:10.1073/pnas.1312197110 (2013).
177 Ries, C. H. *et al.* Targeting tumor-associated macrophages with anti-CSF-1R antibody reveals a strategy for cancer therapy. *Cancer cell* **25**, 846-859, doi:10.1016/j.ccr.2014.05.016 (2014).
178 Hume, D. A. & MacDonald, K. P. Therapeutic applications of macrophage colony-stimulating factor-1 (CSF-1) and antagonists of CSF-1 receptor (CSF-1R) signaling. *Blood* **119**, 1810-1820, doi:10.1182/blood-2011-09-379214 (2012).
179 Huynh, N. T., Passirani, C., Saulnier, P. & Benoit, J. P. Lipid nanocapsules: a new platform for nanomedicine. *International journal of pharmaceutics* **379**, 201-209, doi:10.1016/j.ijpharm.2009.04.026 (2009).
180 Bastiat, G. *et al.* A new tool to ensure the fluorescent dye labeling stability of nanocarriers: a real challenge for fluorescence imaging. *Journal of controlled release : official journal of the Controlled Release Society* **170**, 334-342, doi:10.1016/j.jconrel.2013.06.014 (2013).
181 Harivardhan Reddy, L., Sharma, R. K., Chuttani, K., Mishra, A. K. & Murthy, R. S. Influence of administration route on tumor uptake and biodistribution of etoposide loaded solid lipid nanoparticles in Dalton's lymphoma tumor bearing mice. *Journal of controlled release : official journal of the Controlled Release Society* **105**, 185-198, doi:10.1016/j.jconrel.2005.02.028 (2005).
182 Zhu, S., Li, X., Lansakara, P. D., Kumar, A. & Cui, Z. A nanoparticle depot formulation of 4-(N)-stearoyl gemcitabine shows a strong anti-tumour activity. *The Journal of pharmacy and pharmacology* **65**, 236-242, doi:10.1111/j.2042-7158.2012.01599.x (2013).
183 Reddy, S. T. *et al.* Exploiting lymphatic transport and complement activation in nanoparticle vaccines. *Nature biotechnology* **25**, 1159-1164, doi:10.1038/nbt1332 (2007).
184 Manolova, V. *et al.* Nanoparticles target distinct dendritic cell populations according to their size. *European journal of immunology* **38**, 1404-1413, doi:10.1002/eji.200737984 (2008).
185 Moysan, E. *et al.* An innovative hydrogel of gemcitabine-loaded lipid nanocapsules: when the drug is a key player of the nanomedicine structure. *Soft matter* **10**, 1767-1777, doi:10.1039/c3sm52781f (2014).
186 Le, H. K. *et al.* Gemcitabine directly inhibits myeloid derived suppressor cells in BALB/c mice bearing 4T1 mammary carcinoma and augments expansion of T cells from tumor-bearing mice. *International immunopharmacology* **9**, 900-909, doi:10.1016/j.intimp.2009.03.015 (2009).
187 Suzuki, E., Kapoor, V., Jassar, A. S., Kaiser, L. R. & Albelda, S. M. Gemcitabine selectively eliminates splenic Gr-1+/CD11b+ myeloid suppressor cells in tumor-bearing animals and

enhances antitumor immune activity. *Clinical cancer research : an official journal of the American Association for Cancer Research* **11**, 6713-6721, doi:10.1158/1078-0432.CCR-05-0883 (2005).

188 Tongu, M. *et al.* Metronomic chemotherapy with low-dose cyclophosphamide plus gemcitabine can induce anti-tumor T cell immunity in vivo. *Cancer immunology, immunotherapy : CII* **62**, 383-391, doi:10.1007/s00262-012-1343-0 (2013).

189 Lv, H., Zhang, S., Wang, B., Cui, S. & Yan, J. Toxicity of cationic lipids and cationic polymers in gene delivery. *Journal of controlled release : official journal of the Controlled Release Society* **114**, 100-109, doi:10.1016/j.jconrel.2006.04.014 (2006).

190 Futaki, S. Membrane-permeable arginine-rich peptides and the translocation mechanisms. *Advanced drug delivery reviews* **57**, 547-558, doi:10.1016/j.addr.2004.10.009 (2005).

191 Zhao, Z. X. *et al.* Self-assembly nanomicelles based on cationic mPEG-PLA-b-Polyarginine(R15) triblock copolymer for siRNA delivery. *Biomaterials* **33**, 6793-6807, doi:10.1016/j.biomaterials.2012.05.067 (2012).

192 Apolloni, E. *et al.* Immortalized myeloid suppressor cells trigger apoptosis in antigen-activated T lymphocytes. *Journal of immunology* **165**, 6723-6730 (2000).

193 Wesolowski, R., Markowitz, J. & Carson, W. E., 3rd. Myeloid derived suppressor cells - a new therapeutic target in the treatment of cancer. *Journal for immunotherapy of cancer* **1**, 10, doi:10.1186/2051-1426-1-10 (2013).

194 Ghansah, T. *et al.* Dendritic cell immunotherapy combined with gemcitabine chemotherapy enhances survival in a murine model of pancreatic carcinoma. *Cancer immunology, immunotherapy : CII* **62**, 1083-1091, doi:10.1007/s00262-013-1407-9 (2013).

195 Bergman, A. M., Pinedo, H. M. & Peters, G. J. Determinants of resistance to 2',2'-difluorodeoxycytidine (gemcitabine). *Drug resistance updates : reviews and commentaries in antimicrobial and anticancer chemotherapy* **5**, 19-33 (2002).

196 Komori, S. *et al.* Contribution of thymidylate synthase to gemcitabine therapy for advanced pancreatic cancer. *Pancreas* **39**, 1284-1292, doi:10.1097/MPA.0b013e3181dec17d (2010).

197 Moysan, E., Bastiat, G. & Benoit, J. P. Gemcitabine versus Modified Gemcitabine: a review of several promising chemical modifications. *Molecular pharmaceutics* **10**, 430-444, doi:10.1021/mp300370t (2013).

198 Lobovkina, T. *et al.* In vivo sustained release of siRNA from solid lipid nanoparticles. *ACS nano* **5**, 9977-9983, doi:10.1021/nn203745n (2011).

199 Veltkamp, S. A., Beijnen, J. H. & Schellens, J. H. Prolonged versus standard gemcitabine infusion: translation of molecular pharmacology to new treatment strategy. *The oncologist* **13**, 261-276, doi:10.1634/theoncologist.2007-0215 (2008).

200 Tempero, M. *et al.* Randomized phase II comparison of dose-intense gemcitabine: thirty-minute infusion and fixed dose rate infusion in patients with pancreatic adenocarcinoma. *Journal of clinical oncology : official journal of the American Society of Clinical Oncology* **21**, 3402-3408, doi:10.1200/JCO.2003.09.140 (2003).

201 Boven, E., Schipper, H., Erkelens, C. A., Hatty, S. A. & Pinedo, H. M. The influence of the schedule and the dose of gemcitabine on the anti-tumour efficacy in experimental human cancer. *British journal of cancer* **68**, 52-56 (1993).

202 Francia, G. *et al.* Low-dose metronomic oral dosing of a prodrug of gemcitabine (LY2334737) causes antitumor effects in the absence of inhibition of systemic vasculogenesis. *Molecular cancer therapeutics* **11**, 680-689, doi:10.1158/1535-7163.MCT-11-0659 (2012).

203 Hirai, H. *et al.* C/EBPbeta is required for 'emergency' granulopoiesis. *Nature immunology* **7**, 732-739, doi:10.1038/ni1354 (2006).

204 Sonda, N. *et al.* miR-142-3p prevents macrophage differentiation during cancer-induced myelopoiesis. *Immunity* **38**, 1236-1249, doi:10.1016/j.immuni.2013.06.004 (2013).

# Acknowledgments

I thank my PhD supervisors, Prof. Vincenzo Bronte and Dr. Susanna Mandruzzato, and the PhD school director Prof. Paola Zanovello.

I thank my colleagues who contributed to this work, especially Ilaria Marigo and Giacomo Desantis.

I also thank all the collaborators from other research laboratories: Jean Pierre Benoit, Guillaume Bastiat, Elodye Moysan, Giovanna Lollo and Marion Pitorre (University of Angers); Maria Josè Alonso, Adriana Martinez Ledo and Marcos Garcia Fuentes (University of Santiago de Compostela); Paolo Serafini (University of Miami).

I finally thank my family, all my friends and my roommates for their support during these years.

# Appendix

## Scientific publications

1. Sasso MS, Bronte V, Marigo I. (2014). *Cancer immune modulation and immunosuppressive cells: current and future therapeutic approaches*. In: Alonso MJ and Garcia-Fuentes M. *Nano-Oncologicals: new targeting and delivery approaches*. Advances in Delivery Science and Technology. Springer

2. Marigo I, Zilio S, Desantis G, Mlecnik B, Agnellini A.H.R., Ugel S, Sasso MS, Qualls JE , Kratochvill F, Zanovello P, Molon B, Iezzi M, Lamolinara A, Ries CH, Runza V, Hoves S, Bilocq AM, Bindea G, Galon J, Murray PJ, and Bronte V. *T cell cancer therapy requires CD40/CD40L activation of TNF/iNOS-producing dendritic cells.* Under revision.

## Attended meetings and conferences with written or oral presentation

1. Euronanomed-Lymphotarg project, 2nd annual meeting. Angers, January 30, 2012 (oral presentation).
2. Euronanomed-Lymphotarg project, 3rd annual meeting. Santiago de Compostela, February 21, 2013 (oral presentation)
3. Cancer Bio-Immunotherapy in Siena, XIIth NIBIT Meeting, Siena, October 9 - 11, 2014.
   Ilaria Marigo, Serena Zilio, Giacomo Desantis, Andryelli H.R Agnellini, Stefano Ugel, Maria Stella Sasso, Kevin Leone, Paola Zanovello, Manuela Iezzi, Peter J. Murray, Bernhard Mlencnick, Amelie M. Bilock, Gabriela Bindea, Jerome Galon and Vincenzo Bronte. *The effectiveness of CD8+ T cell mediated immune-therapy against tumor requires a Tip-DC expansion in the tumor microenvironment that acts through the CD40/CD40L signaling pathway* (poster).